THE ROLE OF AKT IN THE PREVENTION OF APOPTOSIS IN HL-60 CELLS, A HUMAN LEUKAEMIC CELL LINE

Chantal Paula Drummond

A dissertation submitted to the Faculty of Science, University of the Witwatersrand, Johannesburg for the Degree of Master of Science

Johannesburg 2005

DECLARATION

I declare that this dissertation is my own, unaided work. It is being submitted for the degree of Master of Science in the University of the Witwatersrand, Johannesburg. It has not been submitted before for any degree or examination in any other University.

Chantal Paula Drummond

28 February 2005

ABSTRACT

Studies on the development of drug resistance in several cancer types, including acute myeloid leukaemia (AML), have implicated the PI3-kinase pathway. This pathway phosphorylates Akt resulting in the activation of proteins involved in cell survival. The aim of this study is to determine the role that Akt plays in survival and the relationship between Akt, IKK and IκB in HL-60 cells. This study demonstrated that etoposide caused apoptosis in HL-60 cells, which was slightly increased when the PI3-kinase pathway was inhibited by LY294002. Stimulation with PDGF resulted in cell proliferation and increased Akt, IKK and IκB phosphorylation. Although pre-treatment with LY294002 decreased the amount of Phospho-Akt, phosphorylation of IKK and IκB still occurred. Therefore additional pathways must be involved in IκB regulation in HL-60 cells. Akt mRNA transcription was decreased when the cells were pre-treated with LY294002 and either PDGF or etoposide. In conclusion, the PI3-kinase pathway plays a minor role in the survival of HL-60 cells and Akt substrates other than IKK are mediating this survival.

DEDICATION

I dedicate this work to my late Grandfather, Mr Ian James Drummond, who sadly passed away on the 30 November 2004 from lung cancer. Thank-you for all of your love and support given to me over the years. Your steely determination was inspiration to us all.

ACKNOWLEDGEMENTS

I would like to express my gratitude to the following people and organizations:

My supervisors, Dr Natalie Whalley and Professor Nerina Savage, for their unwavering support and advice. The members of the Department of Molecular Medicine and Haematology for their technical advice. The members of the Department of Surgery for their assistance with the flow cytometry technique. My friends and family who were always there for me.

The Medical Faculty Endowment Fund, the NHLS, the NRF Thuthuka Programme and the University of the Witwatersrand Faculty Research Committee, for their much appreciated financial support (2000-2004).

ABBREVIATIONS

AML	Acute Myeloid Leukaemia
AO	Acridine orange
APL	Acute Promyelocytic Leukaemia
ATP	Adenosine Triphosphate
BCR	Breakpoint cluster region
BSA	Bovine Serum Albumin
cAMP	Cyclic Adenosine Monophosphate
cDNA	Copy Deoxyribonucleic Acid
CTMP	Carboxyl-terminal modulator protein
DEPC	Diethyl pyrocarbonate
DMSO	Dimethyl sulphoxide
DNA	Deoxyribonucleic Acid
dNTP	Deoxyribonucleoside triphosphates
ECL	Enhanced Chemiluminescence
ECM	Extra cellular matrix
FCS	Foetal calf serum
FKHR	Forkhead transcription factor
GAP	GTPase activating protein
GH	Growth Hormone
GSK-3	Glycogen synthase kinase-3
GTP	Guanine Triphosphate
GTPase	Guanine Triphosphatase

HL-60	Human leukaemic cell line
HSP90	Heat shock protein 90
IGF-1	Insulin-like growth factor 1
IKK	Inhibitor IκB kinase
ILK	Integrin-linked kinase
IRS	Insulin receptor substrate
JNK	Jun N-terminal kinase
kDa	kilo Dalton
LDH	Lactate dehydrogenase
LY294002	2-(4-Morphylinyl)-8-phenyl-4H-benzopyran-4-one
MAPKK	mitogen-activated protein kinase kinase
Met	Meathionine
MEKK	Mitogen-activated protein kinase/ERK kinase kinase
MOPS	3-[N-morpholino] propane sulphonic acid
mRNA	Messenger ribonucleic acid
mTOR	Mammalian target of rapamycin
NADH	Nicatinamide dehydrogenase
NAK	NF-κB activating kinase
NF-κB	Nuclear factor κB
PBS	Phosphate buffered saline
PCR	Polymerase chain reaction
PDK	3-phosphoinositide-dependent protein kinase
PDGF	Platelet derived growth factor
PH-domain	Pleckstrin homology domain

Phospho	Phosphorylated
PI3-kinase	Phosphoinositide 3 kinase
PIK	PI kinase domain
PKA	Protein kinase A
PKB	Protein kinase B (Akt)
PKC	Protein kinase C
PP2A	Protein phosphatase 2A
PS	Phoshatidyl-serine
PTEN	Phosphatases and tensin homologue deleted on chromosome 10
PtdIns	Phosphatidylinositol
Rac	Ras related GTP binding protein
Rb	Retinoblastoma
RNA	Ribonucleic acid
RNases	Ribonucleases
rRNA	Ribosomal ribonucleic acid
RTK	Receptor tyrosine kinase
RT-PCR	Reverse transcription polymerase chain reaction
SDS	Sodium dodecyl sulphate
SDS-PAGE	Sodium dodecyl sulphate poly-acrylamide gel electrophoresis
Ser	Serine
SH2 domain	Src homology 2 domains
TBS-T	Tris buffered saline with Tween-20

Thr	Threonine
Tyr	Tyrosine
TNF-α	Tumour necrosis factor α
U	Units
UV	Ultra Violet
V	Volts

TABLE OF CONTENTS

LIST OF FIGURES

LIST OF TABLES

CHAPTER 1

INTRODUCTION

Cancer is a cell growth disorder, characterised by an autonomous proliferation of genetically dysfunctional cells (Alberts *et al*, 1994; Raven & Johnson, 1996). If the cells continue to replicate in an uncontrolled manner, they lead to a cluster of cells known as a tumour or a neoplasm. A tumour is considered to be non-cancerous or benign if the neoplastic cells remain clustered together, and the mass can generally be removed completely with surgery. Cancerous or malignant tumour cells are able to invade the surrounding tissue, as well as break away from the tumour. These enter the blood or lymph vessels and form secondary tumours known as metastases in other parts of the body (Alberts *et al*, 1994).

Cancers are generally classified according to the tissue and cell type from which they develop. Carcinomas develop from epithelial cells, whereas cancers of the connective tissue or muscle cells are referred to as sarcomas. Other cancers arising from haemopoietic cells, known as leukaemias, and nervous tissue do not fall into these categories (Alberts *et al*, 1994).

Many signalling pathways exist in the cell, and it has been shown that cancer results from a stepwise accumulation of mutations in the pathways affecting growth control, differentiation and cell survival.

A delicate balance exists between the mechanisms that stimulate cell proliferation and programmed cell death. The most commonly described signalling pathways include the Ras/MAPK (Mitogen activated protein kinase) pathway which drives uncontrolled proliferation, the retinoblastoma (Rb) pathway that alters the control of the cell cycle, and apoptosis/cell survival that is regulated by the p53 and PI3-kinase/Akt pathways. Akt has also been implicated in 'anoikis', a process that prevents normal cells from detaching from the extracellular matrix (ECM). It is thought that an alteration in the PI3-kinase/Akt pathway allows cancerous cells to metastasise or drug resistance to develop (Masure *et al*, 1999).

The remainder of the introduction will be focused on the PI3-kinase/Akt and IKK/IκB pathways, and their roles in the prevention of apoptosis with particular interest in leukaemia.

1.1 PHOSPHOINOSITIDE 3-KINASE PATHWAY

1.1.1 STRUCTURE OF PI3-KINASE

Courtneidge and Heber first characterised the PI3-kinase enzyme as an 85 kDa phosphoprotein in 1987 (Domin & Waterfield, 1997). PI3-kinase activity was found to be physically and functionally associated with the transforming activity of viral oncogenes such as SRC tyrosine kinase and polyomavirus middle antigen (Vivanco & Sawyers, 2002). Subsequent cloning and purification of the enzyme revealed that PI3-kinase is a heterodimeric complex consisting of an 85 kDa adaptor (p85) and a 110 kDa catalytic subunit (p110) (Domin & Waterfield, 1997). The p85 regulatory subunit is directly associated with many active tyrosine kinases through the physical interaction of its SH2 domain with phosphotyrosine residues. In some cases, the interaction of p85 and the receptor tyrosine kinases is indirect, occurring through intermediate phosphoproteins, such as insulin receptor substrates IRS1 and IRS2 (Vivanco & Sawyers, 2002). Over the following years numerous PI3-kinase catalytic and regulatory subunits have been described resulting in a classification of the enzyme family according to their structure and probable mechanism of regulation. Seven forms of the catalytic subunit and five forms of associated binding partner/adaptor subunit have been identified in mammals, and have been

divided into three main classes; class I, II and III (Domin & Waterfield, 1997; Astoul *et al,* 2001; Vivanco & Sawyers, 2002).

1.1.2 REGULATION OF PI3-KINASE ACTIVITY

Most of the understanding about the PI3-kinase family has been gained from the study of class I molecules, which consist of a p85 regulatory domain and a p110 catalytic domain. The class I PI3-kinases appear to play a role in almost every receptor mediated signalling event, and are tightly regulated in normal cells by various mechanisms. A pre-formed inactive p85-p110 complex is situated in the cytoplasm of resting cells awaiting activation. When ligand binding to a receptor tyrosine kinase occurs, it results in the activation of kinase activity and transphosphorylation of the receptor tyrosine kinase cytoplasmic tail. The p85-p110 complex is recruited to the receptor by the phosphorylation of tyrosine residues presented within a pTyr-X-X-Met consensus sequence, which acts as docking sites for the class IA adaptor subunit SH2 domains. In some cases the interaction may be with the IRS1/IRS2 signalling intermediates. Lipid kinase activity is activated by phosphopeptide binding to the p85 SH2 domains and the catalytic subunit is brought into close proximity with its lipid substrate by translocation to the plasma membrane. This also results in an increase in PI3-kinase activity by facilitating an interaction with GTP bound ras (Fig. 1.1) (Domin & Waterfield, 1997; Tu *et al*, 2000; Vivanco & Sawyers, 2002).

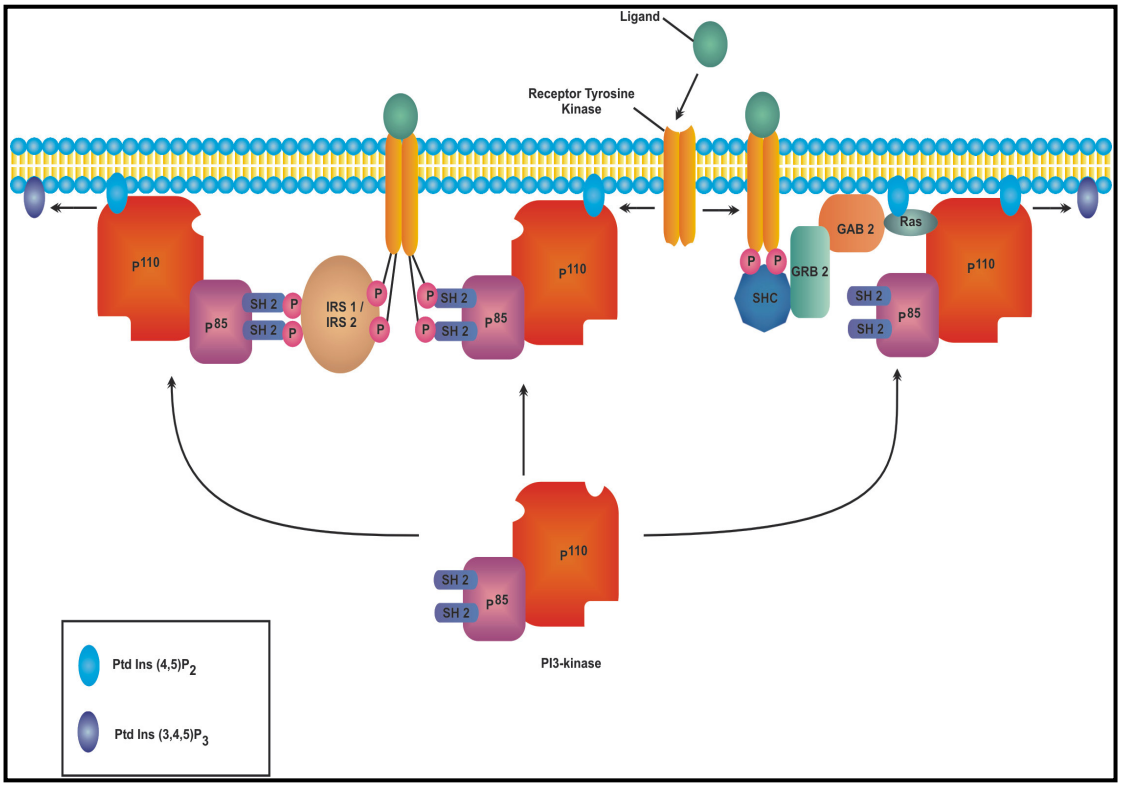

Figure 1.1 Three possible activation pathways of PI3-kinase (Adapted from Vivanco & Sawyers, 2002).

The generation of PtdIns(3,4,5)P_3, a second messenger, from PtdIns(4,5)P_2 is the primary repercussion of PI3-kinase activation. Due to the effects of strict PI3-kinase regulation and the action of several PtdIns(3,4,5)P_3 phosphatases (PTEN, SHIP1 and SHIP2) (Fig. 1.2), PtdIns(3,4,5)P_3 levels are barely detectable in unstimulated mammalian cells. PTEN functions primarily as a PtdIns(3,4,5)P_3 lipid phosphatase that converts PtdIns(3,4,5)P_3 to PtdIns(4,5)P_2, but it is thought to also have activity against protein substrates (Ramaswamy *et al*, 1999;

Burgering & Kops, 2002; Vivanco & Sawyers, 2002). SHIP phosphatases also act on PtdIns(3,4,5)P_3, but remove the phosphate from the 5' position resulting in the production of PtdIns(3,4)P_2 (Fig. 1.2). PtdIns(3,4)P_2, like PtdIns(3,4,5)P_3 act as secondary messengers and recruit proteins, such as Akt, which contain a PH-domain. Both PTEN and SHIP reduce the level of PtdIns(3,4,5)P_3, however PTEN appears to play the major role in the control of the mitogenic effects of phosphoinositides. This has been shown as knockout mutations in *Pten* give a stronger cancer phenotype in mice than *Ship1* (Vivanco & Sawyers, 2002).

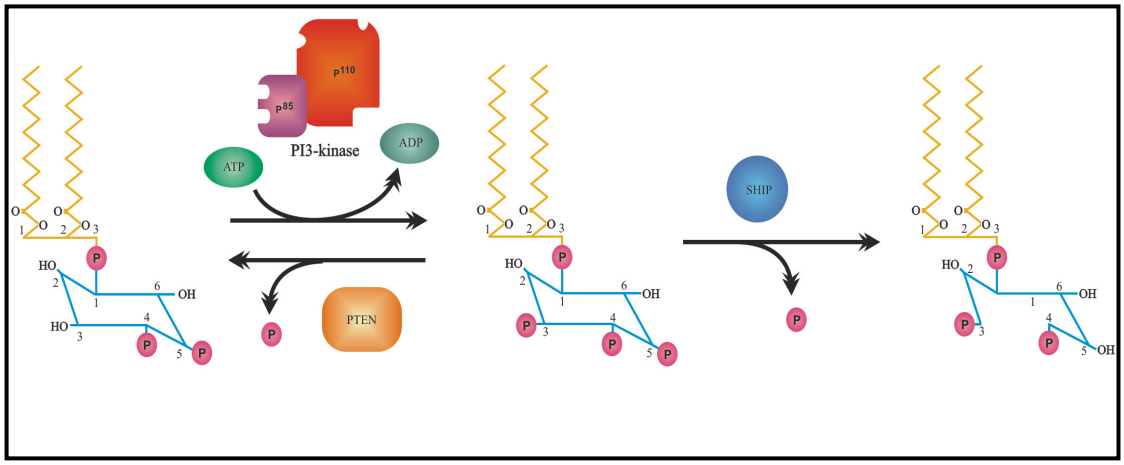

Figure 1.2 Phosphoinositol 3-kinase (PI3-kinase) phosphorylation of PtdIns(4,5)P_2 at the D3 position giving rise to the second messenger PtdIns(3,4,5)P_3. PtdIns(4,5)P_2 is regenerated by the dephosphorylation of PtdIns(3,4,5)P_3 by PTEN. Dephosphorylation of PtdIns(3,4,5)P_3 by SHIP1/2 occasionally occurs at the D5 position forming PtdIns(4,5)P_2. (Adapted from Vivanco & Sawyers, 2002).

1.1.4 DOWNSTREAM TARGETS OF PI3-KINASE

The PI3-kinase pathway appears to have several downstream targets as the phospholipid products of PI3-kinase bind to the pleckstrin homology (PH) domains of proteins. This either modifies their activity or causes them to be translocated to the membrane (Domin & Waterfield, 1997).

.

Evidence has shown that even though activation of $p70^{S6}$ kinase is a result of Ser/Thr protein kinase independent of the Raf/MAPK pathway, it is an important downstream target of PI3-kinase. $p70^{S6}$ kinase plays a key role in G1 to S phase transition in the cell cycle, by phosphorylating the 40S ribosomal protein S6 in response to mitogenic stimuli (Domin & Waterfield, 1997).

Rac, the ras related GTP binding protein is also thought to be a downstream target of PI3-kinase. The protein is said to activate the JNK/stress activated protein kinase, which phosphorylates c-jun (Domin & Waterfield, 1997).

Activation of calcium-independent isoforms of protein kinase C and protein kinase C related kinases appear to be the result of binding to 3' phosphoinositides. This has been found *in vitro* and is thought to be the case in whole cells, but the specificity of this activation is a contentious issue (Domin & Waterfield, 1997).

PDK1 or 3-phosphoinositide-dependent protein kinase is activated by PI3-kinases, PtdIns(3,4,5)P_3 and PtdIns(3,4)P_2. Due to the presence of a PH domain, it is thought that PI3-kinase activity causes PDK1 to be translocated to the membrane. PDK1 also contains a catalytic domain with homology to cAMP-dependent protein kinase (PKA) Akt and protein

kinase C (PKC) subfamily (Brazil & Hemmings, 2001; Burgering & Kops, 2002).

Akt, also called protein kinase B, is a Ser/Thr kinase and is the cellular homologue of the retroviral oncogene v-akt. This kinase will be discussed in more detail below.

1.2 AKT/PROTEIN KINASE B

Staal and co-workers first described Akt/Protein kinase B in 1977. They discovered a transforming murine leukaemia virus (AKT8) which had a high incidence of spontaneous lymphoma in the mink epithelial cell line CCL-64. The inability of AKT8 to induce focus formation in other cell lines such as NIH3T3 fibroblasts suggested that the virus contained an undescribed oncogene. The isolation of the retrovirus from AKT8 infected mink lung epithelial cells showed that AKT8 contained a cell-derived oncogenic sequence called Akt. The hypothesis that this gene played a role in the pathogenesis of human malignancy was strongly supported by the identification of two human homologues, Akt1 and Akt2, and the amplification of a fragment of the *Akt1* gene in gastric adenocarcinoma cells. Further research showed evidence of the oncogenic potential of Akt when they demonstrated that the AKT8 virus induced tumour formation,

specifically thymic lymphoma, in nude mice (Staal, 1987; Bellacosa *et al*, 1991; Brazil & Hemmings, 2001).

No further research on the properties of Akt was reported until 1991, when three independent research teams identified genes corresponding to PKB/Akt. The first was from Jones and co-workers identifying a gene encoding a serine/threonine protein kinase, named Rac (related to the A and C kinases) and was subsequently renamed *PKBα/Akt1.* Akt was shown to have *in vitro* kinase activity with histone H1 as a substrate. Similar work by Bellacosa and colleagues later that year described the cloning of *v-Akt* by fusing the cDNA of the viral GAG protein and the α-isoform of Akt. These results showed that a strong similarity exists between the *v-Akt* and protein kinase C sequence and when run on a SDS-PAGE there was a retarded migration suggesting phosphorylation of the protein (Bellacosa *et al*, 1991; Brazil & Hemmings, 2001). Lastly a PCR screening approach used by Coffer and Woodget demonstrated the significant homology of PKB to protein kinase C and protein kinase A. Akt contains a centrally located catalytic domain, which shows a high degree of homology to those of both protein kinase C and protein kinase A, 75% and 65% respectively (Andjelkovic *et al*, 1996; Brazil & Hemmings, 2001). The combination of these results and the discovery of the second form of Akt, PKBβ/Akt2, identified Akt as a widely expressed phospho-protein kinase (Okano *et al*, 2000; Brazil & Hemmings, 2001).

Staal and co-workers detected amplification of *Akt1* in gastric adenocarcinoma, resulting in further investigation of the role of the Akt genes in human cancers. Similarly Cheng and colleagues demonstrated the amplification of the *Akt2* gene in two ovarian carcinoma cell lines. This led to the conclusion that amplification of Akt genes may contribute to the pathogenesis of certain cancers and opened the door for the investigation of the role of Akt in many cellular processes including glucose metabolism, transcription, apoptosis, proliferation, migration, angiogenesis and cell growth (Staal, 1987; Brazil & Hemmings, 2001).

1.2.1 THE STRUCTURE OF AKT

The analysis of the amino acid sequence of Akt revealed an N-terminal region with homology to a modular domain called the pleckstrin homology (PH) domain. The PH domain, containing ~100 amino acids, has been identified in more than 90 signalling and cytoskeletal molecules including Akt, RasGAP, mSOS and β-spectrin, many of which are associated with membranes (Andjelkovic *et al*, 1996; Stokoe, *et al*, 1997; Brazil & Hemmings, 2001). This PH domain was thought to mediate the interaction of Akt with other proteins. Fesik and co-workers demonstrated that PtdIns(3,4,5)P_2 could bind to the PH domain of proteins, leading to the hypothesis that phospholipids interacted with the PH domain of Akt (Stokoe *et al*, 1997; Brazil & Hemmings, 2001).

In 1995, experiments on the Akt homologue in *Drosophila melanogater*, DRAC-PK, revealed that the protein has a 75% homology to the human isoforms, and is ubiquitously expressed throughout the *Drosophila* life cycle. Akt activity in *Drosophila* appears to be developmentally regulated as it is ~8 fold higher in adult flies than in early embryos (Andjelkovic *et al*, 1996; Brazil & Hemmings, 2001). It was also shown that the PH domain of Akt mediates protein-protein interactions. The identification of a relationship between PI3-kinase activity and Akt activation revealed that the membrane phospholipids generated by PI3-kinase were essential for the activation of Akt (Brazil & Hemmings, 2001).

Three main isoforms of Akt have now been identified in mammalian cells: PKBα/Akt1, PKBβ/Akt2 and PKBγ/Akt3. The amino acid sequences for Akt2 and Akt3 have 81% and 83% homology with Akt1 respectively. Akt has two phosphorylation sites required for full activation, on Akt1 they are at Thr^{308} and Ser^{473}, but on Akt2 and Akt3 they are at $Thr^{309/305}$ and $Ser^{474/472}$ respectively. PKBα/Akt1 has been found to be overexpressed in the breast cancer epithelial cell line (MCF-7), PKBβ/Akt2 is overexpressed in a number of ovarian and pancreatic cancers, with both appearing to be ubiquitously expressed. Akt3 is expressed predominantly in the brain, heart and kidney (Alessi *et al*, 1996; Masure *et al*; 1999; Okano *et al*, 2000).

1.2.2 AKT REGULATION

Both the PH domain and the phosphorylation of Akt appeared to regulate Akt activity. This concept was supported by data showing that Akt was activated by both serum stimulation and protein phosphatase inhibitors (such as pervanadate). The kinase activity of Akt was inhibited by incubating cells with protein phosphatase 2A (PP2A), suggesting that Akt activity is controlled by reversible phosphorylation on both serine and threonine residues (Andjelkovic *et al*, 1996; Brazil & Hemmings, 2001). Chaperone protein heat-shock protein 90 (HSP90) protects Akt from dephosphorylation by PP2A hence preventing its inactivation. The recently identified carboxy-terminal modulator protein (CTMP) has also been shown to bind to Akt, inactivating it and preventing phosphorylation and downstream signalling (Vivanco & Sawyers, 2002). Alessi, Andjelkovic and colleagues demonstrated the exact mechanism of this phospho-regulation by treating cells with insulin or insulin-like growth factor (IGF-1), causing Akt to be activated by phosphorylation on residues Thr^{308} and Ser^{473}. The addition of either of the PI3-kinase pathway inhibitors, wortmannin or LY294002, or the mutation of these amino acid residues caused a decrease in Akt activity. A model of Akt activation was becoming apparent. Full activation of Akt appeared to require the recruitment of Akt to the plasma membrane. The PH domain binds to PtdIns(3,4,5)P_3 and phosphorylation occurs on Thr^{308} in the T-loop of the catalytic domain and Ser^{473} in the C-terminus of the α isoform by one or

more upstream kinases (Andjelkovic *et al*, 1998; Brazil & Hemmings, 2001).

An intensive search for the upstream kinases responsible for phosphorylating Akt was sparked by the discovery that phosphorylation on the serine and threonine residues was essential for the regulation of Akt. Within a year a kinase was purified from both rabbit skeletal muscle and rat brain that phosphorylated Akt on Thr^{308} activating the kinase. Consistent with previous work, it was shown that insulin stimulated Thr^{308} and Ser^{473} phosphorylation was abolished when PI3-kinase was inhibited. It was also demonstrated that this protein was activated by the products of PI3-kinase, PtdIns(3,4,5)P_3 and PtdIns(3,4)P_2, leading to it being named 3-phosphoinositide-dependent protein kinase or PDK1. The cloning of PDK1 revealed a C-terminal PH domain thought to be involved in lipid binding and a catalytic domain with homology to cAMP-dependent protein kinase (PKA) Akt and protein kinase C (PKC) subfamily. The PH domain suggests that PI3-kinase activity causes PDK1 to be translocated to the membrane, however the catalytic activity of PDK1 appears to be constitutive and remains largely unchanged after PI3-kinase activation. It is therefore thought that PI3-kinase activity is not only responsible for the membrane localisation of PDK1, but regulates both the localisation and activation of Akt (Stephens *et al,* 1998; Brazil & Hemmings, 2001; Burgering & Kops, 2002). The phosphorylation of Akt by PDK1 appears to be conformationally regulated, as the PH domain of Akt masks its

activation site. Therefore Akt must bind to PtdIns(3,4,5)P_3 or PtdIns(3,4)P_2, causing the auto-inhibition to be relieved and allowing PDK1 to access Thr^{308} on the activation loop (Toker & Newton, 2000).

The kinase responsible for the phosphorylation of the C-terminal hydrophobic Ser^{473} residue remains elusive. A number of possibilities have been postulated, these include MAPKAP kinase 2, Akt, PDK1, ILK, and PRK2 (Andjelkovic *et al*, 1998; Tu *et al*, 2000; Brazil & Hemmings, 2001). Recent reports have provided conflicting views on the control of phosphorylation on this site. The regulation of the Ser^{473} has been shown to be both mitogen- and PI3-kinase-dependent, leading to the proposal that the upstream kinase is also in the PI3-kinase pathway but distinctly different from PDK1. The kinase was therefore provisionally named PDK2. ILK has been shown to increase Ser^{473} phosphorylation in transfected cells, however the mechanism is indirect suggesting that ILK is not the mysterious PDK2 (Toker & Newton, 2000).

1.2.4 DOWNSTREAM TARGETS OF AKT

Glycogen synthase kinase-3 (GSK-3) was the first downstream substrate of Akt to be identified. Akt is stimulated and GSK-3 is inhibited when cells are treated with insulin. The inhibition of GSK-3 occurs when Akt phosphorylates Ser^{21} in GSK-3α and Ser^{9} in GSK-3β. It was noted that the addition of a PI3-kinase inhibitor prevented the activation of Akt and

the inhibition of GSK-3. These findings suggested that the Akt pathway may play a role in the control of physiological processes such as glycogen and protein synthesis (Alessi *et al*, 1996; Brazil & Hemmings, 2001) (Fig. 1.3).

Further experimentation with cerebellar granule neurons showed that the removal of serum or growth factors such as IGF-1 caused apoptosis. Evidence provided by Yao and Cooper showed that growth factor mediated cell survival required a PI3-kinase signal that was independent of $p70^{S6}$ kinase. Dudek and co-workers substantiated this by demonstrating that cerebellar granule cell survival mediated by IGF-1 was completely dependent on PI3-kinase activity and involved Akt with no $p70^{S6}$ kinase activity. The expression of wild-type Akt enhanced the survival of neurons in the absence of growth factors, however neurons with dominant negative mutants of Akt appeared to have increased apoptosis in the presence of serum. These results pointed out a pivotal role that Akt plays in the neuronal survival pathway, suggesting that Akt may influence pathological conditions of the brain including hypoxic/ischaemic-induced injury and neurodegenerative disorders (Brazil & Hemmings, 2001) (Fig. 1.3).

The possibility that Akt had an anti-apoptotic role led to the search for downstream targets involved in cell survival. The first downstream target identified was BAD, a pro-apoptotic factor. When phosphorylated its pro-

apoptotic function in haematopoietic cells, in response to ligands such as interleukin-3, is inhibited. It was also observed that Akt translocated to the nucleus in growth factor stimulated cells indicating that suppression and/or upregulation of gene expression could be another anti-apoptotic mechanism controlled by the kinase. Other downstream targets involved in cell survival include mTOR which is responsible for protein translation (Fig. 1.3). Pro-apoptotic factors which are inhibited by Akt phosphorylation include ASK and caspase-9 (Brunet *et al*, 1999; Borgatti *et al*, 2000; Jones *et al*, 2000; Madge & Pober, 2000; Tang *et al*, 2000; Zhou *et al*, 2000; Brazil & Hemmings, 2001; Tang *et al*, 2001; Burgering & Kops, 2002; Shin *et al,* 2002; Steelman *et al*, 2004) (Fig. 1.3).

Akt was found to phosphorylate and inactivate the newly discovered human homologues of the *Caenorhabditis elegans* gene encoding Daf-16 (FKHRL1, FKHR and AFX) otherwise known as the Forkhead family of transcription factors. It was observed that stimulation by growth factors caused Akt dependent phosphorylation and inhibition of FKHRL1 function. The transcription of death genes such as Fas ligand gene was suppressed and cell survival was promoted (Brunet *et al*, 1999; Brazil & Hemmings, 2001). The activation of IKKα resulting in the degradation of IκB and stimulation of NF-κB has also been linked to Akt. Recently Akt has been implicated in the inhibition of apoptosis in cells treated with a number of agents and treatments including Fas ligation, UV radiation and etoposide (Brunet *et al*, 1999; Borgatti *et al*, 2000; Jones *et al*, 2000;

Madge & Pober, 2000; Tang *et al*, 2000; Zhou *et al*, 2000; Brazil & Hemmings, 2001; Tang *et al*, 2001; Burgering & Kops, 2002; Steelman *et al*, 2004) (Fig. 1.3).

The search for more Akt downstream targets is continuing, a recent publication described the use of a peptide library to find Akt substrates and defined the optimal substrate sequence (Table 1.1). Sufficient phosphorylation occurs when the sequence motif is Arg-Xaa-Arg-Yaa-Zaa-Ser/Thr-Hyd, where Xaa is any amino acid, Yaa and Zaa are small residues except glycine, and Hyd is a bulky hydrophobic residue (Phe, Leu) (Alessi *et al*, 1996). This consensus peptide phosphorylation sequence for Akt has been derived from small peptides with relatively low affinities, and may not represent the *in vivo* situation completely. It appears that Akt plays a major role in cell signalling as the diverse list of substrates (Table 1.1) is constantly increasing. These substrates are not only involved in apoptosis, but also in metabolism, cytoskeleton regulation and various other cellular processes (Brazil & Hemmings, 2001).

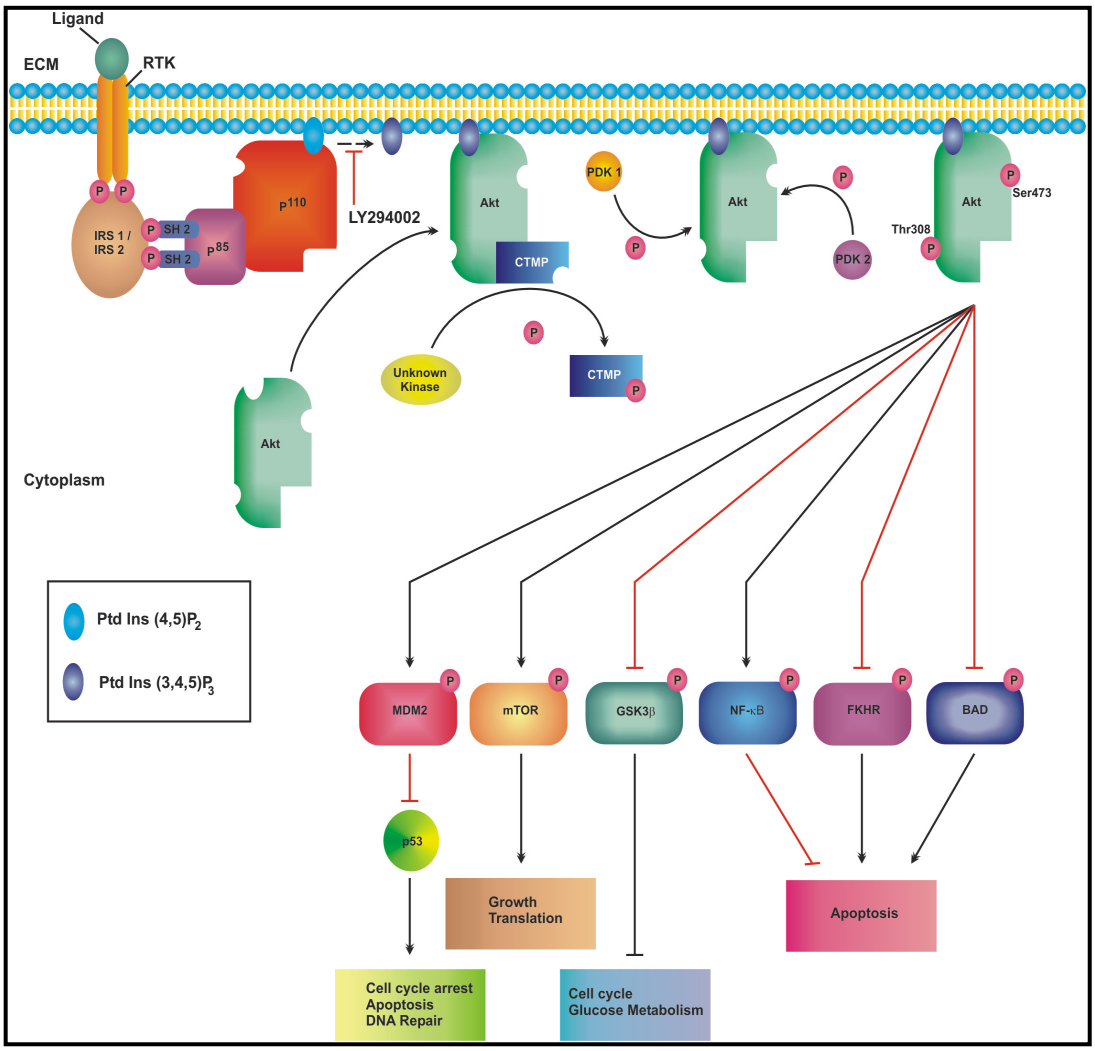

Figure 1.3 The process of Akt phosphorylation, showing the subsequent activation and inhibition of several downstream targets, resulting in cellular growth, survival and growth. The black arrows indicate the targets that are activated, whereas the red arrows indicate targets that are inhibited. (Adapted from Vivanco & Sawyers, 2002).

Table 1.1 The current list of published Akt substrates. The amino acid phosphorylated by Akt is in bold (Brazil & Hemmings, 2001).

Protein	Akt Phosphorylation Sites	Species	Effect of Phosphorylation
BAD	^{107}RSRHS**S**Y^{113}	Human	Blocks BAD-induced apoptosis
C-Raf	^{130}RGRSR**S**A^{137}	Human	Inhibits C-Raf activity
B-Raf	^{254}RQRST**S**T^{260} ^{423}RERKS**S**S^{429}	Human	Inhibits B-Raf activity
BCRA-1	^{504}KKRRP**T**S^{510}	Human	Interferes with nuclear localization of BCRA-1
CREB	^{128}LSRRP**S**Y^{134}	Human	Increased association with CBP and p130
eNOS	^{1174}RIRTQSF**S**L^{1181}	Human	Activates eNOS and leads to NO production
FKHRL-1	^{248}RRRAV**S**M^{254}	Human	Inhibits transcriptional activity of FKHRL1
GSK-3α	^{16}RARTS**S**F^{22}	Human	Inactivates GSK-3 activity
GSK-3β	^{4}RPRTS**S**F^{10}	Human	Inactivates GSK-3 activity
IκB kinase-α	^{18}RERLG**T**G^{24}	Human	Activates transcriptional activity of NF-κB
IRS-1	^{297}RSRTE**S**I^{303}	Murine	Protects IRS-1 from action of PYPase
mTOR	^{2443}RTRTD**S**Y^{2449}	Murine	Activates mTOR activity
PDE-3B	^{268}RPRRR**S**S^{274}	Murine	Inactivates PDE-38
PFK-2	^{460}RMRRN**S**F^{467} ^{478}RPRNT**S**V^{484}	Bovine	Activates PFK-2
Rac1	^{66}RIRPL**S**Y^{72}	Human	Inhibits Rac1-GTP binding
hTERT	^{819}RIRGK**S**Y^{825}	Human	Enhances telomerase activity
p21CIP1	^{139}RKRRQ**T**S^{146}	Human	Causes cytoplasmic localization of p21CIP1
Nur77	^{345}RGRLP**S**K^{351}	Human	Inhibits transcriptional activity of Nur77

1.3 THE IKK PATHWAY AND NF-κB REGULATION

Stimulation of the IKK pathway occurs in response to many different stimuli, including cytokines, growth factors, bacterial products, viral infection, physiological, physical and oxidative stress, receptor ligands and some pharmaceutical drugs and chemicals. Activation of IKK causes IκB to be ubiquitinated and degraded, releasing the nuclear transcription factor NF-κB and allowing it to move into the nucleus (Beraud *et al*, 1999; Delhase *et al*, 2000; Perkins, 2000).

1.3.1 IKK PROTEIN COMPLEX

The IKK protein complex was isolated as a >700 kDa complex consisting of three proteins, IκB kinase (IKK) α, β and γ. IKKα (IKK1) and IKKβ (IKK2) are catalytic subunits whereas IKKγ/NEMO (NF-κB essential modulator) plays a regulatory role, and is required for IKK activation by upstream pathways (Perkins, 2000; Madrid *et al*, 2001). IKK proteins are Ser/Thr kinases characterised by a Leucine zipper and a helix-loop-helix protein interaction motif. The Leucine zippers of IKKα and β allow the proteins to heterodimerize, a requirement for kinase activity (Beraud *et al*, 1999). Another high molecular weight IKK complex was recently discovered, adding to the complexity of the pathway. This complex contains IKKε, which is homologous to, but does not associate with IKKα

and IKKβ. The IKKε complex appears to activate NF-κB by phorbal esters and cross-linking, not by TNF-α or ILK-1 (Perkins, 2000).

Kinases responsible for the phosphorylation at Thr^{23} and activation of IKK complexes include members of the mitogen-activated protein kinase kinase (MAPKK) family, such as NF-κB-inducing kinase (NIK) and mitogen-activated protein kinase/ERK kinase kinase (MEKK) 1, 2 and 3. Others include members of the atypical protein kinase C family, Akt/PKB, and two IKKα and IKKβ related proteins, IKKi and NF-κB activating kinase (NAK). The exact contribution of each pathway is still unclear and varies with different experimental conditions (Perkins, 2000).

1.3.2 THE IκB PROTEIN FAMILY

Another multigene family was discovered when the IκB gene was cloned. This family including IκBβ, IκBε and Bcl3, is structurally characterised by 5 to 7 ankyrin-repeat motifs. These motifs mediate the interaction with the Rel homology domain of NF-κB (Beraud *et al*, 1999; Perkins, 2000). The C-termini of p100 and p105 contain similar repeats and can function as IκB-like proteins, retaining NF-κB complexes in the cytoplasm prior to proteolytic cleavage (Shah *et al*, 1999; Hsu *et al*, 2000; Perkins, 2000; Schmitz *et al*, 2001). IκB proteins contain two conserved Ser residues, Ser^{32} and Ser^{36} on IκBα, Ser^{19} and Ser^{23} on IκBβ, Ser^{18} and Ser^{22} on IκBε,

within their N-terminal domain (Beraud *et al*, 1999; Perkins, 2000). Once the Ser^{32} and Ser^{36} residues on IκBα are phosphorylated, IκB is ubiquitinated and degraded by the 26S proteosome (Beraud *et al*, 1999; Romashkova *et al*, 1999; Delhase *et al*, 2000; Perkins, 2000; Pomerantz & Baltimore, 2000; Schmitz *et al*, 2001).

1.3.3 NF-κB

NF-κB was first discovered as a nuclear transcription factor in mature B cells that bound to an element in the kappa immunoglobulin light chain enhancer, hence its name. It was found that NF-κB was a complex consisting of two subunits with molecular weights of 50 kDa (p50) and 65 kDa (p65). This complex is found in an inactive cytoplasmic form bound to the inhibitor protein IκB in most cell types. Treatment of cells with inflammatory cytokines, TNF-α and IL-1, released NF-κB from IκB allowing its nuclear translocation and confirming NF-κB's involvement in the immune response. Other NF-κB target genes were identified, including cytokines, chemokines, cytokine- and immuno-receptors, adhesion molecules, acute-phase proteins, stress-responsive genes and HIV-1 (Perkins, 2000). The isolation of the p50 gene revealed that it encoded for a 105 kDa protein that required proteolytic cleavage to generate p50. It was found that the DNA-binding and dimerization domain of p50 was significantly homologous to the viral oncoprotein v-Rel, its

cellular counterpart c-Rel and Dorsal (the *Drosophila melanogater* developmental protein) (Perkins, 2000; Schmitz *et al*, 2001). Shortly afterwards p65 cDNA was isolated, confirming this relationship. A multigene NF-κB family was established by the discovery of two other highly homologous proteins, p100 (p52) and Rel-B. The members of this family all contain a ~300 amino acid N-terminal DNA binding and dimerization domain. Several of these proteins, c-Rel, RelB and p65 (RelA) contain a nonhomologous transactivation domain at their C-termini, and do not require proteolytic cleavage to generate their active forms (Beraud *et al*, 1999; Shah *et al*, 1999; Perkins, 2000; Schmitz *et al*, 2001). p52 (NF-κB2) is similar to p100/50 (NF-κB1) as it is generated by the proteolytic cleavage of p100. The most commonly observed form of NF-κB is a p50-p65 heterodimer (Shah *et al*, 1999; Perkins, 2000; Schmitz *et al*, 2001).

1.3.4 AKT AND THE IKK PATHWAY

NF-κB appears to be stimulated rapidly in response to many stimuli, including cytokines, growth factors, bacterial products, viral infection, physiological, physical and oxidative stress, receptor ligands and some pharmaceutical drugs and chemicals (Beraud *et al*, 1999; Delhase *et al*, 2000; Perkins, 2000). Several pathways are activated by these stimuli and result in the phosphorylation of IκB. Ozes and colleagues

demonstrated that Akt was required for NF-κB activation by TNF-α in 293, HeLa and ME-180 cells (Ozes *et al*, 1999; Perkins, 2000). Zhou and associates found evidence that Akt activity was essential for the stimulation of both IKKα and β, for IκB phosphorylation and NF-κB activation in several breast cancer cell lines (Zhou *et al*, 2000). Furthermore in primary rat and human fibroblasts it was shown that NF-κB activation by PDGF and not TNF-α or phorbol esters, required Akt (Romashkova *et al*, 1999; Perkins, 2000). In MCF-7 breast carcinoma cells it was found that Akt signalling activated NF-κB in both a TNF-α-dependent and –independent manner (Burow *et al*, 2000). Contrasting evidence by Kane and co-workers demonstrated that Akt did not activate NF-κB in Jurkat cells, but along with phorbal esters resulted in an enhanced degradation of IκB (Kane *et al*, 1999; Perkins, 2000). Two groups, Sizemore and colleagues and Madrid and co-workers, contradicted these findings by examining the IL-1 or oncogenic H-Ras-mediated activation of NF-κB in HepG2 and NIH 3T3 cells respectively. They reported that Akt could activate NF-κB transactivation, however it was not at the IκB level of phosphorylation and NF-κB nuclear translocation. They found that Akt stimulated the p65 (RelA) transactivation domain to induce transcription (Sizemore *et al*, 1999; Delhase *et al*, 2000; Madrid *et al*, 2000; Perkins, 2000). An overlapping role of the IKK complexes could explain these discrepancies, as both dominant-negative IKKε and IKKα/β proteins have been shown to inhibit phorbol-ester-mediated NF-κB activation. IKK activation and expression

may vary in different cell lines or under different growth conditions, resulting in conflicting results (Perkins, 2000).

1.4 ACTIVATION OF IKK BY THE PI3-KINASE/AKT PATHWAY

The PI3-kinase/Akt pathway has been linked to three main biological processes vital to the progress of cancer development, survival, proliferation and cell growth. As previously mentioned, there is an increasing number of downstream targets responsible for the development and survival of cancer cells (Okano *et al*, 2002; Vivanco & Sawyers, 2002). In this study, one biological process, survival, and one downstream pathway; IKK, IκB and NF-κB, was highlighted for analysis.

With the binding of an appropriate ligand to the RTK, SH2 domains on the p85 subunit of the preformed inactive PI3-kinase complex bind to the phospho-tyrosine residues on the receptor. This brings the p110 catalytic in close proximity to its substrate, PtdIns(4,5)P_2. PI3-kinase phosphorylates PtdIns(4,5)P_2 at the D3 position forming the second messenger PtdIns(3,4,5)P_3, which is necessary for the binding of Akt's pleckstrin-homology domain (Fig 1.2). Akt is recruited to the membrane, where it binds to PtdIns(3,4,5)P_3, and an unknown kinase phosphorylates and releases the inhibitor CTMP. The binding of Akt to PtdIns(3,4,5)P_3

conformationally changes Akt, exposing Thr308 which is phosphorylated by PDK-1. This phosphorylation is necessary and sufficient for Akt activation, however maximum activation is achieved with the phosphorylation of Ser473 by PDK-2. Akt is then able to activate its downstream pathways, including IKK which is phosphorylated on the IKKα subunit at Ser180 and on the IKKβ subunit at Ser181. Phosphorylated IKK in turn phosphorylates IκB on Ser 32 and Ser36 resulting in the release of NF-κB. The phosphorylated IκB is ubiquitinated and degraded by the 26S proteosome (Franke *et al*, 1997; Frech *et al*, 1997; Okano *et al,* 2000; Brazil & Hemmings, 2001; Vivanco & Sawyers, 2002; Brazil *et al*, 2004). This allows NF-κB to move from the cytoplasm to the nucleus where it activates the transcription of anti-apoptotic genes including those involved in the regulation of inflammation and immune responses, viral replication, nitric oxide production, cell-cell interactions, apoptosis and proliferation (Fig 1.4) (Franke *et al*, 1997; Frech *et al*, 1997; Janssen-Heininger *et al*, 2000; Okano *et al,* 2000; Ryan *et al,* 2000; Brazil & Hemmings, 2001; Vivanco & Sawyers, 2002; Brazil *et al*, 2004).

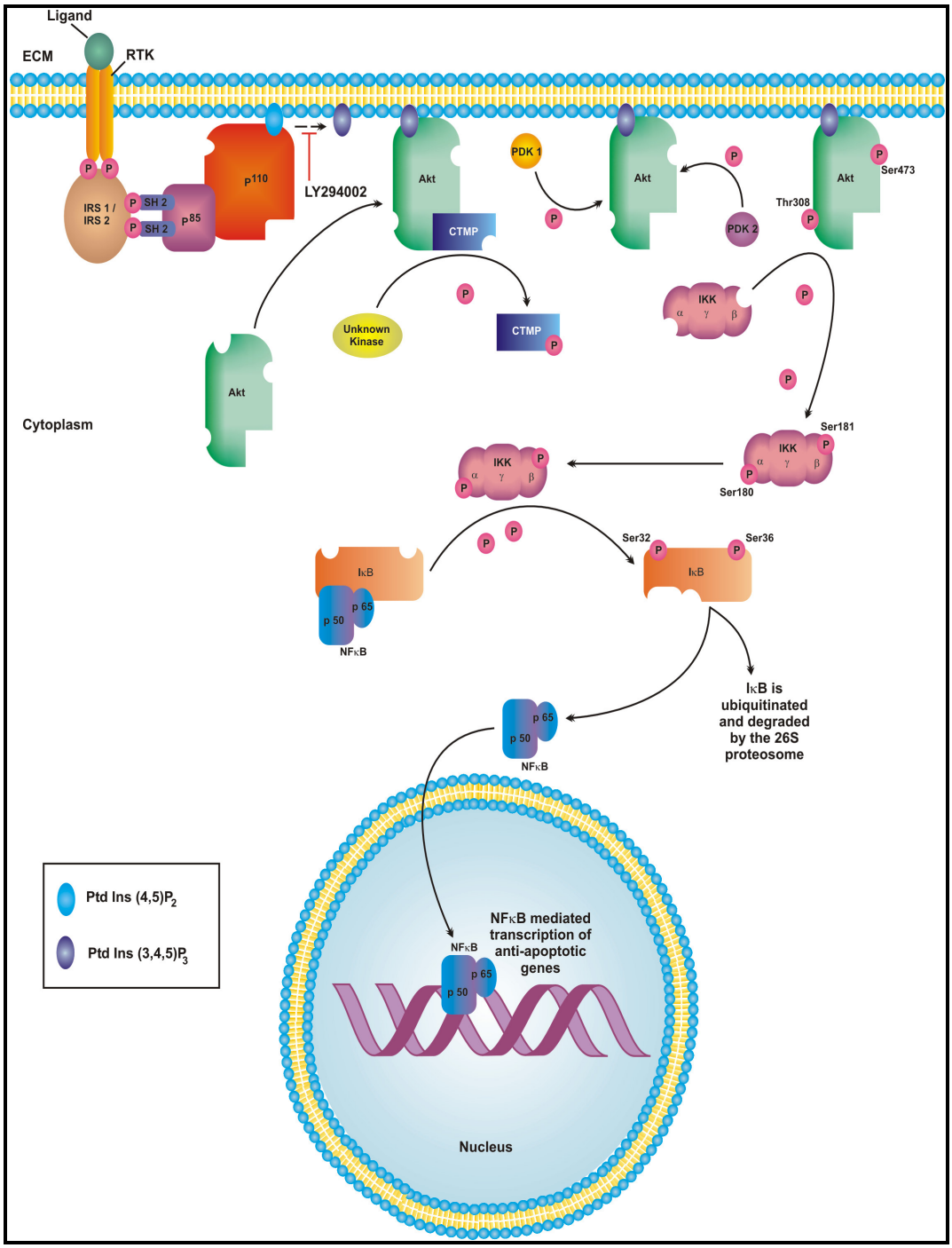

Figure 1.4 The proposed PI3-kinase/Akt pathway showing the activation of IKK, IκB and IKK.

1.5 CHEMICAL INHIBITORS OF THE PI3-KINASE/AKT PATHWAY

Identification of specific inhibitors is extremely useful in the characterisation of intracellular signalling cascades or networks. Two specific PI3-kinase pathway inhibitors, wortmannin and LY294002, have been extensively used to define the role of this kinase and its products in cells, however many new inhibitors are being developed and tested daily.

1.5.1 WORTMANNIN

Wortmannin is a fungal metabolite which has been shown to specifically inhibit the PI3-kinase pathway. Many specific inhibitors are unable to pass through the cell membrane, however wortmannin is cell-permeant which allows whole cell studies to be performed on the PI3-kinase pathway. Wortmannin binds covalently and irreversibly to the p110 catalytic subunit of the PI3-kinase molecule (Ui *et al*, 1995). It has recently been found that L802 present in the kinase domain of PI3-kinase in conjunction with wortmannin covalently modifies the β-phosphate of ATP to a Schiff base, preventing phosphorylation (Steelman *et al*, 2004).

1.5.2 LY294002

2-(4-Morphylinyl)-8-phenyl-4H-1-benzopyran-4-one (LY294002) was first described by Vlahos and colleagues in 1994, when they synthesised several chromones from the initial and relatively unsuccessful PI3-kinase inhibitor, quercetin. One of these chromones, LY294002, was found to be a selective inhibitor of PI3-kinase with a 2.7-fold greater potency than quercetin. LY294002 is a competitive inhibitor of the ATP-binding site of PI3-kinase, however does not inhibit several other ATP-requiring enzymes, unlike quercetin (Vlahos *et al*, 1994).

In a recent study, treatment of cells with LY294002 resulted in dephosphorylated Akt and BAD in leukaemic cell lines and AML as well as decreased clonogenic growth of the AML cells. This inhibition of colony-forming was less pronounced in normal myeloid progenitor cells signifying that LY294002 may selectively target leukaemic cells over normal haemopoietic cells. This is indicative that inhibition of the PI3-kinase pathway with LY294002 may have significant therapeutic implications in AML therapy (Zhao *et al*, 2004).

1.5.3 OTHER PI3-KINASE INHIBITORS

Many scientific groups have deemed wortmannin and LY294002 unsatisfactory in the inhibition of PI3-kinase, as downstream kinases that are dependent on PI3-kinase activity are also presumably inactivated. An Akt inhibitor 1L-6-hydroxy-methyl-chiro-inositol 2*(R)*-2-*O*-methyl-3-*O*-octadecylcarbonate described by Martelli and co-workers (2003), has been shown to decrease the resistance of leukaemic cells to cytotoxic drugs and ionizing radiation. A plant derived pigment called curcumin, was used to inhibit prostrate cancer cell growth, and was shown to reduce Akt phosphorylation on Ser473. Degeulin was synthesised from the natural plant compound rotenone, and was found to inhibit human bronchial epithelial cell proliferation. The constitutively activated Akt in this cell line was inhibited by degeulin without interfering with the PI3-kinase activity. Meuillet and colleagues (2003) identified a group of D-3-deoxy-phospatidyl-myo-inositols that traps Akt in the cytosol, and prevents its activation by binding to its PH domain (Brazil *et al*, 2004).

The increased specificity being discovered with these new inhibitors lays a platform for the further advancement in our understanding of the PI3-kinase pathway. Pro-survival pathway inhibitors used in conjunction with cytotoxic drugs to obtain a higher percentage of apoptosis, may prove useful in the future both in the laboratory and in the clinic.

1.6 APOPTOSIS AND NECROSIS

An important part of the development, maintenance and growth of a tissue is the ability to control the death of damaged cells. There are two distinct types of cell death, the first being an accidental cell death or necrosis, which can be induced by lethal physical, chemical or biological injury. The second is programmed cell death (PCD) otherwise known as apoptosis (Vermes *et al*, 1997; Story & Kodym, 1998).

1.6.1 NECROSIS

Necrosis is not seen in normal tissue development, but occurs in response to injury or toxic damage. The process of necrosis is not biologically controlled and starts when the cell membrane is damaged. This results in the disruption of osmotic homeostasis as the selective permeability and ion-pumping capacity of the cell membrane is lost. The influx of cations causes an almost instantaneous swelling of the cell and its organelles, the cellular metabolic pathways collapse and poisoning of respiration pathways occur. Random DNA degradation and further membrane disruption occurs with the activation of Ca^{2+}-dependent degradative enzymes, such as phospholipases, hydrolases, proteases and endonucleases. The cell eventually bursts due to the osmolytic imbalance, and a cache of lysosomal and degradative enzymes are

released. These elicit an inflammatory response in the adjacent viable cells and can result in a zone of necrotic cells radiating from a necrotic centre in a tissue (McKenna, 1996; Vermes *et al*, 1997; Story & Kodym, 1998; Golstein *et al*, 2003).

1.6.2 APOPTOSIS

Programmed cell death (PCD) was first described by Kerr, Wyllie and Currie in 1972. They named the natural ordered elimination of cells from a tissue apoptosis, which, in classic Greek describes the loss of leaves from a tree in autumn (McKenna, 1996; Story & Kodym, 1998). Apoptosis is a genetically mediated form of cell death and plays an integral role in normal tissue development. It is involved in organogenesis, tissue homeostasis and remodelling, and the removal of auto-reactive clones by editing of the immune system. In contrast to necrosis, which affects a large number of cells in one area, apoptosis characteristically affects scattered individual cells and usually does not cause an inflammatory response (McKenna, 1996). The process of apoptosis has been described as an active bio-energy saving cell-elimination mechanism, which removes aged, unwanted or damaged cells. The cellular contents of precious caloric value are phagocytosed by adjacent cells or macrophages and recycled (Vermes *et al*, 1997).

1.6.1.1 Morphology of Apoptotic Cells

Apoptosis occurs by a specific pattern and is characterised by several distinct morphological changes. One of the first changes is the severing of junctions with neighbouring cells and the loss of specialised membrane structures such as microvilli. The integrity of the cell membrane and the mitochondria however, remains initially intact. The cytoplasm and nucleus become condensed and the chromatin aggregates along the nuclear membrane. Degradation at the internucleosomal linker sites of the cellular DNA yields fragments in multiples of 180 base pairs giving the nucleus a segmented appearance. The membrane appears to be blebbing and convoluted as the endoplasmic reticulum is transformed in to vesicles, which fuse to the cellular membrane. The cell membrane becomes rigid due to the cross-linking of the membrane proteins before the cell is broken apart into small vesicles called apoptotic bodies. The apoptotic bodies contain remnants of the cell as well as several apparently intact organelles. These remain in the extracellular space until they are phagocytosed by the neighbouring cells or by the macrophages (Vermes *et al*, 1997; Story & Kodym, 1998; Corfe, 2002; Golstein *et al*, 2003).

No damage to the surrounding cells occurs, and no inflammatory response is initiated during apoptosis. This is due to the surface changes on the apoptotic cells and the appropriate receptors on the macrophages and neighbouring phagocytic cells. There is increasing evidence that a

phosphatidyl-serine (PS) flip-flop phenomenon occurs in apoptotic cells, and that the exposed PS may act as a recognition site for the phagocytic cells. It is also thought that this change in architecture of the cell membrane and the altering of the surface hydrophobicity and charge may be recognised by the macrophages (Vermes *et al*, 1997; Corfe, 2002).

1.6.1.2 The Apoptotic Pathways

Although apoptosis may be triggered by a wide variety of stimuli, there are essentially two pathways that control this process. The first can be thought of more as murder than suicide. Cells contain a large number of receptors on the surface membrane, and several of them are death receptors. The presentation of an appropriate ligand for a death receptor causes these to form a multi-protein complex called the death-induced signalling complex (Fig 1.5). This complex triggers the direct activation of caspase-8, which belongs to a proteinase family known as the caspases. The caspases are thought to be activated solely and specifically during apoptosis. Certain caspases can auto-activate and can then activate other caspases and a variety of other cellular substrates. These are involved in the breaking down and packaging of the cellular components into apoptotic bodies (Vermes *et al*, 1997; Green & Reed, 1998, Thornberry & Lazenbnik, 1998; Li & Yuan, 1999; Adrain & Martin, 2001).

The second pathway involves intracellular signalling that targets the mitochondria, where several of the Bcl-2 protein family members are situated. These include proapoptotic Bak and Bax, and the anti-apoptotic Bcl-x_L and Bcl-2 proteins. Bcl-x_L and Bcl-2 may also be present in the endoplasmic reticulum and the nuclear membrane in some cell types, and often Bax is found in the cytosol. Once apoptosis is stimulated Bax is recruited to the mitochondria where it binds to Bak (Fig 1.5). This complex forms pores in the membrane, allowing the release of cytochrome *c* into the cytoplasm and the loss of mitochondrial membrane potential. The apoptosome, a protein complex of pro-caspase 9 and APAF-1, binds with the released cytochrome *c*. This leads to the activation of caspase-9, which activates pro-caspase 3 and 7 and the other apoptotic substrates in the same manner of the first pathway (Vermes *et al*, 1997; Green & Reed, 1998, Thornberry & Lazenbnik, 1998; Li & Yuan, 1999; Adrian & Martin, 2001; Pommier *et al*, 2004) (Fig 1.5).

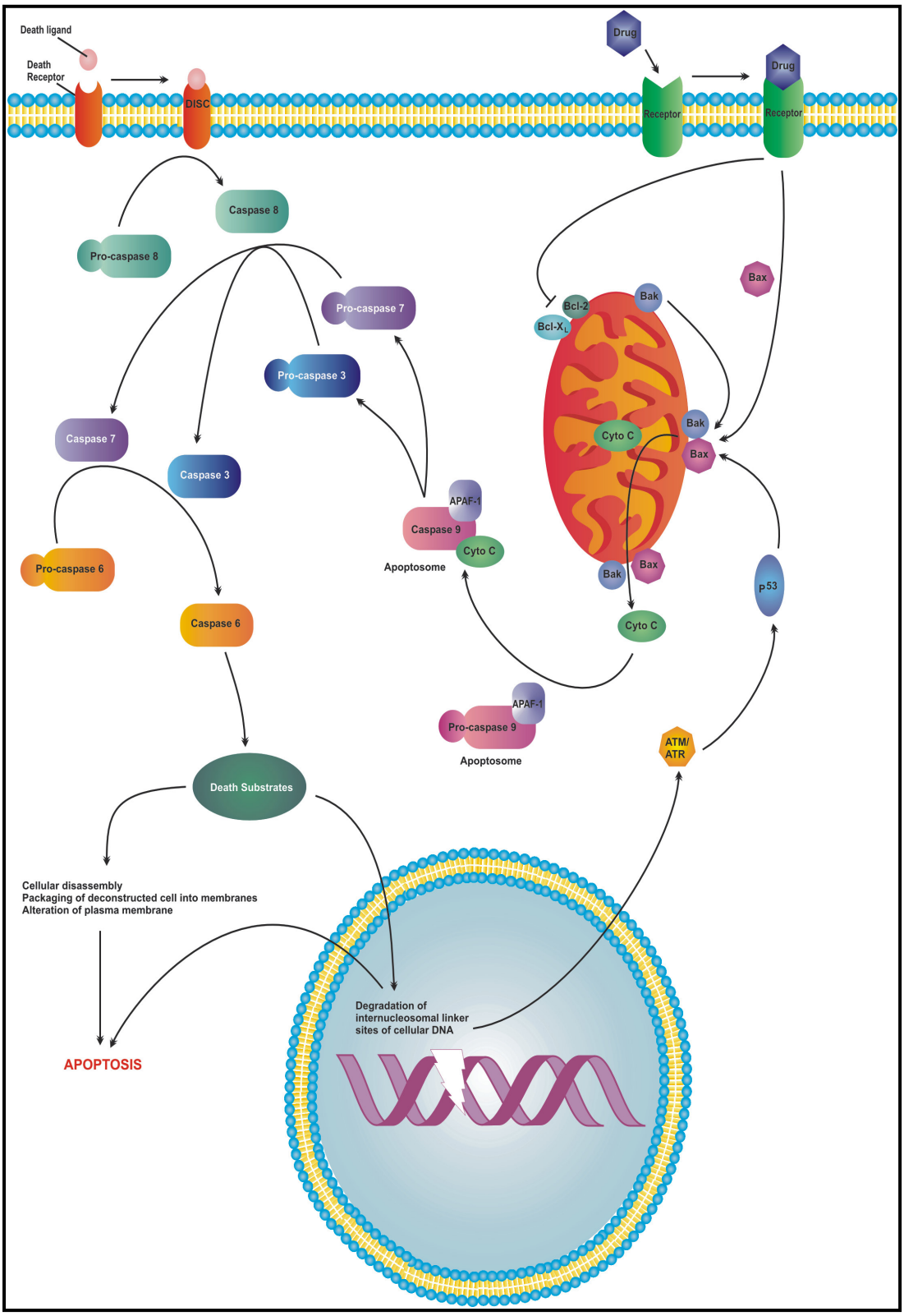

Figure 1.5 A diagrammatic representation of the two apoptotic pathways

1.7 THE CYTOTOXIC DRUG ETOPOSIDE

Doxorubicin and etoposide are both topoisomerase II inhibitors, and are both active chemotherapeutic agents used in clinical oncology, particularly in breast cancer and leukaemia, respectively. The exact mechanism of etoposide's antineoplastic effect is unknown, however there are two theories. The first is that it acts at the premitotic stage of cell division to inhibit DNA-synthesis. This is cell cycle-dependent and phase-specific as it has maximum effect on the S and G_2 stages of cell division. The second theory is that the topoisomerase II inhibition results in DNA damage, causing cytochrome c to be released from the mitochondria. This is followed by the activation of caspase 9 and the effector caspases that were previously described (Fig. 1.5) (Yang *et al*, 2001; USP DI(R) Drug Information for the Health Care Professional, 2003).

Treatment of patients with etoposide has been shown to cause acute leukaemia (onset 2 to 3 years), therefore the risk-benefit must be carefully considered by the health care professional. Etoposide is generally used in life-threatening situations or in serious diseases for which other medications cannot be used or are ineffective (USP DI(R) Drug Information for the Health Care Professional, 2003).

1.8 THE HL-60 PROMYELOCYTIC LEUKAEMIA CELL LINE

The HL-60 cell line was derived from a 36-year-old Caucasian female with acute promyelocytic leukaemia (APL). This cell line has proved to be valuable in several areas of research as the cells proliferate continuously in suspension culture with a doubling time of ~36 to 48 hours. The cells can also be induced to differentiate into four different cell types; granulocytes, monocytes, macrophage-like cells and eosinophils, using various agents (Collins, 1987).

HL-60 cells have proven to be invaluable in the study of oncogenic structure and expression in normal and leukaemic cell proliferation and differentiation. The cell line exhibits several specific genomic mutations involving the cellular oncogenes c-*myc*, N-*ras* and p53. This reinforces the concept that the development of cancer is from a series of genomic mutations (Collins, 1987).

1.9 OBJECTIVES OF THIS STUDY

Drug resistance is proving to be a serious limiting factor in the treatment of many leukaemias. O'Gorman and co-workers (2000) recently demonstrated that an increase in apoptosis resulted in response to

cytotoxic drugs after the inhibition of the PI3-kinase pathway. They studied the regulation of BAD in relation to the PI3-kinase/Akt pathway and found no changes. Thus they postulated that alternate targets of Akt may be responsible for drug resistance in AML (O'Gorman *et al*, 2000). This project aims to determine whether inhibition of the PI3-kinase pathway results in increased apoptosis in HL-60 cells, and to determine the role of IKK in the prevention of apoptosis.

The specific aims of the project are:

1. To monitor cell growth/survival when HL-60 cells were treated with PDGF and etoposide in conjunction with LY294002.
2. To determine qualitatively (confocal microscopy and DNA fragmentation) and quantitatively (flow cytometry) whether HL-60 cells undergo apoptosis when treated with the cytotoxic drug etoposide and/or LY294002.
3. To investigate the expression of Total Akt, activated Akt (phosphorylated) and its mRNA, phospho-IKK and phospho-IκB in HL-60 cells after exposure to:
   (i) growth factors (PDGF)
   (ii) inducers of apoptosis (etoposide)
   in the presence and absence of PI3-kinase inhibitor LY294002.

These aims will help to demonstrate the roles that Akt and IKK play in the prevention of apoptosis in HL-60 cells.

CHAPTER 2

MATERIALS AND METHODS

2.1 HL-60 CELL CULTURE

The sources of all the chemicals and equipment used are listed in Appendix 1.1 and the preparation of the reagents used for culturing are described in Appendix 2.1.

2.1.1 MAINTENANCE CULTURE CONDITIONS

The Human leukaemic cell line HL-60 was purchased from the American Type Culture Collection (Maryland, USA). The cells were grown in a humidified atmosphere of 5% CO_2: 95% air at 37°C. Tissue culture flasks were used to maintain the cells in sterile-filtered RPMI-1640 medium. The medium contained 22 mM $NaHCO_3$, 100 U/L penicillin, 100 µg/L streptomycin and 2.5 mg/L fungizone with 10% heat-inactivated foetal calf serum (FCS). RPMI-1640 medium stored for more than 3 weeks was resupplemented with 2mM glutamine, as it has a half-life of 3 weeks.

2.1.1.1 Passaging and feeding cells

HL-60 cells are a non-adherent cell line and have a doubling time of ~36-48 hours. Every two days the cells were allowed to settle, and approximately half of the used medium was poured off and replaced with fresh medium. Once the cells had reached confluence, they were passaged into fresh culture flasks at a split ratio of 1:5. The cultures were regularly examined using light microscopy (200x) for morphological signs of cellular damage or deterioration.

2.1.1.2 Cell counting and viability determination

The cells were counted and the viability determined using the trypan blue exclusion test. Cells (100µl) were removed from the culture flask and added to an equal volume of trypan blue dye. The cell suspension (100 µl) was placed in a haemocytometer and examined at 200x magnification. All of the unstained cells in the central square of the grid were counted. The volume of the grid is 10^{-4} ml therefore the number of cells per ml could be determined.

$$\text{No. cells/ml} = \text{No. cells in central grid} \times 10^{4} \times \text{dilution factor}$$

The viability of the cells was determined by counting the number of blue-stained dead cells in the central grid. The percentage of unstained viable cells to blue-stained dead cells could then be calculated.

2.1.1.3 Cell cryopreservation and recovery

At regular intervals cells were removed from the cultures and stored frozen at -70°C. The cells were allowed to grow to the late log phase when they were at high confluence. A volume containing approximately 10 x 10^6 cells was removed from the flasks and the cells pelleted by centrifuging at 500 rpm for 5 minutes at 20°C. The medium was discarded and the cells resuspended in 1 ml FCS. An equal volume of freezing mixture consisting of 40% sterile glycerol and 60% culture medium was added. The cell suspension was then transferred into sterile cryotubes and frozen slowly, wrapped in cotton wool at -20°C overnight and then stored at -70°C until required.

The cells were recovered from frozen storage by rapidly thawing in a water bath at 37°C. Ten volumes of warm culture medium were added drop-wise to the cell solution reducing osmotic shock. Centrifugation (500 rpm for 5 min at 20°C) was used to remove the freezing solution, and the cells were resuspended in 10 ml of fresh culture medium. The cells were

placed in a small sterile tissue culture flask and maintained as previously described.

2.1.2 CULTURE CONDITIONS OF EXPERIMENTS

For use in experiments, the HL-60 cells were counted (Chapter 2.1.1.2) and the appropriate number of cells for the experiment (refer to specific experiments) were placed in sterile Nunc tubes. The medium was removed by centrifuging at 500 rpm for 5 min (20°C). The cells were resuspended in RPMI-1640 with 10% FCS without fungizone, as it interferes with etoposide, and placed in sterile petri dishes. The cells were stimulated with various agents (Chapter 2.2) and then placed in sterile Nunc tubes and centrifuged at 2000 rpm for 10 min (4°C). The pellets were washed three times by resuspending in PBS and centrifuging at 4°C for 10 min (2000 rpm). The washed pellets were resuspended in the appropriate buffer for each experiment.

2.2 STIMULATION OF CELLS

The suppliers of all the chemicals are listed in Appendix 1.2, and the preparation of all the reagents is described in Appendix 2.2.

2.2.1 PLATELET DERVIVED GROWTH FACTOR

A stock solution of Platelet Derived Growth Factor (PDGF) (10 ng/µl) was dissolved in 4 mM HCl + 0.1% BSA. Cells (20 x 10^6) were plated into 15 mm sterile petri dishes in a final volume of 2 ml. The cells were incubated with 50 ng/ml PDGF for 15 min and 30 min as these times were found to give optimal phosphorylation of Akt. Two controls were prepared, the first, the blank had no stimulants added, and in the second the cells were incubated for 30 min with HCl-BSA at the same concentration as the experimental samples. This was done to ensure that the PDGF and not the HCl-BSA were responsible for the results obtained.

2.2.2 APOPTOSIS INDUCING AGENTS

Two different apoptosis inducing agents were used: (i) Cyclohexamide was used primarily as a positive control as literature cites it as causing apoptosis in HL-60 cells and (ii) the chemotherapeutic drug etoposide. Stock solutions of cyclohexamide and etoposide were prepared at 3 mg/ml and 30 mg/ml in DMSO respectively. DMSO at the same concentration as the cytotoxic agents was added to the controls. Cyclohexamide (3 µg/ml) and etoposide (60 µg/ml) were incubated with the cells for 4, 24 and 48 hrs depending on the experiment.

2.2.3 THE PI3-KINASE INHIBITOR - LY294002

LY294002 was dissolved in DMSO and added at 25 μM 1 hour prior to the addition of PDGF and the apoptosis inducers. In the experiments with PDGF, an extra control was set up with both DMSO and HCl-BSA.

2.2.4 NECROSIS POSITIVE CONTROL

It is important to have a necrosis positive control with which to compare the experimental results. The necrosis control was prepared by plating the cells in an identical manner to the samples for the experiment. The cells were then subjected to 6 cycles of freeze/thawing at -70°C for 5 minutes each.

2.3 GROWTH/CYTOTOXICITY ASSAY

This assay is a rapid method allowing viable cell number to be determined in proliferation, cytotoxicity, cell attachment, chemotaxis and apoptosis. Mosmann first described the original form of this assay, the MTT assay, in 1983. The MTT assay has many problems including serum protein precipitation caused by the addition of organic solvent, interference of phenol red, incomplete solubilization of formazan crystals resulting in a

lowered sensitivity and the stability of the coloured product. Many of these problems have been solved by the use of the CellTitre 96® Non-Radioactive Cell Proliferation Assay kit (Promega).

The source of the kit and reagents used are listed in Appendix 1.3. The dilutions used are described in Appendix 2.3.

2.3.1 HARVESTING OF CELLS FOR ASSAY

Cells (4 x 10^6 cells) were removed from the flasks and centrifuged at 500rpm (20°C) for 5 minutes. The medium was removed and the cells resuspended in 2 ml of 10% FCS RPMI.

2.3.2 PREPARATION OF ASSAY PLATES

2.3.2.1 Proliferation Assay

The effects of PDGF (10, 30, 50, 70 and 90 ng/ml) with and without 25 μM LY294002 were evaluated in this assay. Stock solutions (4X) of HCl-BSA, DMSO, LY294002 and PDGF (at each concentration) were prepared in 10% FCS RPMI. Stock solutions (25 μl) of HCl-BSA (in triplicate), DMSO (in triplicate) and PDGF (two sets in triplicate) were added to the wells of a

sterile 96 well plate (Fig. 2.1). To each well, 25 µl 10% FCS RPMI was added except one set of PDGF in triplicate, to which 25 µl stock LY294002 was added. Two blanks (in triplicate) containing 50 µl 10% FCS RPMI were prepared. Thus the final volume in each well was 50 µl.

PDGF PDGF + 25 µM LY294002

10 ng/ml	30 ng/ml	50 ng/ml	70 ng/ml	90 ng/ml	10 ng/ml	30 ng/ml	50 ng/ml	70 ng/ml	90 ng/ml
10 ng/ml	30 ng/ml	50 ng/ml	70 ng/ml	90 ng/ml	10 ng/ml	30 ng/ml	50 ng/ml	70 ng/ml	90 ng/ml
10 ng/ml	30 ng/ml	50 ng/ml	70 ng/ml	90 ng/ml	10 ng/ml	30 ng/ml	50 ng/ml	70 ng/ml	90 ng/ml
Blank	10 % FCS	25 µM LY	HCl-BSA	DMSO					
Blank	10 % FCS	25 µM LY	HCl-BSA	DMSO					
Blank	10 % FCS	25 µM LY	HCl-BSA	DMSO					

Figure 2.1 Schematic representation of the 96 well plate prepared for the proliferation assay

The cell suspension (50 µl (100 000 cells) prepared as described above (2.8.1), was added to each well, except one blank (in triplicate), where 50 µl of medium was added. The plate was incubated at 37°C in the incubator for 48 hours.

2.3.2.2 Cytotoxicity Assay

The percentage of cell survival was determined in this assay by the incubation of cells with five different concentrations of etoposide (20, 40, 60, 80 and 100 µg/ml) with and without 25 µM LY294002.

A 4X stock solution of DMSO, each concentration of etoposide and LY294002 was prepared in 10% FCS RPMI. Stock solutions (25 µl) of DMSO (in triplicate), and etoposide (two sets in triplicate) were added to the wells of a sterile 96 well plate (Fig 2.2). To each of the above wells 25 µl of 10% FCS RPMI was added, except the second set of etoposide concentrations, to which 25 µl LY294002 stock was added. Two blanks (in triplicate) were prepared by adding 50 µl 10% FCS RPMI to the wells. The final volume of each well was 50 µl.

The cell suspension (50 µl (100 000 cells) prepared as previously described (Chapter 2.2.1), was added to each well, except one blank (in

triplicate), where 50 µl of medium was added. The plate was incubated at 37°C in the incubator for 48 hours.

Etoposide ⟷ Etoposide + 25 µM LY294002

20 µg/ml	40 µg/ml	60 µg/ml	80 µg/ml	100 µg/ml	20 µg/ml	40 µg/ml	60 µg/ml	80 µg/ml	100 µg/ml
20 µg/ml	40 µg/ml	60 µg/ml	80 µg/ml	100 µg/ml	20 µg/ml	40 µg/ml	60 µg/ml	80 µg/ml	100 µg/ml
20 µg/ml	40 µg/ml	60 µg/ml	80 µg/ml	100 µg/ml	20 µg/ml	40 µg/ml	60 µg/ml	80 µg/ml	100 µg/ml
Blank	10 % FCS	25 µM LY	DMSO						
Blank	10 % FCS	25 µM LY	DMSO						
Blank	10 % FCS	25 µM LY	DMSO						

Figure 2.2 Schematic representation of the 96 well plate prepared for the cytotoxicity assay

2.3.3 COLOUR DEVELOPMENT

Dye solution (15µl) was added to each well and the plates were incubated for 4 hours at 37°C at 5% CO_2, to allow the formation of the formazan crystals. After 4 hours, 100µl of the Solubilizing/Stop solution was added. It was no longer necessary to keep the plate sterile and it could be incubated at room temperature for 1 hour, but better solubilization occurred at 37°C. After 1 hour, the contents of the wells were gently mixed using a multichannel pipette and care was taken to prevent the formation of bubbles. The plate was placed in the 96 well plate reader and the plate was gently shaken for 30 seconds to ensure a uniformly coloured solution. The absorbance was read at 570nm, as the maximum absorbance for formazan is 570nm. A reference wavelength of 630nm was used to reduce background contributed by cell debris, fingerprints and other nonspecific absorbance.

The plate was allowed to stand overnight in a humidified chamber at room temperature to completely solubilize the formazan crystals. The absorbance readings were then taken again and compared with the first readings.

2.4 PROTEIN EXTRACTION PROTOCOLS

The suppliers for the chemicals used are listed in Appendix 1.4 and the preparation of the buffers is described in Appendix 2.4.

The extraction of protein from cells is a very important first step in analysis, and therefore the choice of extraction buffer and method is important. This is to ensure that the target proteins are immunoreactive and undegraded. A small-scale pilot study was conducted using five lysis buffers (Table 2.1) with two extraction techniques to determine which buffer and method gave optimal protein concentration and the least protein degradation.

Two Protocols were used for protein extraction.

2.4.1 PROTOCOL 1

This protocol was used for lysis buffers: A, B, D, and E. The cells were counted (Chapter 2.1.1.2) and 20 x 10^6 cells were seeded in 60 mm petri dishes. After stimulation (Chapter 2.2) the cells were washed as previously described in 2.1.2. Lysis buffer (100 µl) was added to the cells and placed in an Eppendorff tube. The cells were lysed with an initial 15 minutes of freezing at -70°C. This was followed with 3 cycles of freeze

thawing of 5 min each. The lysates were centrifuged in a bench top centrifuge at 14 000 rpm (4°C) for 3 min, the pellet was discarded, to obtain a supernatant with dissolved proteins. An equal volume of loading buffer was added to each sample and then boiled at 100°C for 3 min. The samples were stored at -70°C until required for electrophoresis.

2.4.2 PROTOCOL 2

This protocol was used for lysis buffer C. The cells were counted (Chapter 2.1.1.2) and 20 x 10^6 cells were seeded in 60 mm petri dishes. After the cells were stimulated (Chapter 2.2) they were washed as previously described in Chapter 2.1.2. The cells were resuspended in 100 µl lysis buffer C and the DNA was sheared by sonicating the sample, while on ice, for 13 seconds at high frequency. The extracts were boiled for 5 min, and then centrifuged in an Eppendorff microcentrifuge at 4°C for 5 min. The pellet was discarded, obtaining a supernatant with dissolved proteins. The samples were stored at -70°C until required for electrophoresis.

Table 2.1 Composition of lysis buffer used in protein extraction from HL-60 cell culture

BUFFERS	**COMPOSITION**
Buffer A	20 mM Tris-HCl (pH 7.5), 0.25 M Sucrose, 1% Triton X-100
Buffer B	20 mM Tris-HCl (pH 7.5), 0.25 M Sucrose, 1% Triton X-100, 1 mM PMSF
Buffer C (SDS-lysis buffer)	62 mM Tris-HCl (pH 6.8), 2% SDS, 10% glycerol, 0.5% β-mercaptoethanol
Buffer D	20 mM Tris-HCl (pH 7.5), 100 mM NaCl, 1% Triton X-100, 0.1% SDS, 1 mM Na_3VO_3, 1 mM PMSF, 50 mM NaF
Buffer E (Akt lysis buffer)	20 mM Tris-HCl (pH 7.2), 150 mM NaCl, 10% glycerol, 1% Triton X-100, 10 mM NaF, 30 mM Sodium pyrophosphate, 1 mM EDTA, 1 mM Na_3VO_3, 1 mM PMSF

2.5 TOTAL PROTEIN DETERMINATION

The Lowry-Folin technique was used to determine the concentration of the protein samples. The sources of the chemicals used are listed in Appendix 1.5, and the preparation of all the reagents are described in Appendix 2.5. All standards and samples were performed in duplicate. A standard curve was prepared with bovine serum albumin (BSA). Protein concentrations of 0, 25, 50, 75, 100 and 150 µg were prepared in 1 ml of distilled water. SDS interferes with the reaction, therefore for the proteins extracted with lysis buffer C, 10 µl of the lysis buffer was added to each of the standards of the standard curve. Each sample (10 µl) was added to 990 µl of distilled water. Working Reagent A was freshly prepared by adding the following components in strict order with constant stirring: 1 ml 2% w/v sodium potassium tartrate, 1 ml 1% w/v copper sulphate and 100 ml 2% sodium carbonate in 0.1 M NaOH. Working reagent A (5 ml) was added to each tube then vortexed and allowed at stand for 15 min at room temperature. A 1:1 dilution of Folin & Ciocalteau Reagent was freshly prepared with distilled water, and 0.5 ml was added to each tube. The samples were vortexed and placed in the dark for 30 min allowing a characteristic blue colour to develop.

The absorbance was read at 750 nm on the Beckman DU-65 spectrophotometer using the Lowry-Folin program. A standard curve was constructed by plotting the protein concentration of each standard against

the absorbance reading. Total protein concentration of each sample was determined by plotting the absorbance reading of the sample against the standard curve.

2.6 SDS-PAGE ELECTROPHORESIS

The suppliers of the chemicals used for SDS-PAGE are listed in Appendix 1.6, and the preparation of reagents, stacking and resolving gels, molecular weight markers, buffers and stains are described in Appendix 2.6.

A mini gel system was used for electrophoresis. The dimensions of each gel were 8 cm x 10 cm with a thickness of 1.5 mm. All components of the apparatus were thoroughly washed, and rinsed with distilled water and then with 70% ethanol to remove any contaminants.

The percentage gel used is dependent on the size of the protein in question. The higher the percentage of the gel, the smaller the pore sizes. For example, a 15% gel separates proteins with a M_r in the range of 100 000 to 10 000. Generally a 12.5% resolving gel with a 4% stacking gel was poured.

Identical concentrations (40 μg) of the protein samples were added into the wells of each gel using a microtitre syringe. Protein molecular weight markers (5μl), treated in the same manner as the protein lysates, were also run on the gels.

The electrophoresis unit was attached to a cooling system that was set to 4°C before running the gels. A Hoefer Scientific Instruments power pack was used to run each gel at 10 mA for ±1 hour (or until through the stacking gel). Thereafter the gels were run at 15 mA per gel for ±2 hours.

Once the dye front had reached the bottom of the resolving gel, the power pack was switched off and the gels removed. The gels were stained for protein with Coomassie Brilliant Blue R-250 stain followed by an overnight incubation in destain or western blotted onto nitrocellulose paper for immunodetection.

2.7 WESTERN BLOTTING

The source of the materials used is described in Appendix 1.7 and the details regarding the preparation of the reagents are given in Appendix 2.7.

The gels were removed from between the plates and gently washed with tap water to remove any excess SDS that might hinder the transfer. Nitrocellulose paper was cut to the same size as the gel, care was taken ensuring that the nitrocellulose was not touched to avoid contamination. Both the gel and the paper were equilibrated in the transfer buffer to remove any excess SDS and air bubbles. This also reduces the possibility of band distortion and poor resolution.

The cartridge was assembled, by placing the gel and the nitrocellulose between two sponges and four pieces of filter paper. All air bubbles were removed from the sponges, before the cassette was closed and placed in the Transfer Electrophoresis Unit TE series with the membranes facing the anode (positive electrode) and the gel facing the cathode (negative electrode). The gel was transblotted at a constant current of 200 mA (maximum voltage) for 2 hours at 4°C.

Once completed the blots were either stained with Amido black stain for 1 hour and placed in destain overnight or immunoblotted.

2.8 IMMUNOBLOTTING

The sources of the chemicals are listed in Appendix 1.8, and the preparations of the reagents used for immunoblotting are described in Appendix 2.8. Details of the concentrations of the four antibodies and the blocking buffers used are described in Table 2.2.

After the transfer of protein from the SDS-PAGE to the nitrocellulose, all the membranes were trimmed to prevent a background outline. The membranes were washed in TBS-T for 5 minutes at room temperature to remove the excess transfer buffer. Incubating with freshly prepared respective blocking buffers for 1 hour at room temperature blocked any non-specific binding sites on the membrane. The primary antibodies were diluted in freshly prepared primary antibody dilution buffer. This was placed with the membranes in glass petri dishes and incubated overnight at 4°C with gentle agitation. The blots were washed six times (5 min each) with TBS-T. The secondary antibodies were diluted in freshly prepared secondary antibody dilution buffer and incubated with the membrane for 1 hour at room temperature with gentle agitation. The blots were washed six times (10 min each) in TBS-T.

Table 2.2 The four antibodies used, their concentrations and blocking buffers

1° Antibody	Type	Blocking Buffer	1° Ab Dilution	2° Antibody	2° Ab Dilution
Total Akt	Poly-clonal	BSA	1:75 000	Donkey anti Rabbit	1:100 000
Phospho-Akt	Poly-clonal	BSA	1:25 000	Donkey anti Rabbit	1:100 000
IκB	Mono-clonal	Milk powder	1:50 000	Sheep anti Mouse	1:100 000
IKK	Poly-clonal	BSA	1:25 000	Donkey anti Rabbit	1:100 000

All four proteins; Total Akt, Phospho-Akt, Phospho-IκB and Phospho IKKα/β were detected using the enhanced chemiluminescence technique (Whitehead *et al*, 1979). The Advanced ECL^{TM} kit was used for detection, and the protocol was carried out in the dark room following the provided instructions. After washing the membranes in TBS-T, the excess TBS-T was drained and the membrane was placed on plastic cling film, with the protein side up. Equal volumes (500 µl) of ECL Detection Solution 1 and Solution 2 (final volume required is 125 µl/cm^2 membrane) were mixed and added to the membrane. The membrane was incubated for 1 min at

room temperature, before the excess reagent was drained off and the blot wrapped in a fresh piece of cling film. All air pockets were gently smoothed out, and the membrane placed protein side up in a film cassette. This was exposed to X-ray film for 2, 10 and 30 seconds and 1 min. The film was removed and developed. Depending on the intensity of the bands, the film may be exposed to a fourth piece of film for 2 minutes or longer.

2.9 CONFOCAL MICROSCOPY

Apoptosis can be detected by morphological changes according to the method described by Gibson and colleagues (1999). The assay was used to detect the morphological changes in cells treated with etoposide, cyclohexamide and LY294002. The technique allows the different stages of apoptosis and necrosis to be visualised by the differential uptake of two fluorescent DNA binding dyes. Acridine orange (AO) appears green and can be taken up by viable cells. Ethidium bromide (EB) is an orange dye and can only enter the cell once the cell membrane has been compromised. Healthy cells (H) therefore appear green, early apoptotic cells (EA) also appear green but condensation of the nucleus is very apparent as a solid green mass. Once the cells have entered late apoptosis (LA), the membrane has lost its selective permeability and ethidium bromide can enter. These cells can still appear green, but they

are more commonly an orange colour with the nuclear material appearing as large orange granules. The last stage of apoptosis is the packaging of the cellular contents into the apoptotic bodies. These are orange but are often not visible. Necrotic cells (N) are generally larger than healthy cells, and as the membrane is compromised they appear as large orange bodies (Fig. 4.6)

The suppliers of all equipment and reagents used for confocal microscopy are listed in Appendix 1.9, and the preparation of the acridine orange-ethidium bromide dye is described in Appendix 2.9. Cells (1×10^6) were seeded in 15 mm petri dishes with a final volume of 1 ml, as previously described (Chapter 2.1.1.2). After stimulation (Chapter 2.2) with various combinations of the inducers for 24 hrs, 20 µl of 100 mg/ml acridine orange and 100 mg/ml ethidium bromide in PBS was added to the cells. The cells were viewed at 40X magnification using the fluorescence microscope. Photographs of 3 fields from each sample were taken and analysed.

2.10 FLOW CYTOMETRY

Flow cytometry is a very precise and widely used technique. Cells can be stained with a variety of different stains, before they are passed in single file through a stream of sheath fluid. A focused laser beam is then directed at the cells, and depending on the granularity, nuclear condensation, membrane permeability and stain uptake, the light is scattered in different directions. This allows specific cell populations in the sample to be isolated and quantitated (Glencross, 1994).

This assay was based on the determination of membrane integrity and two stains; propidium iodide and YO-PRO-1 were used. The normal healthy cells do not get stained by either dye, however the YO-PRO-1 dye binds to the exposed phosphatidyl-serine (PS) on the membranes of apoptotic cells. Cells with intact or viable membranes do not allow propidium iodide to enter. Once the cell becomes necrotic or the membrane is compromised, the propidium iodide enters the cell and stains the DNA.

The suppliers of all equipment and reagents used for flow cytometry are listed in Appendix 1.10, and the preparation of the solutions is described in Appendix 2.10. As flow cytometry is a very sensitive technique it requires a relatively small number of cells (100 000). Cells (1.5×10^6) were plated in 15 mm petri dishes. After stimulation, as described in

Chapter 2.2, for 48 hrs the cells were centrifuged at 1 000 rpm for 10 min at 20°C and resuspended in 1 ml of PBS. From this approximately 3 x 10^5 cells (200 µl) was resuspended in 800 µl of ice-cold PBS in flow cytometry tubes. The remaining cells were used to determine DNA fragmentation. The samples were placed on ice and 0.5 µl of 1mM YO-PRO-1 and 1 µl of 1mM propidium iodide were added. The samples were gently vortexed, and incubated on ice for 20 min. Control tubes were prepared with no dye added, and one was prepared with only YO-PRO-1 and another with just propidium iodide. The samples were gently vortexed, to ensure they were in suspension, prior to inserting into the flow cytometer. The percentage of viable, apoptotic and necrotic cells was measured with the use of argon laser excitation at 488 nm.

2.11 DNA FRAGMENTATION

2.11.1 DNA EXTRACTION

Three different extraction protocols with different lysis buffers (Table 2.3) were used to extract DNA. The sources of all the chemicals and equipment used are listed in Appendix 1.11. The composition and preparation of the solutions and buffers are described in Appendix 2.11.

Cells (1 x 10^6) were seeded in 30 mm Nunc petri dishes. After treatment with various agents (Chapter 2.2), the cells were washed with cold PBS as previously described (Chapter 2.1.2).

For Protocol 1, DNA lysis buffer 1 (100 µl) was added to the cells, which were then incubated at 37°C for 30 min. Proteinase K (50 µl of a 10 mg/ml solution) was added to the samples and incubated for a further 30 min at 37°C. An equal volume of gel loading buffer was added to stop the reaction. The samples were stored at -70°C until required.

For Protocol 2, DNA lysis buffer 2 (500 µl) was added to the cells and incubated for 30 min at 37°C. One-tenth volume (50 µl) of 3 M sodium acetate and two volumes of ice cold ethanol (1000 µl) were added. This was incubated at -70°C for 20 min. The samples were centrifuged using an Eppendorff micro-centrifuge for 5 min at 13 000 rpm. The supernatants were discarded and the pellets washed twice in 70% ethanol. The pellets were air dried, then resuspended in 100 µl TE buffer. The samples were stored at -70°C until required.

For Protocol 3, the cells were placed directly in Eppendorff tubes labelled 'B' (bottom). The samples were centrifuged in a micro-centrifuge at 3 000 rpm for 10 min (4°C). The supernatants were transferred to new Eppendorff tubes labelled 'S' (supernatant). TTE buffer (500 µl) was added to the pellets in the tubes labelled B, and this was vigorously

vortexed until the pellet was resuspended. The B tubes were centrifuged at 10 000 rpm for 10 min (4°C). The supernatants were transferred to new Eppendorff tubes labelled 'T' (top), and the pellets in B were gently resuspended in 500 µl TTE buffer. Tubes S, B and T had 100 µl of ice cold 5 M NaCl added and they were vigorously vortexed for 10 seconds. Ice cold isopropanol (700 µl) was added to each tube and they were vortexed again. Precipitation of the DNA was allowed to occur by incubating the tube at 20°C overnight. The DNA was recovered by centrifuging in a microcentrifuge at 4°C (10 000 rpm) for 10 min. The supernatants were removed and the pellets washed in 500 µl ice cold 70% ethanol. The samples were spun down in a micro-centrifuge for 10 min at 10 000 rpm (4°C). The supernatants were discarded and the excess fluid removed by inverting the tubes on absorbent paper towel for 30 min. The DNA pellets were air dried for 3 hours before they were resuspended in 50 µl TE buffer and incubated at 37°C for 48 hours. Loading buffer (50 µl) was added to each sample, which was then heated in a heating block at 65°C for 10 min. The samples were stored at -70°C until required.

Table 2.3 Composition of lysis buffers used in DNA extraction from HL-60 cells

Lysis Buffer	Composition
Protocol 1	1 M Tris- HCl (pH 7.4), 0.5 M EDTA (pH 7.5), 1 % RNAse- A, 0.25% NP-40
Protocol 2	1 M Tris- HCl (pH 7.4), 0.5 M EDTA (pH 7.5), 1 % RNAse- A, 0.25% NP-40
Protocol 3 (TTE Buffer)	TE buffer (pH 7.4), 0.2 % Triton-X

2.11.2 DETERMINATION OF DNA CONCENTRATION

The DNA was diluted 1:100 in TE buffer. The absorbance was measured using a spectrophotometer at two wavelengths, firstly 260 nm and secondly at 280 nm. Nucleic acids have optimal absorbance at 260 nm, whereas proteins absorb light optimally at 280 nm. The 260/280 ratio was determined. A low ratio indicated that high concentrations of proteins were present in the sample, the higher the ratio the purer the DNA. An absorbance of 1 at wavelength 260 nm indicates a DNA concentration of

50 ng/µl. The calculation for the determination of DNA concentration is as follows:

DNA Concentration = Absorbance X 50 X Dilution factor

2.11.3 VISUALISATION OF DNA FRAGMENTATION

Agarose (1 g) was dissolved in 100 ml 1X TEA buffer by boiling. The solution was allowed to cool until it was approximately 60°C. Ethidium bromide (3 µl) was added and the solution mixed well. Ethidium bromide intercalates with nucleic acids and fluoresces under ultra violet (UV) light. The solution was poured into the casting chamber, the combs inserted. The gel was allowed to set for 20 min.

Once the gel had set the chambers of the running system were filled with 1X TEA buffer. Each sample (10 µl) (protocol 1 and 2) were mixed with approximately 3 µl loading buffer (protocol 3 already mixed with loading buffer) and placed in the wells. The samples were run at 60 V for 1 hour. The gels were viewed using the Syngene gel viewing system.

2.12 THE LACTATE DEHYDROGENASE (LDH) ASSAY

Apoptosis 'packages' the cellular contents into small vesicles, whereas necrosis is characterized by the disruption and loss of membrane integrity. As a consequence, the cellular contents including LDH are released into the medium, allowing the LDH activity to be measured and the degree of necrosis determined. This study, in conjunction with the other apoptosis detection techniques, was used to confirm cell death due to apoptosis and not necrosis. The LDH activity in culture medium was determined at RT by measuring the decrease in NADH absorbance at 340 nm with time.

$$\text{Pyruvate} + \text{NADH} \rightarrow \text{Lactate} + \text{NAD}$$

The suppliers of the reagents and equipment used are listed in Appendix 1.12, and the preparation of the buffers is described in Appendix 2.12. The medium from samples prepared for DNA fragmentation and flow cytometry assays were collected and stored at -70°C until analysis. All reagents for this assay were freshly prepared prior to the assay and placed on ice to prevent any enzymatic degradation. The reaction was performed by placing LDH buffer in a quartz curvette (1 cm) along with 87 mM monosodium pyruvate and 4.5 mM NADH (Final volume = 2.8 ml). Sample (200 µl) was added to the curvette, which was mixed by inverting twice. The LDH activity was measured by monitoring the decrease in

NADH absorbance at 340 nm with time using a Perkin-Elmer spectrophotometer equipped with a chart recorder. The reaction was allowed to take place at RT at a chart speed of 40 mm/min. The LDH activity was calculated from the slopes of the chart recordings and expressed as nmoles NADH converted/min. The negative control had medium not exposed to cells added to the curvette, whereas the positive control had 0.1 μg LDH added to the LDH buffer, pyruvate and NADH.

Activity was calculated from the chart readings and expressed as μmoles NADH converted/min. The absorbance of 1 mmol of NADH is 6.22, therefore the following calculation was used to calculate μmole NADH converted/min:

$$\text{LDH Activity} = \frac{\Delta\text{Absorbance/time}}{\Sigma}$$

Where $\Sigma = 6.22$

2.13 EXTRACTION, QUANTIFICATION AND ANALYSIS OF RNA

Total cellular RNA is susceptible to degradation by Ribonucleases (RNases), therefore all work surfaces were sterilised with 10% bleach and

70% ethanol prior to and after use. All equipment and tips were autoclaved and solutions were made up with Diethyl Pyrocarbonate (DEPC) treated water. The suppliers of all chemicals, and equipment used are listed in Appendix 1.13. Buffers and reagents used for the RNA work were prepared according to the recipes described in Appendix 2.13.

2.13.1 RNA EXTRACTION WITH TRI-REAGENT™

Cells (5 x 10^6) cells were seeded in 30 mm Nunc petri dishes, and stimulated with various agents (Chapter 2.2) according to the experimental conditions. After stimulation, the cells were centrifuged at 1500 rpm for 10 minutes. The medium was discarded and 1 ml of Tri-Reagent™ was added to the pellet. Aspirating several times with a pipette lysed the cells, which were then transferred to an Eppendorff tube. If necessary this cell suspension can be stored at -70°C for up to a month. The samples were centrifuged in an Eppendorff centrifuge at 12 000 rpm for 10 min at 4°C. The supernatants were transferred to a clean Eppendorff and allowed to stand at RT for 10min, before adding 200 µl chloroform. The tubes were vortexed for 15 sec and left to stand at RT for 10 min. The samples were centrifuged at 12 000 rpm at 4°C for 10 min which resulted in the development of 3 layers. The bottom phase was red and contained protein, the thin middle layer was white and consisted of DNA and the top phase, containing the RNA, was colourless (aqueous). The upper layer

was transferred to a new Eppendorff, care was taken not to touch the interphase with the pipette tip. Isopropanol (500 µl) was added to each sample, which was then vortexed and allowed to stand for 10 min at RT. A tiny RNA pellet was obtained after the tubes were centrifuged at 12 000 rpm at 4°C for 10 min. The supernatant was discarded and the pellet was dried by inverting the tube for several minutes on absorbent paper. The RNA pellet was washed by adding 1 ml 75% ethanol, briefly vortexing, and centrifuging at 4°C for 10min at 12 000 rpm. The ethanol was discarded and the pellets were allowed to air-dry until they become translucent. The RNA was resuspended in 20 µl DEPC water by aspiration, and heated to 55°C for 10 min. The extracted RNA was stored until required at -70°C.

2.13.2 TOTAL CELLULAR RNA QUANTIFICATION

The RNA was diluted 1:250 in DEPC water. The absorbance was measured using a spectrophotometer at two wavelengths, firstly 260 nm and secondly at 280 nm. Nucleic acids have optimal absorbance at 260 nm, whereas proteins absorb light optimally at 280 nm. The 260/280 ratio was determined. A low ratio indicated that high concentrations of proteins were present in the sample. Ratios of 1.8 or higher were considered pure enough for further use. An absorbance of 1 at wavelength 260 nm indicates an RNA concentration of 40 ng/µl. RNA concentration is calculated as follows:

$$\text{RNA concentration } (\mu g/ml) = \frac{\text{Absorbance X 40 X Dilution factor}}{0.001}$$

2.13.3 DETERMINATION OF RNA INTEGRITY

RNA is extremely susceptible to degradation from both endogenous and exogenous origins. The integrity of the RNA was therefore evaluated using denaturing agarose gel electrophoresis. Total cellular RNA run on a denaturing agarose gel separated into three distinct bands. Each one represents a major RNA species produced in the cells, namely, the 28S, 18S and 5S ribosomal RNA (rRNA). Degraded RNA appeared as a smear.

Agarose (0.5 g) was dissolved in 50 ml of 1X MOPS (pH 5.5 –7.0) solution by boiling. The solution was allowed to cool until it was approximately 60°C, before formamide (denaturant) and ethidium bromide were added. Ethidium bromide intercalates with nucleic acids and fluoresces under ultra violet (UV) light. The solution was poured into the casting chamber, the combs inserted. The gel was allowed to set for 20 min.

Total cellular RNA (10 μg) was added to 15 μl RNA sample buffer. The samples were denatured by heating at 65°C for 10 minutes, before they

were loaded onto the gel. The gels were run in a 1X MOPS buffer containing ethidium bromide at 65 V (constant current) for approximately 1 hour at RT. The RNA was visualised using the Syngene gel viewing system

2.14 REVERSE TRANSCRIPTION-POLYMERASE CHAIN REACTION ANALYSIS

Reverse transcription-polymerase chain reaction (RT-PCR) technique allows the semi-quantitative analysis of gene expression (transcription of specific mRNA species) within the cell. The total cellular RNA is transcribed into cDNA using reverse transcription. This is followed by the amplification of a specific cDNA region to detectable levels using polymerase chain reaction (PCR).

The suppliers for the kits, primers and other chemicals used are listed in Appendix 1.14. The exact details for the preparation of the buffers and reagents for the RT- and multiplex- PCR are described in Appendix 2.14.

2.14.1 REVERSE TRANSCRIPTION

Reverse transcription was performed using the Promega cDNA synthesis kit. A master mix was prepared containing 1X Reverse Transcription Buffer, 1 mM of each of the four dNTPs, 5 mM $MgCl_2$, 20 U RNase Inhibitor, 15-20 U AMV Reverse Transcriptase and 0.5 μg Oligo $(dT)_{15}$ Primer, which binds to the poly A tails of the RNA. Master mix (10.1 μl) was added to 1 μg of RNA in an Eppendorff, and was made up to a final volume of 20 μl with nuclease free water. A blank sample was included in each reverse transcription run, and had the total cellular RNA solution replaced with nuclease free water. The reverse transcription was performed in the Hybaid Touchdown Thermocycler as follows; 45 min at 42°C, 5 min at 95°C and finally at 4°C for 5 min. The cDNA was stored at -70°C until PCR analysis was performed.

2.14.2 MULTIPLEX PCR

The sequence of *AKT1* was obtained from the Gene Bank, Accession number NM_005163. The two primer sequences used were obtained from Okano and colleagues (2000) and are designed in less conserved 5' or 3' non-coding regions to avoid any potential cross reactivity among the *AKT* isoforms. The resulting forward and reverse primers (Table 2.4 and Fig. 2.3) resulted in the amplification of a 383 bp *AKT1* product. The

internal standard used for the semi-quantitative analysis of *AKT1* was the housekeeping gene *GAP-DH* which is a 587 bp product.

Table 2.4 The oligonucleotide primer sequences for *AKT1* and *GAP-DH*

mRNA	Product Size	Primer Sequence	
AKT1	383 bp	**Forward**	5' GCTGGACGATAGCTTGGA 3'
		Reverse	3' CATGACAGATAGCTGGTG 5'
GAP-DH	587 bp	**Forward**	5' CCCTTCATTGACCTCAACTACATG 3'
		Reverse	3' GACTTGCCCTTCGAGTGACCGTAC 5'

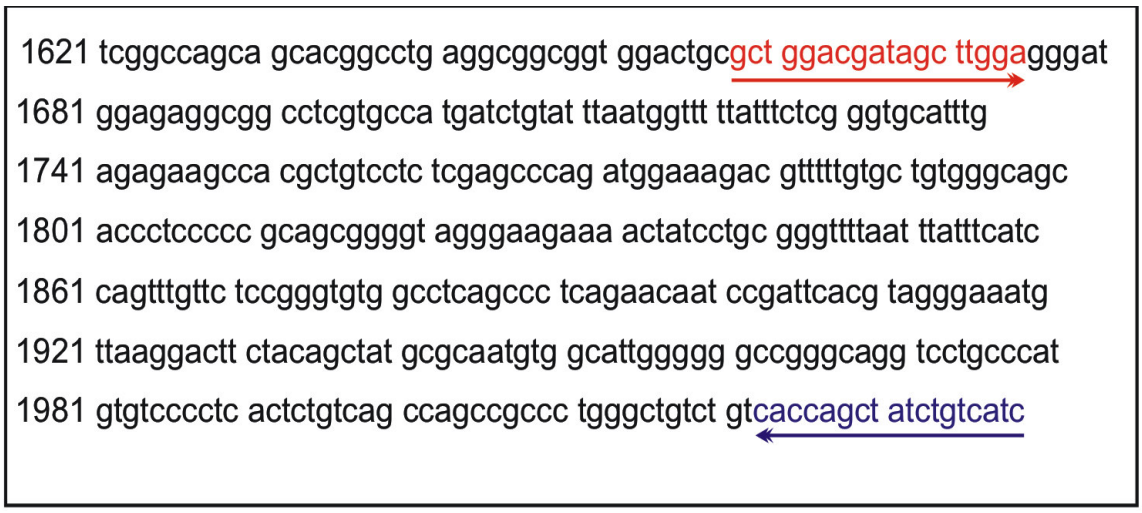

Figure 2.3 The sequence for the Human AKT1 gene and primer annealing positions. The red text and arrow indicates the forward primer and the blue arrow and text indicates the reverse primer.

The PCR was performed using the Roche PCR Core Kit™. Prior to performing the PCR, the cDNA was diluted with 80 µl of nuclease free water. The cDNA (10 µl) was added to a pre-prepared master mix (14 µl) containing 0.4 µM and 0.05 µM of each of the *AKT1* and *GAP-DH* primers respectively, 1X PCR Reaction Buffer with 1.5 mM $MgCl_2$, 0.2 mM dNTPs and 2.5 U *Taq* polymerase, made up to a final volume of 50 µl with nuclease free water. The PCR reaction mixture was overlaid with mineral oil to prevent evaporation. Three controls were also prepared. The first had the cDNA replaced with nuclease-free water to ensure that no contamination was present in the PCR master mix. The second and third had only one set of primers added to each. This was done to ensure that the amplification of the two products did not interfere with each other.

The PCR was performed using a Hybaid Touchdown Thermocycler. The cDNA was denatured at 94°C for 1 min, and then the primers were annealed at 55°C for 1 min. Extension occurred at 72°C for 1 min. This was repeated for 30 cycles, and then held at 4°C until the samples were retrieved. The PCR products were stored at 4°C until subjected to electrophoresis.

Agarose (2 g) was dissolved in 100 ml 1X TEA buffer by boiling. The solution was allowed to cool until it was approximately 60°C. Ethidium bromide (3 µl) was added to the solution and mixed well. The solution

was poured into the casting chamber and the combs inserted. The gel was allowed to set for 20 min.

The chambers of the running system were filled with 1X TEA buffer. Each sample (10 µl) were mixed with approximately 3 µl bromophenol blue loading buffer and placed in the wells. The chamber was closed and the samples run at 65 V for 1 hour. The PCR product was viewed using the Syngene gel viewing system. The size of the product was determined by comparing its size relative to that of the 100 bp DNA Molecular Weight Marker.

2.15 ENDONUCLEASE RESTRICTION ANALYSIS OF *AKT1* PCR PRODUCT

The suppliers of the restriction enzymes and their buffers are listed in Appendix 1.15.

To confirm that the amplified product was the correct sequence, a PCR control sample that was amplified with just the *AKT1* primers was subjected to restriction analysis. Three different restriction enzymes were used, XhoI, AvaI and HaeIII. The cleavage sites for these enzymes were obtained from Restriction Mapper (www.restrictionmapper.org), and the cleavage positions are shown in Table 2.5 and Figure 2.4.

Each enzyme is supplied with its own 10X reaction buffer (Buffer M, H and B for XhoI, AvaI and HaeIII respectively). The preparation of the restriction enzyme master mixes are described in Appendix 2.15. PCR product (6µl) was added to 14 µl of the master mix in an Eppendorff tube, making a final volume of 20 µl. The samples were incubated at 37°C for 24 hrs and the resulting products were run on a 2% agarose gel as previously described.

Table 2.5 The list of recognition sites and resultant fragments obtained for the three restriction enzymes used

Restriction Enzyme	Recognition Site	Cleavage Sites	Resulting Fragment Sizes
AvaI	CYCGRG	1717, 1750	33, 70, 279
HaeIII	GGCC	1680, 1871, 1951	33, 78, 80, 191
XhoI	CTCGAG	1750	103, 279

Figure 2.3 The sequence for the Human AKT1 gene and the cleavage sites of the restriction enzymes. The blue arrow heads indicate the cleavage sites for Ava I, the green arrow heads indicate the cleavage sites for Hae III and the red arrow head indicates the cleavage site for Xho I.

CHAPTER 3

RESULTS

3.1 GROWTH/CYTOXICITY ASSAY

3.1.1 GROWTH ASSAY

Cells (50 000) were treated with 25 μM LY294002 for 1 hour prior to the addition of the different concentrations of PDGF (in triplicate). Figure 3.1 is the graphical representation of the mean % growth for the four experiments, and shows a decrease in the mean % growth when 25 μM LY294002 was added.

The results obtained had large standard deviations hence were considered to be non-reproducible. A preliminary study using the Trypan Blue exclusion test (results not shown) demonstrated a 10% increase in cell growth when the HL-60 cells were treated with the recommended (Sigma) PDGF concentration of 50 ng/ml. Hence, the recommended PDGF concentration (50 ng/ml) was used in the remainder of the experiments, as was the recommended concentration of LY294002 (25 μM).

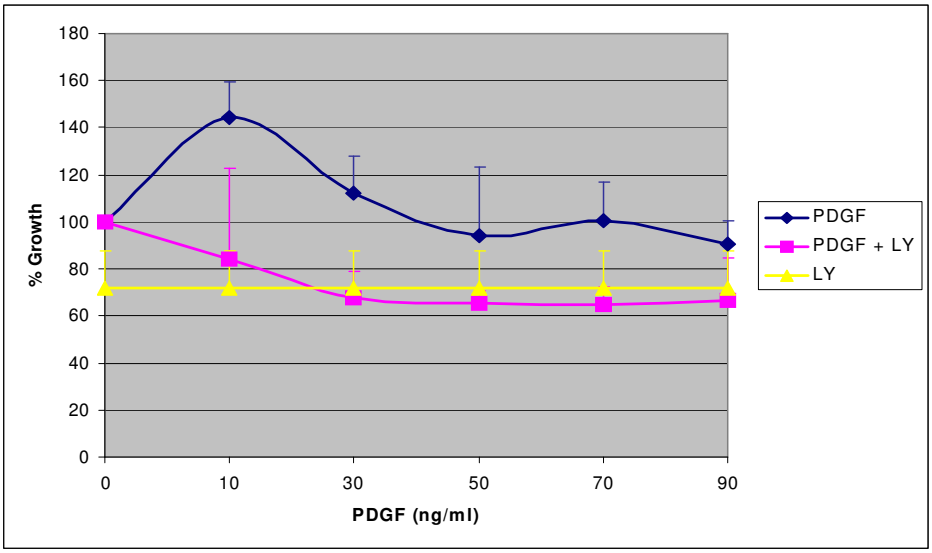

Figure 3.1 A graphical representation of the mean and standard deviation of the % growth for four experiments (in triplicate) of 50 000 HL-60 cells treated with various concentrations of PDGF and 25 µM LY294002 for 48 hours

3.1.2 CYTOTOXICITY ASSAY

Cells (50 000) were treated with 25 µM LY294002 for 1 hour prior to the addition of the different concentrations of etoposide for 48 hours (in triplicate). Figure 3.2 is a graphical representation of the mean % survival of the three experiments, and indicates that the addition of 25 µM LY294002 results in a slight increase in cell death. The experiment had low standard deviations and is therefore more reproducible.

A large amount of cell death occurred between 0 µg/ml and 20 µg/ml etoposide (Fig. 3.2), therefore three experiments (in triplicate) were conducted with a range of etoposide between 0 µg/ml and 10 µg/ml. Figure 3.3 indicates that the HL-60 cells continue to grow in concentrations of etoposide less than 0.1 µg/ml, but a large percentage of cells die when the concentration of etoposide is increased to 1 µg/ml.

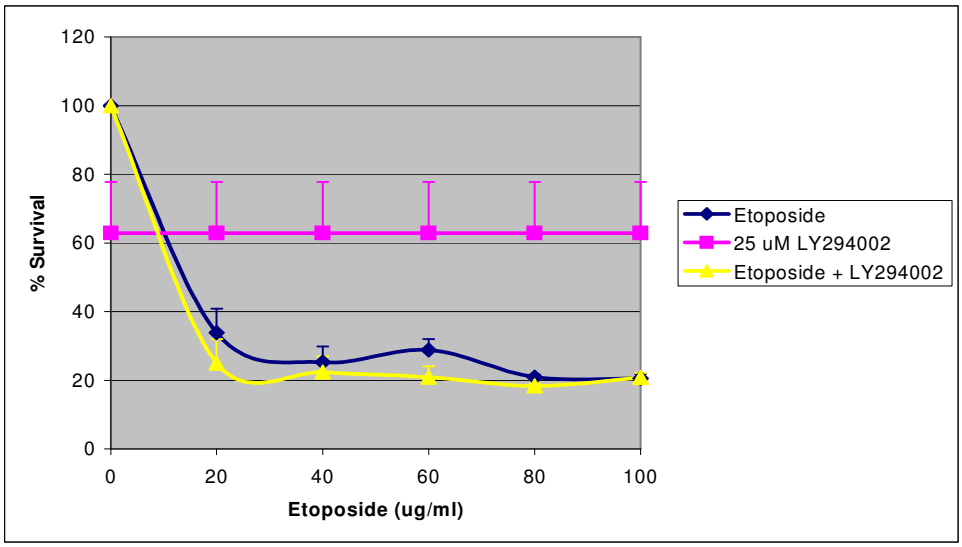

Figure 3.2 A graphical representation of the mean and standard deviation of the % survival for three experiments (in triplicate) of 50 000 HL-60 cells treated with various concentrations of etoposide and 25 µM LY294002 for 48 hours

The recommended concentration (Sigma) of etoposide was 60 µg/ml, and was shown to cause cell death with this technique. Etoposide was therefore used at a concentration of 60µg/ml for all further experimental procedures.

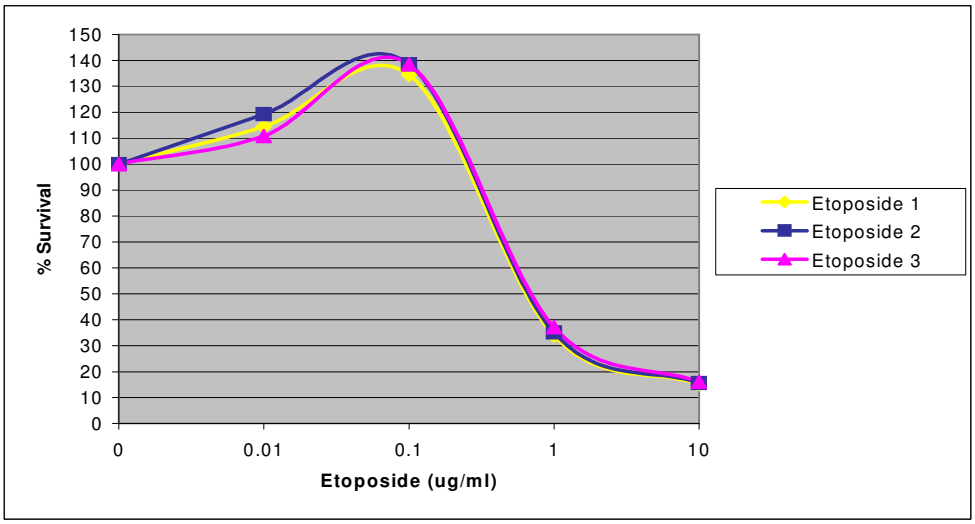

Figure 3.3 A graphical representation of the % survival three experiments (in triplicate) of 50 000 HL-60 cells treated with a concentration range of etoposide for 48 hours

3.2 IMMUNOBLOTTING

The first step in the immunoblotting assay was to determine which protein extraction buffer to use. Protein was extracted from 20 x 10^6 HL-60 cells using the five extraction buffers described in Chapter 2.4 (results not shown). The SDS-lysing buffer (Buffer C) gave high protein yields (Chapter 2.5) however the samples were very globular and difficult to load on the SDS-PAGE gels. The protein also appeared as smears on the gels when stained with Coomassie Blue stain (Chapter 2.6). Buffers A and B

gave very low protein yields and were therefore not used. Protein extracted with Buffer D gave high protein yields, however when immunoblotted no Phospho-Akt was present. This was probably due to phosphatase activity in the lysate, as no phosphatase inhibitors were present in the lysing buffer. The Akt lysing buffer (Buffer E), containing phosphatase inhibitors, also had a high protein yield, and when the samples were immunoblotted the Phospho-Akt was present. It was therefore decided to use the Akt lysing buffer to extract protein for the experimental procedures.

A time trial was conducted (in triplicate) by adding 50 ng/ml PDGF to the HL-60 cells for 5, 10, 15, 30, 45 and 60 minutes. The resultant blots indicated that optimal phosphorylation of Akt occurs at 15 and 30 minutes (results not shown). Therefore, for the remaining experiments these time frames were used.

Protein was extracted from HL-60 cells (20×10^6) stimulated with 25 μM LY294002 for 1 hour, prior to the addition of 50 ng/ml PDGF for 15 and 30 minutes. The protein (40 μg) was then run on a SDS-PAGE, western blotted and immunoblotted with Akt, Phospho-Akt, Phospho-IκB and Phospho-IKK antibodies. The experiment was repeated several times and a representative of the resulting blots are shown in Figure 3.4. In all experiments performed the blot of total Akt was used as a loading control.

Figure 3.4 A representation of the four immunoblots obtained from 40 μg protein extracted from HL-60 cells (20 x 10^6) treated with 25 μM LY294002 for 1 hour before 50 ng/ml PDGF was added for 15 and 30 min. 1 = Untreated Cells, Cells treated with: 2 = DMSO, 3 = HCl-BSA, 4 = LY294002, 5 = 15 min PDGF, 6 = 30 min PDGF, 7 = 15 min PDGF + LY294002 and 8 = 30 min PDGF + LY294002.

The changes in the intensity of the bands is difficult to detect with the naked eye, therefore they were scanned using the Genesnap Tools program. The resulting band densities were plotted in Fig. 3.5.

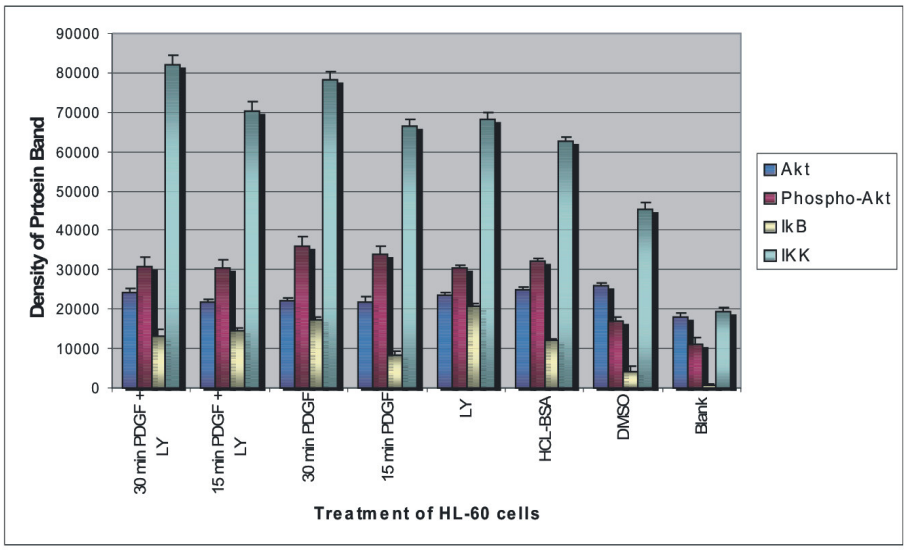

Figure 3.5 The mean protein band intensities from three experiments of Akt, Phospho-Akt, Phospho-IκB and Phospho-IKK.

Figure 3.5 shows that when the cells are stimulated with 50 ng/ml PDGF there is an increase in Akt phosphorylation, however when 25 μM LY294002 is added 1 hour prior to the addition of PDGF there is a decrease in phosphorylation. This decrease is more apparent with the 30 minute period, however the significance is dubious. A high amount of IκB phosphorylation occurs when the cells are treated with LY294002 for 1 hour, as well as when they are stimulated with PDGF for 30 minutes. Stimulation of cells for 15 minutes with PDGF seems to have no marked affect on IκB phosphorylation, however a slight decrease in IκB phosphorylation is shown after the cells have been treated with LY294002 and PDGF for 30 minutes. IKK phosphorylation increases dramatically with all the treatments (Fig. 3.5).

3.3 ACRIDINE ORANGE-ETHIDIUM BROMIDE ASSAY

The acridine orange-ethidium bromide assay is a morphological assay, which allows the different stages of cell death to be identified. The uptake of the two fluorescent dyes by the cells in these different stages is described in Chapter 2.11. Figure 3.6 is a schematic representation and Figure 3.7 is an enlarged photographic representation of the different stages of cell death, and assists in the interpretation of the photographs.

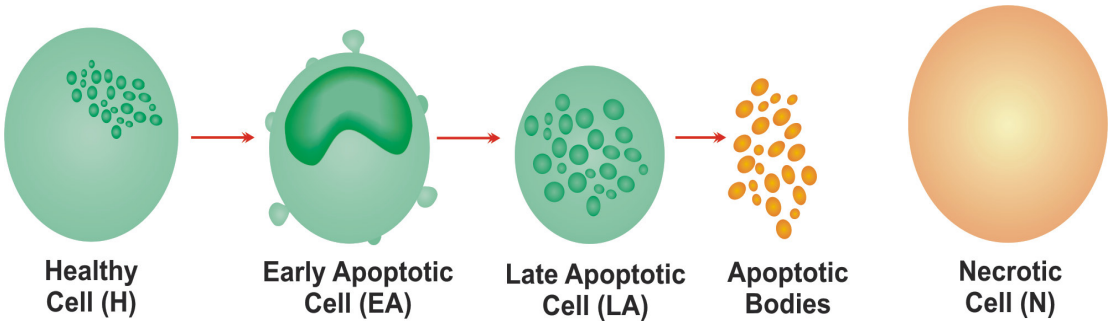

Figure 3.6 A schematic illustration of the different stages of apoptosis and of necrosis, showing the differential uptake of acridine orange and ethidium bromide.

The assay was repeated three times and the images in this section are a representation of the results obtained. For all the experiments 1 x 10^6 HL-60 cells were grown in 15 mm petri dishes for 48 hours before being viewed and photographed at 400X magnification with the confocal microscope.

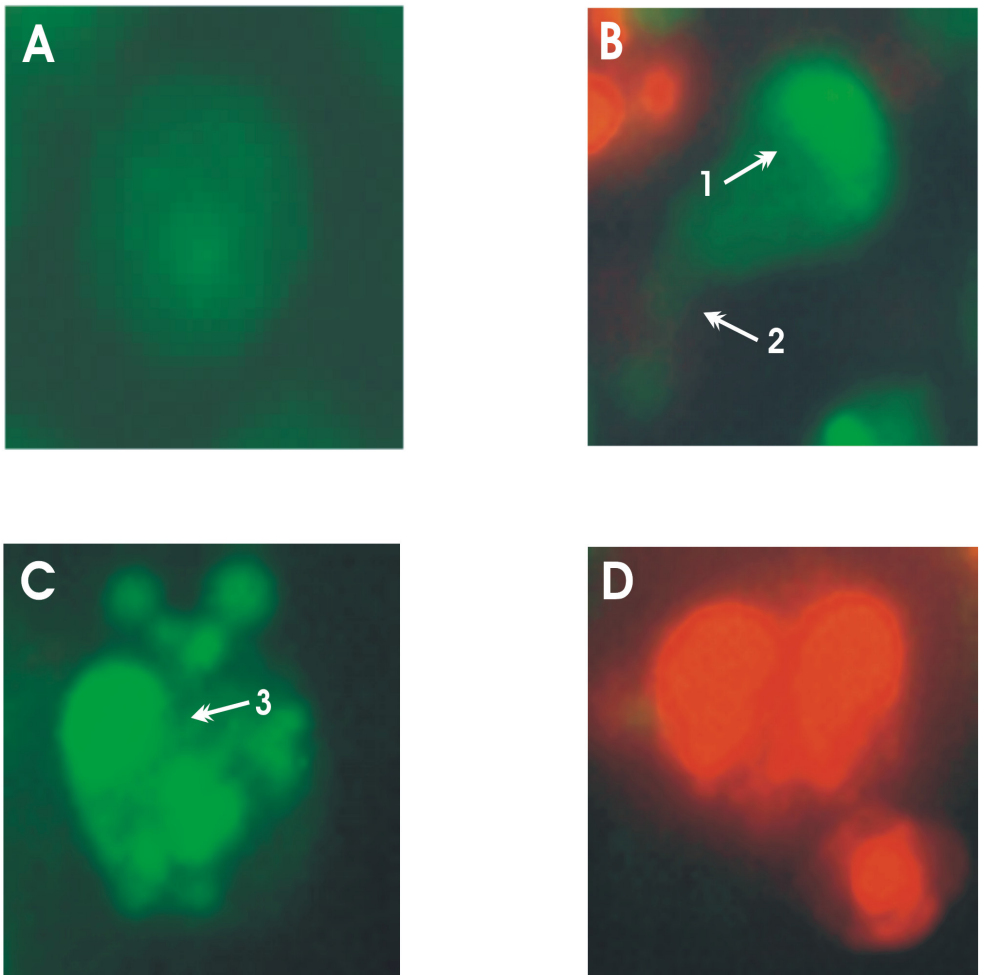

Figure 3.7 An enlarged photographic representation of HL-60 cells in the different stages of apoptosis and necrosis, showing the differential uptake of acridine orange and ethidium bromide. Panel A represents normal cells, B is a cell undergoing early apoptosis with 1 indicating the characteristic 'horse shoe' shape of the condensed nucleus and 2 showing membrane blebbing. Panel C represents a cell undergoing late apoptosis with 3 indicating the very granular cytoplasm. Panel D is a necrotic cell.

A number of control samples were prepared and are described by Figures 3.8-11. Figure 3.8 is HL-60 cells that have been growing under normal conditions; the majority of cells in the field are healthy (H), as they appear green with a non-granular cytoplasm. Normal cell death does occur under these conditions and is represented by the late apoptotic cells (LA). A large orange necrotic cell (N) is also present in this field of view. DMSO is the vehicle used for etoposide, cyclohexamide and LY294002, and it is therefore essential to ensure that the stimulants and not the vehicle are causing cell death. Figure 3.9 is HL-60 cells stimulated with DMSO for 48 hours, and the cells appear very similar to those in Figure 3.8. LY294002 (25 μM) was added to the HL-60 cells in Figure 3.10; the cells appear to be healthy (H), with a small proportion entering early apoptosis (EA) evident by the presence of membrane blebbing and nuclear condensation. The membrane blebbing is not apparent in the photographs, but was present when the cells were viewed under the microscope. The necrosis control (Fig. 3.11) has several large orange necrotic cells (N) present as well as cells undergoing apoptosis (EA), however no normal cells are visible. The experimental samples of the HL-60 cells treated with various combinations of apoptosis inducing agents and the PI3-kinase pathway inhibitor LY294002 are shown in Figures 3.12-17. Etoposide (60 μg/ml) was added to the cells in Figure 3.12 and although a few healthy cells (H) are present, the majority of cells have entered early (EA) and late (LA) apoptosis. The HL-60 cells Figure 3.13 were treated with both 60 μg/ml etoposide and 25 μM LY294002. No normal cells are present as most of

the cells are in early apoptosis (EA) and the remainder have entered late apoptosis (LA). Cyclohexamide (3 μg/ml) has been reported to be an apoptosis control for HL-60 cells, however, Figure 3.14 indicates otherwise as most of the cells are healthy (H), with a few exhibiting nuclear condensation and membrane blebbing (visible under microscope but lost in reproduction) indicative of early (EA) and late (LA) apoptosis. The addition of both 3 μg/ml cyclohexamide and 25 μM LY294002 (Fig. 3.15) also proved to have no extensive effect, as most of the cells are healthy (H) with a small number exhibiting early apoptosis (EA). HL-60 cells treated with both 60 μg/ml etoposide and 3 μg/ml cyclohexamide (Fig. 3.16) exhibit a large proportion of cells in early apoptosis (EA) as the cells have nuclear condensation and characteristic horseshoe shaped nuclei, membrane blebbing (visible under microscope but lost in reproduction) is also evident. The remaining small proportion of cells are in late apoptosis (LA) as the cells appear either green or orange with large orange granules (nuclear material) present in the cytoplasm. In Figure 3.17 the cells have been treated with all three stimulants, 60 μg/ml etoposide, 3 μg/ml cyclohexamide and 25 μM LY294002. The proportion of cells in early (EA) and late (LA) apoptosis appears to be equal, and no healthy cells are present.

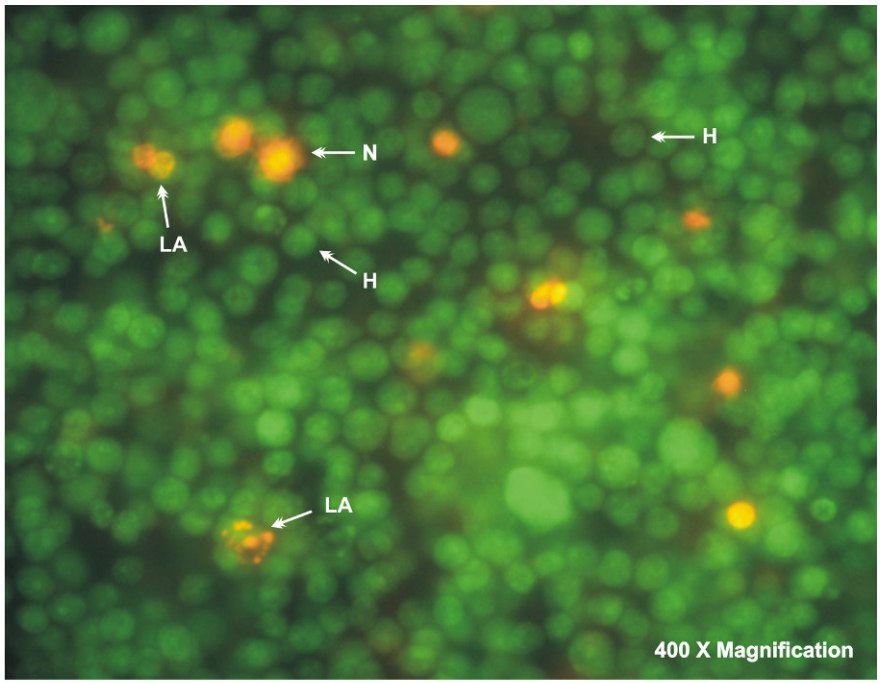

Figure 3.8 HL-60 cells (1 x10^6) grown under normal conditions for 48 hours. H = healthy cells, N = necrotic cells, LA = late apoptosis

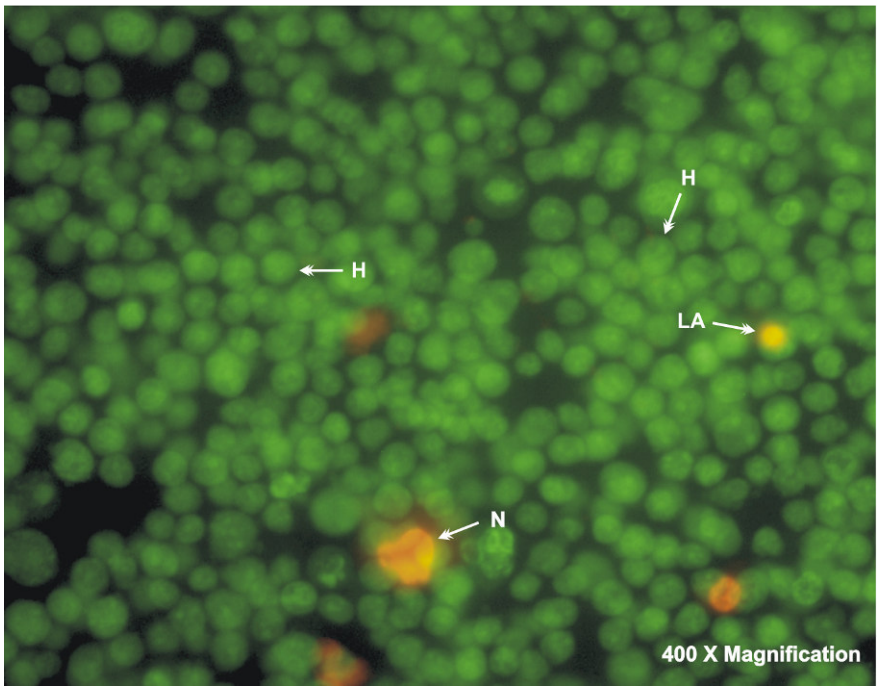

Figure 3.9 HL-60 cells (1 x10^6) stimulated with DMSO, the vehicle for etoposide, cyclohexamide and LY294002 for 48 hours. H= healthy cells, N = necrotic cells, LA = late apoptosis

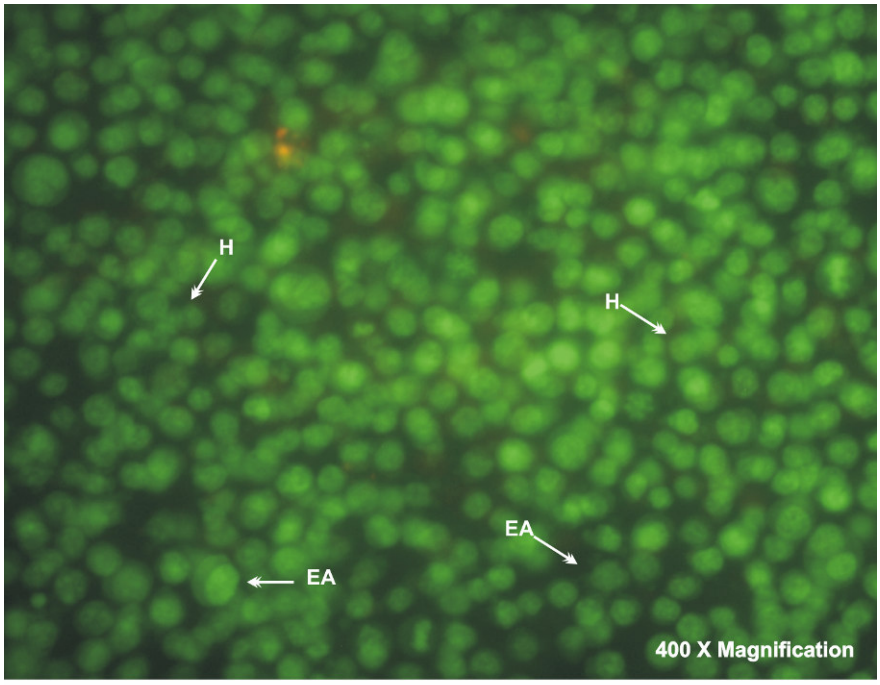

Figure 3.10 HL-60 cells (1 x 10^6) stimulated with the PI3-kinase pathway inhibitor LY294002 (25µM) for 48 hours. H = healthy cells, EA = early apoptosis

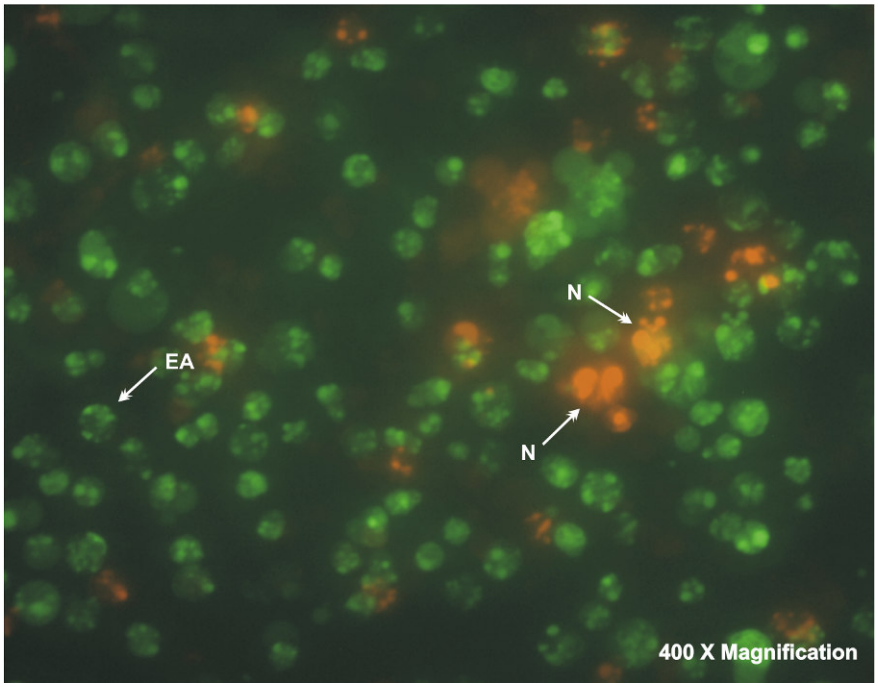

Figure 3.11 HL-60 cells (1 x 10^6) subjected to freeze-thawing to give a necrosis positive control. N = necrotic cells, EA = early apoptosis

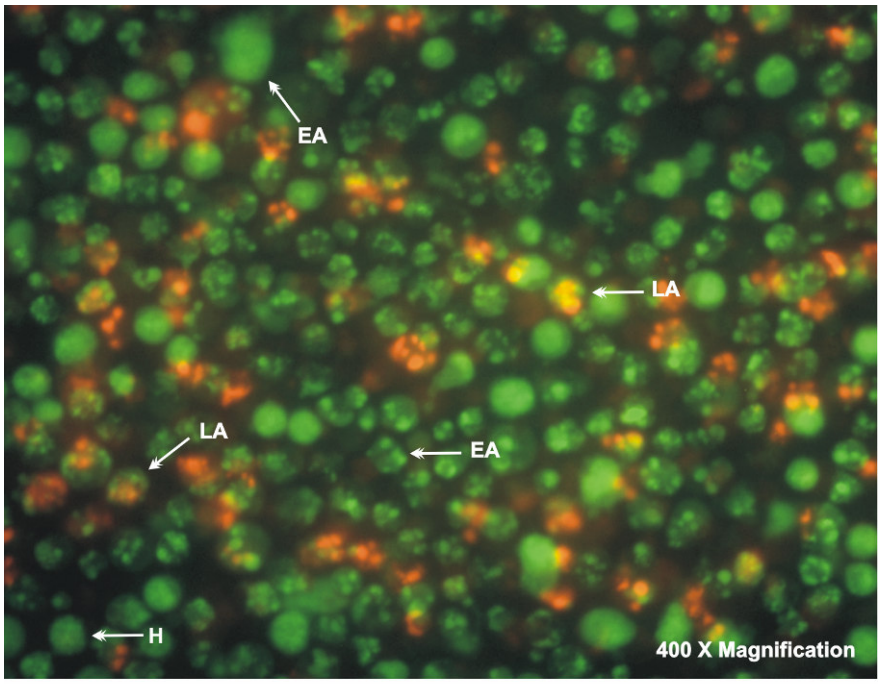

Figure 3.12 HL-60 cells (1 x 10^6) stimulated with 60 μg/ml etoposide for 48 hours. H = healthy cells, EA = early apoptosis, LA = late apoptosis

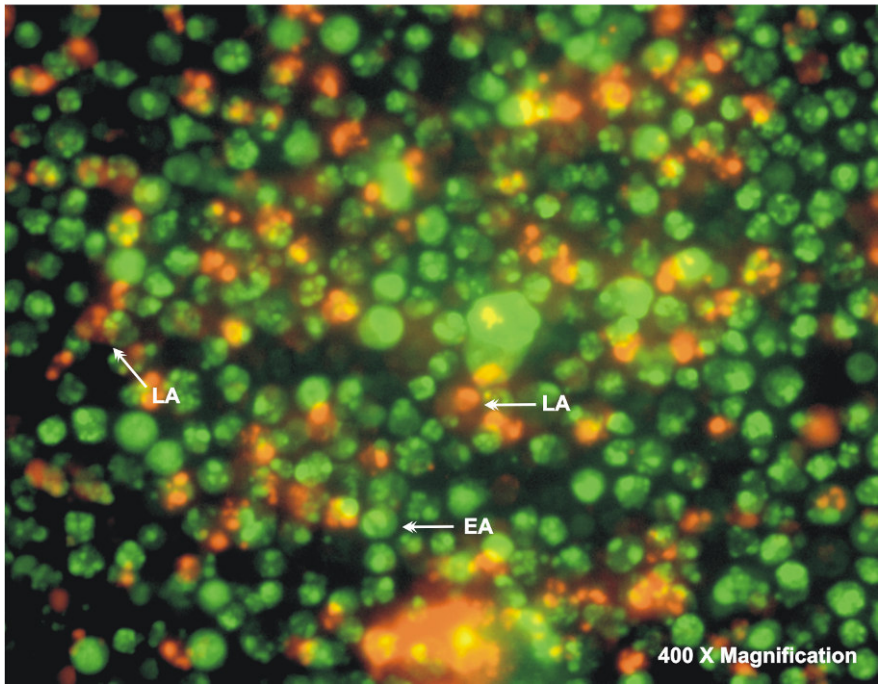

Figure 3.13 HL-60 cells (1 x 10^6) stimulated with 25μM LY294002 for 1 hour before 60 μg/ml etoposide was added, then incubated for a further 48 hours. EA = early apoptosis, LA = late apoptosis

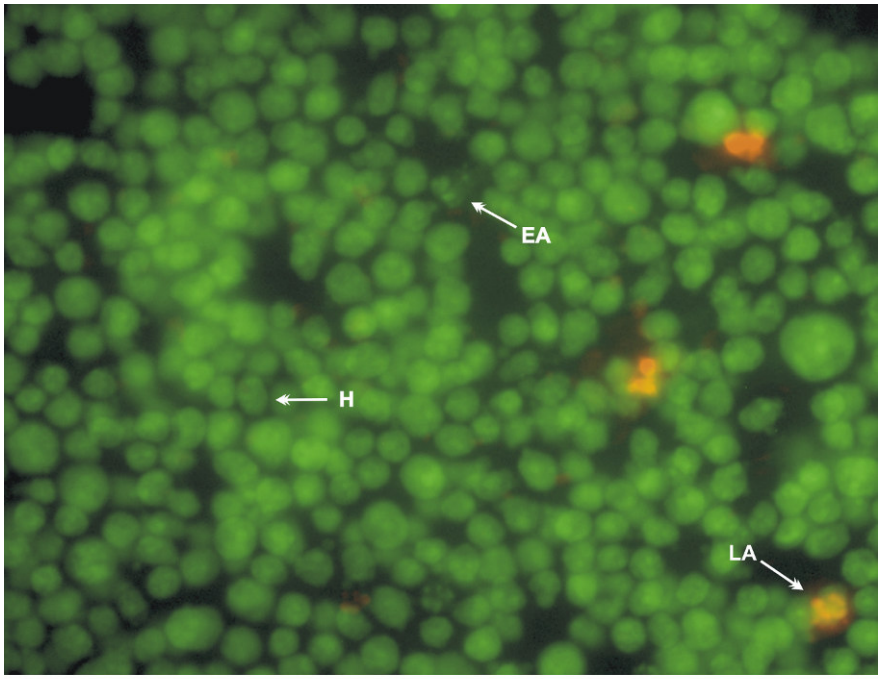

Figure 3.14 HL-60 cells (1 x 10^6) treated with 3 μg/ml cyclohexamide for 48 hours. H = healthy cells, EA = early apoptosis, LA = late apoptosis

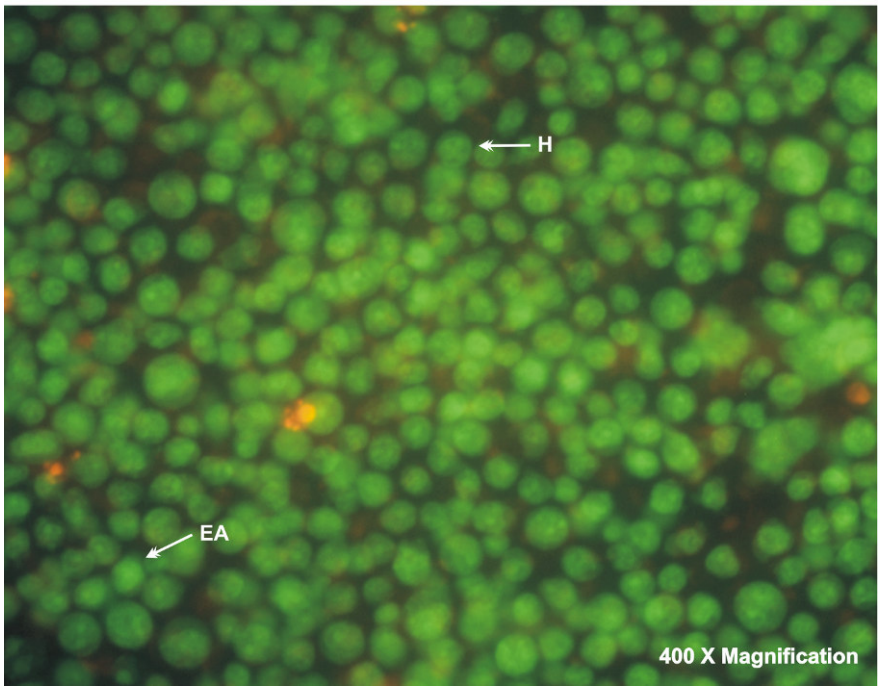

Figure 3.15 HL-60 cells (1 x 10^6) treated with 25 μM LY294002 for 1 hour prior to the addition of 3 μg/ml cyclohexamide and then incubated for a further 48 hours. H = healthy cells, EA = early apoptosis

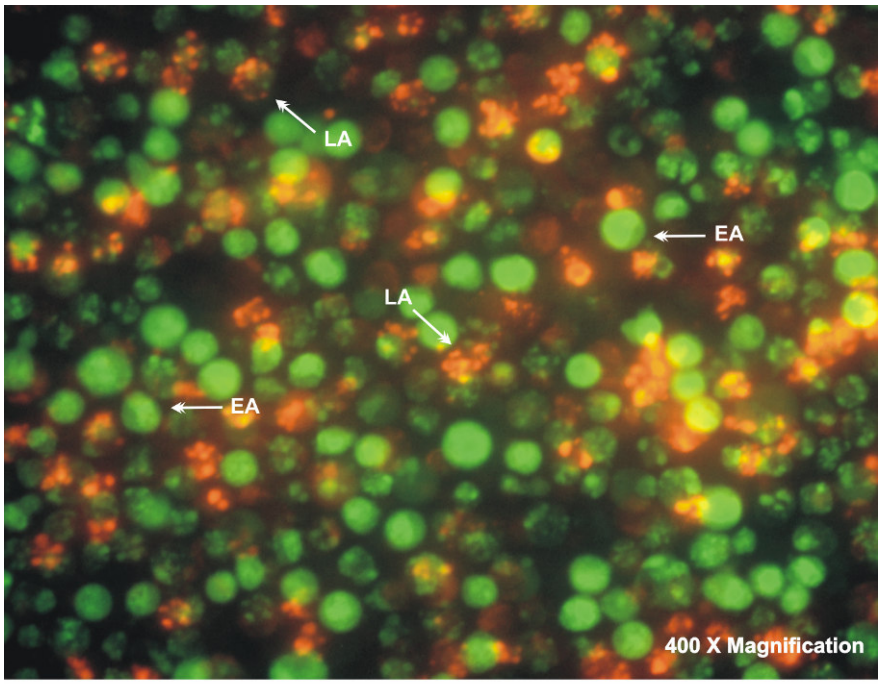

Figure 3.16 HL-60 cells (1 x 10^6) stimulated with 60 µg/ml etoposide and 3 µg/ml cyclohexamide for 48 hours. EA = early apoptosis, LA = late apoptosis

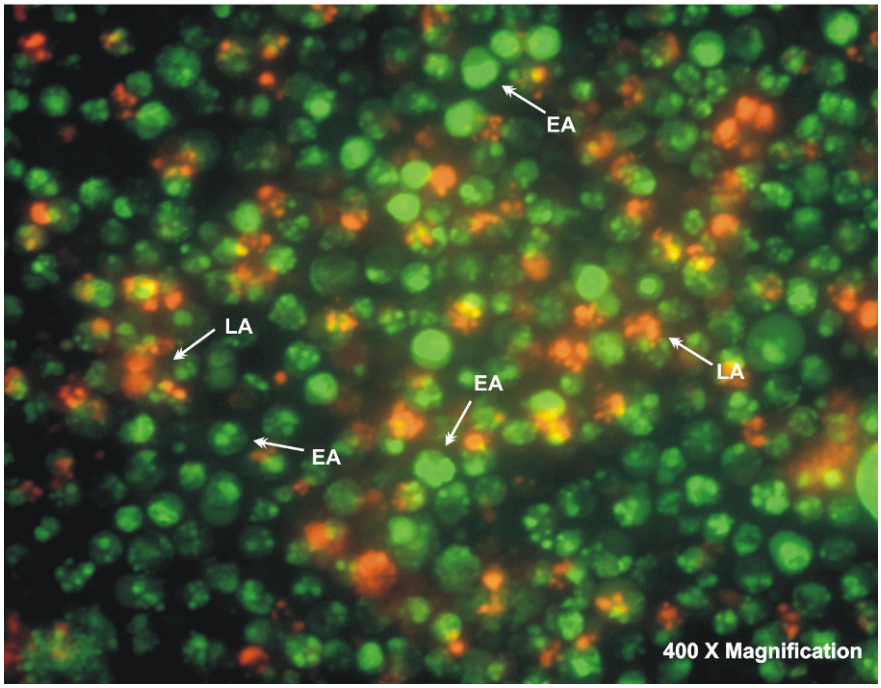

Figure 3.17 HL-60 cells (1 x 10^6) incubated with 25 µM LY294002 (one hour) before the addition of 60 µg/ml etoposide and 3 µg/ml cyclohexamide for 48 hours. EA = early apoptosis, LA = Late apoptosis

3.4 FLOW CYTOMETRY

Flow cytometry was performed (3 experiments) on 3 x 10^3 HL-60 cells treated with 60 μg/ml etoposide, 3 μg/ml cyclohexamide and 25 μM LY294002 for 48 hours. Figure 3.18 (A-J) are representative dot plots that were obtained from these samples when they were stained with YO-PRO-1 and propidium iodide. Each of these dot plots contains four quadrants labelled 1-4 that help to separate the different cell populations. The different colours can also differentiate the cell populations. The black indicates viable cells, the green indicates apoptotic cells and red indicates necrotic cells. The dot plots also appear to have a characteristic 'scorpion tail' pattern. Quadrant 1 contains cellular debris and the necrotic cells are present in quadrant 2. Quadrant 3 consists of normal viable cells and quadrant 4 contains the apoptotic cells. The percent of each population was calculated by COULTIER(R) EPICS(R) program and were plotted in Figure 3.19.

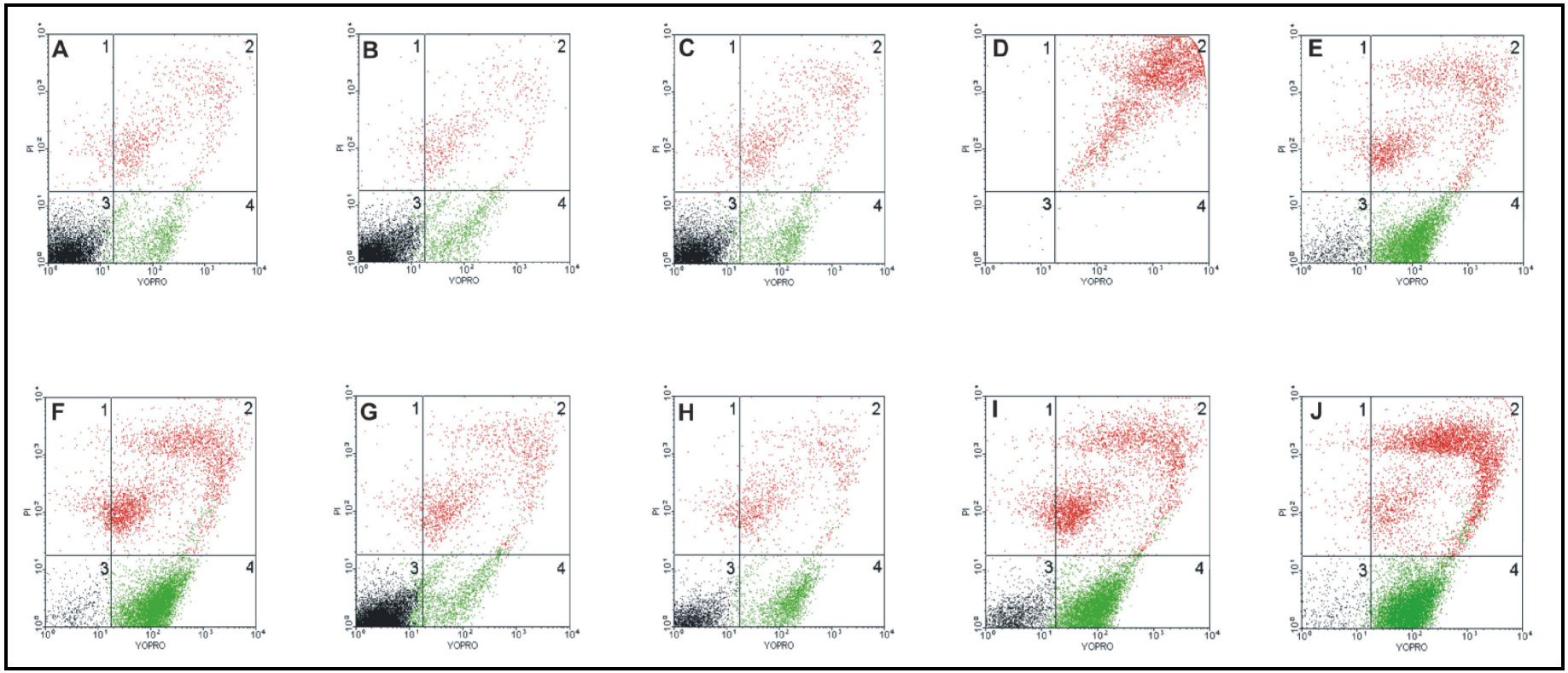

Figure 3.18 Representative dot plots obtained from 3 x 105 HL-60 cells passed through the Beckman-Coultier Flow cytometer after being stained with YO-PRO-1 and propidium iodide. The cells were treated with 25 μM LY294002 for 1 hour prior to the addition of 60 μg/ml etoposide and 3 μg/ml cyclohexamide for 48 hours. A = Untreated cells (Blank), Cells treated with: B = DMSO, C = LY294002, D = Necrotic Control, E = etoposide, F = etoposide + LY294002, G = cyclohexamide, H = cyclohexamide + LY294002, I = etoposide + cyclohexamide and J = etoposide + cyclohexamide + LY294002.

Figure 3.18 A-D are the control samples, where A is HL-60 cells grown under normal conditions, B are the cells treated with the vehicle DMSO, C are cells stimulated with 25 μM LY294002 and D is the necrotic control. Figure 3.18 A-C and Figure 3.19 indicate that the majority of the cell populations are normal (96.45%, 96.23% and 93.3% respectively), however negligible apoptosis (1.36%, 1.52% and 2.19%) and necrosis (0.96%, 0.88% and 1.84%) do occur. In the necrotic control the majority of the cells appear to be undergoing necrosis (90.37%), and a large amount of cell debris is present (8.69%) Fig. 3.18 D & Fig. 3.19).

A large proportion of cells treated with 60 μg/ml etoposide undergo apoptosis (45.36%), however when they are treated with 25 μM 294002 for 1 hour prior to the addition of etoposide, the number of cells undergoing apoptosis is increased to 53.08% (Fig. 3.18 E-F & Fig. 3.19). Cyclohexamide (3 μg/ml) causes a small amount of apoptosis (1.97%), which is increased when 25 μM LY294002 is added (6.91%) (Fig. 3.18 G-H & Fig. 3.19). The stimulation of cells with etoposide and cyclohexamide results in 37.45% apoptosis, but when LY294002 is added it is increased to 52.72% (Fig. 3.18 I-J & Fig. 3.19).

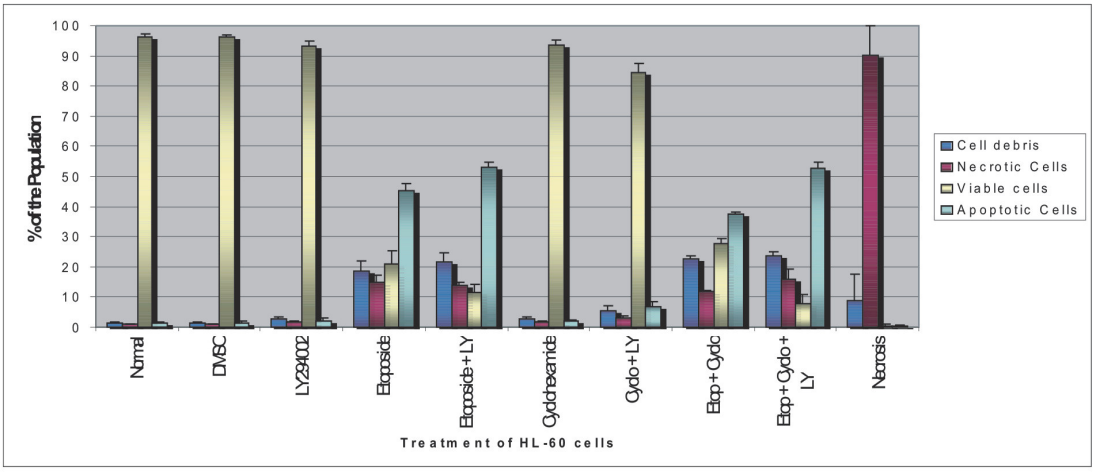

Figure 3.19 The mean and standard deviation of the percentage of the HL-60 cell population from 3 experiments that are viable, apoptotic or necrotic after pre-treatment with 25 μM LY294002 for 1 hour prior to the addition of 60 μg/ml etoposide or 3 μg/ml cyclohexamide for 48 hours.

3.5 DNA FRAGMENTATION

DNA fragmentation was performed on 1 x 10^6 HL-60 cells treated with combinations of 60 μg/ml etoposide, 3 μg/ml cyclohexamide and 25 μM LY294002 for both 48 and 72 hours. This was repeated numerous times with several different techniques, however no DNA fragmentation was present. Figure 3.20 A-C demonstrates the DNA obtained using Protocol

3 (Chapter 2.9.1). The only DNA present on these gels appears as smears (Fig 3.20).

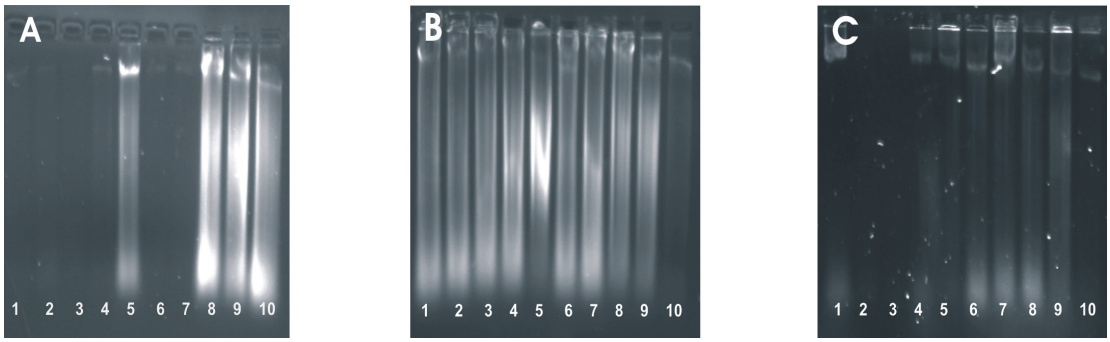

Figure 3.20 DNA extracted from 1 x 10^6 HL-60 cells using Protocol 3. The 1% agarose gel A shows the 'S' fraction, B shows the 'T' fraction and C shows the 'B' fraction of the extraction after 48 hours of stimulation. Cells treated with: 1 = Normal conditions, 2 = DMSO, 3 = LY294002, 4 = etoposide, 5 = etoposide + LY294002, 6 = cyclohexamide, 7 = cyclohexamide + LY294002, 8 = etoposide + cyclohexamide, 9 = etoposide + cyclohexamide + LY294002 and 10 = necrosis control.

3.6 THE LDH ASSAY

The cytotoxicity assay indicated that a large amount of cell death occurred when the HL-60 cells were treated with 0.01 μg/ml – 10 μg/ml etoposide for 48 hours. The LDH activity in the medium was therefore tested at this concentration range with the addition of 25 μM LY294002. The medium of cells treated for 48 hours with the recommended and most commonly used concentration of 60 μg/ml etoposide was also tested.

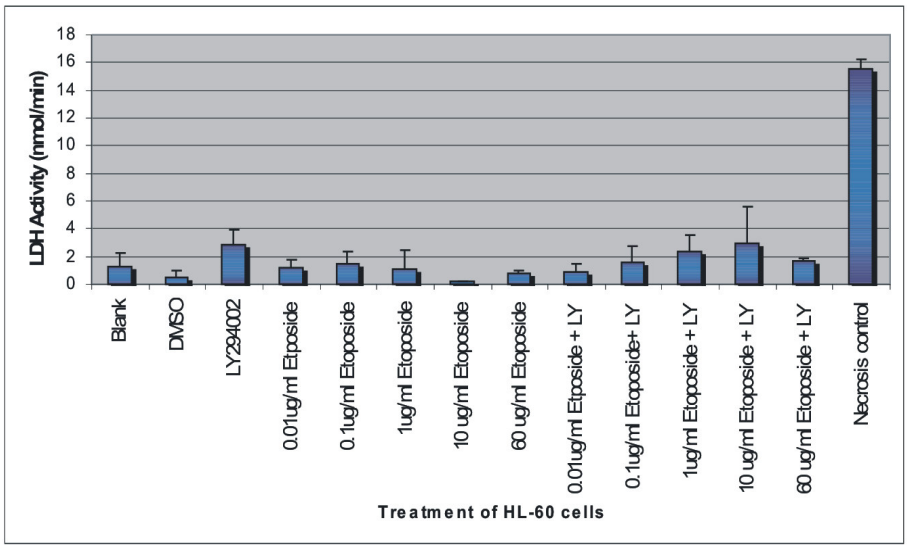

Figure 3.21 The mean and standard deviation of LDH activity (nmol/min) in culture medium of three experiments of HL-60 cells treated with a concentration range of etoposide and 25 μM LY294002.

Figure 3.21 is the mean of the LDH activity for three experiments, a LDH positive control was also tested by adding 10 U of LDH to the reaction in

place of the test medium. The LDH positive control (not represented on the graph) had an activity of 94.054 nmol/min, demonstrating that the assay was working. The LDH activity in all the test samples were negligible, with most activities under 2 nmol/min. The exception being the samples treated with 25 μM LY294002, 1μg/ml etoposide + LY294002 and 10 μg/ml etoposide + LY294002. The necrosis control, as expected, had the highest LDH activity of 15.5 nmol/min (Fig. 3.21).

3.7 RNA ANALYSIS

RNA was extracted from 5 x 10^6 HL-60 cells treated with 25 μM LY294002 for 1 hour before 50 ng/ml PDGF was added for 15 and 30 minutes. This was performed in triplicate and if the absorbance ratio (260 nm/280) nm was less than 1.8 the experiment was discarded and performed again. RNA was also extracted from cells treated with the combination of 25 μM LY294002 and 60 μg/ml etoposide for 4 hours. It appeared that the addition of etoposide had a detrimental effect on the integrity of the RNA as the highest purity obtained was 1.5. Nonetheless, RT-PCR was still performed in triplicate on these samples.

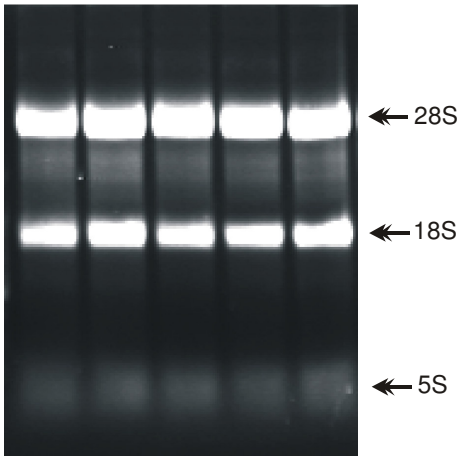

Figure 3.22 A 2% agarose gel showing 5 different RNA extractions. The arrows indicate the three major RNA species (28S, 18S and 5S).

The quality of RNA was also checked using agarose gel electrophoresis, and any samples that did not exhibit three crisp bands were discarded. Figure 3.22 is a representative gel showing RNA extracted from 5 samples. All three major RNA species (28S, 18S and 5S) are present and there is no smearing of the bands.

3.8 REVERSE TRANSCRIPTION-POLYMERASE CHAIN REACTION ANALYSIS

The RT-PCR was performed on 1 μg of RNA extracted from the samples (in triplicate) described in Chapter 2.7. These were then subjected to multiplex PCR.

3.8.1 RESTRICTION ENZYME ANALYSIS OF AKT PCR PRODUCT

Three cDNA products were subjected to PCR with the Akt forward and reverse primers. These PCR products were then digested with 3 restriction enzymes (Ava I, Hae III and Xho I), and run on a 2% agarose gel. The products obtained with each of the restriction enzymes, Xho I (103 bp and 279 bp), Ava I (33 bp, 70 bp and 279 bp) and Hae III (33 bp, 78 bp, 80 bp and 191 bp) proved that the Akt primers were amplifying the correct product as is shown in Figure 3.23. The 33 bp cDNA fragments are not visible on the gel as they are too small, and the 79 and 80 bp fragments obtained with the Hae III enzyme are difficult to differentiate due to the similarity in size (Fig 3.23).

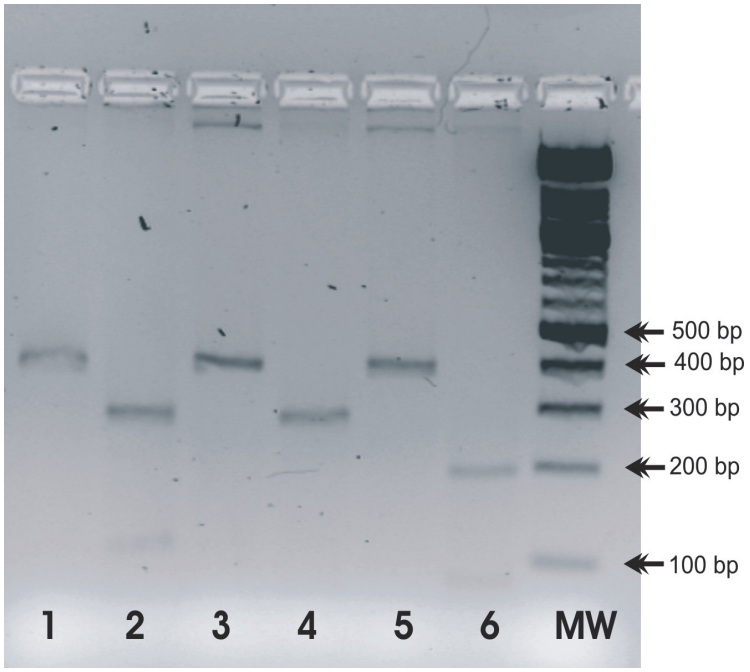

Figure 3.23 A 2% agarose gel showing the Akt PCR product cut by the three restriction enzymes, Ava I, Hae III and Xho I. Lanes 1, 3 and 5 contain uncut control cDNA products, Lane 2 is the Xho I products, lane 4 is the Ava I products, lane 6 is the Hae III products and lane MW is the 100 bp molecular weight ladder.

3.8.2 MULTIPLEX PCR OF HL-60 CELLS STIMULATED WITH PDGF

The multiplex PCR gave two bands, the first was 587 bp (GAP-DH) and the second was 383 bp (Akt). Figure 3.24 is a representative 2% agarose gel of HL-60 cells stimulated with 50 ng/ml PDGF and 25 μM LY294002.

The intensities of the bands were scanned using the Genesnap Tools program. The GAP-DH band was used as a control band and the ratio is compared to Akt in Figure 3.24.

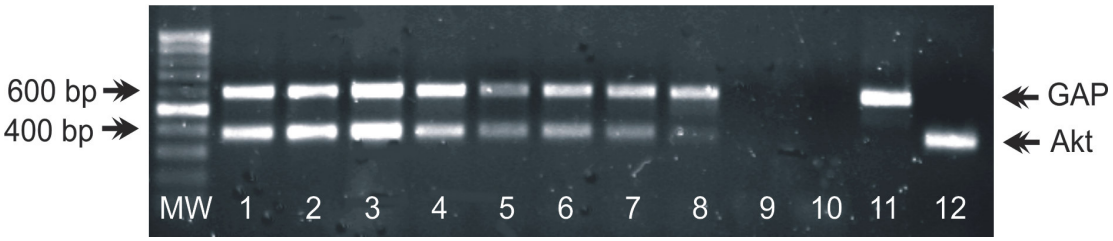

Figure 3.24 A 2% agarose gel showing the multiplex PCR of RNA extracted from 1 x 10^6 HL-60 cells stimulated with 25 μM LY294002 for 1 hour prior to the addition of 50 ng/ml PDGF for two different time periods. MW represents the 100 bp DNA ladder. Lanes 1-4 are control samples; 1 = cells grown in 10% FCS, 2 = DMSO, 3 = HCl-BSA and 4 = 25 μM LY294002. Lanes 5-8 are the test samples; 5 = PDGF (15 min), 6 = PDGF (30 min), 7 = PDGF (15 min) + LY294002 and 8 = PDGF (30 min) + LY294002. Lanes 9-12 are once again control samples; 9 = The RT-PCR blank, 10 = the multiplex PCR blank, 11 = normal cells with the GAP-DH primers and 12 = normal cells with the Akt primers.

The band intensity of the two PCR products GAP-DH and Akt of the 10% FCS control are very similar and give a ratio of Akt/GAP-DH of 0.95. The Akt/GAP-DH ratios were not significantly different in the samples treated with PDGF. However the Akt band intensities and the ratio for the samples treated with 25 μM LY294002 were decreased in the presence and absence of PDGF, indicating a decrease in Akt mRNA expression when the PI3-kinase pathway is inhibited (Figs. 3.24 & 3.25).

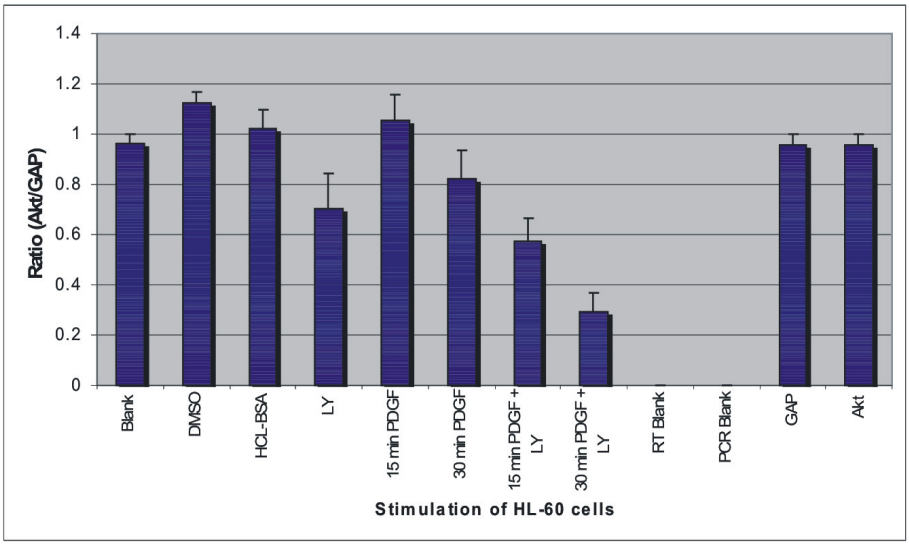

Figure 3.25 The mean and standard deviation of the ratio of Akt/GAP-DH showing the changes in the Akt mRNA expression obtained from 3 experiments when the HL-60 cells (1 x 10^6) were treated with 50 ng/ml PDGF for various time periods with the combination of 25 μM LY294002.

3.8.3 MULTIPLEX PCR OF CELLS TREATED WITH ETOPOSIDE

Figure 3.26 is a representative gel of the multiplex PCR conducted on the RNA extracted from HL-60 cells treated for 4 hours with 60 μg/ml etoposide in addition to the treatment with 25 μM LY294002 for 1 hour (in triplicate). The intensities of the bands were scanned using the Genesnap Tools program as previously described, and plotted as ratios in Figure 3.27.

The intensity of all of the Akt bands and Akt/GAP ratios were very low, however when the cells were treated with 25 μM LY294002 as well as with etoposide, the Akt bands were absent. This was not the case with cyclohexamide and LY294002 (Figs 3.26 & 3.27).

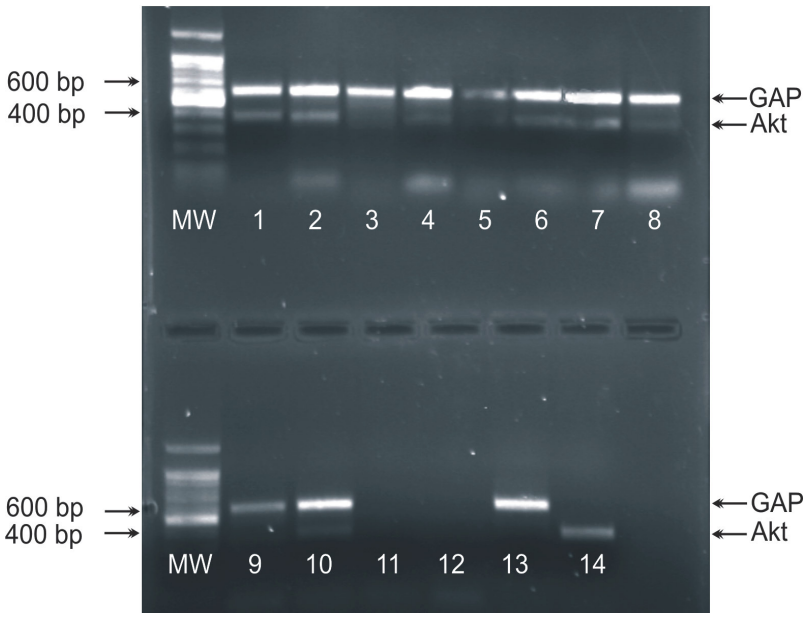

Figure 3.26 A 2% agarose gel showing the multiplex PCR of RNA extracted from 1 x 106 HL-60 cells treated with 25 μM LY294002 1 hour prior to the addition of etoposide (60 μg/ml) and cyclohexamide (3 μg/ml) for 4 hours. MW represents the 100 bp DNA ladder. Lanes 1-3 are control samples; cells treated with: 1 = normal conditions, 2 = DMSO and 3 = 25 μM LY294002. Lanes 4-10 are test samples; cells treated with: 4 = etoposide, 5 = etoposide + LY294002, 6 = cyclohexamide, 7 = cyclohexamide + LY294002, 8 = etoposide + cyclohexamide, 9 = etoposide + cyclohexamide + LY294002 and 10 = Necrosis. Lanes 11-14 are once again control samples; 11 = the RT-PCR blank, 12 = the multiplex PCR blank, 13 = normal cells with the GAP-DH primers and 14 = normal cells with the Akt primers.

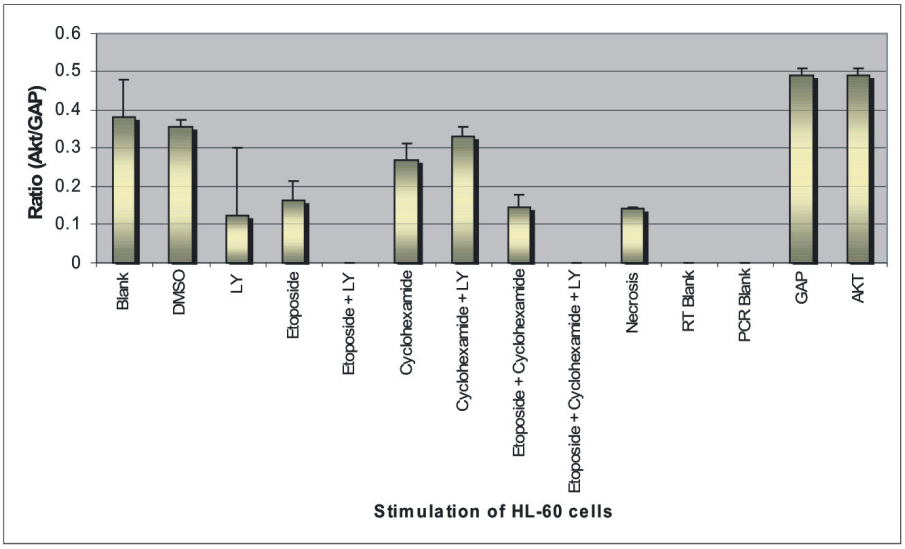

Figure 3.27 The mean and standard deviation of the ratio of Akt/GAP-DH showing the changes in the Akt mRNA expression obtained from three experiments when the HL-60 cells (1 x 10^6) were treated with 60 μg/ml etoposide and 3μg/ml cyclohexamide for 4 hours with the combination of 25 μM LY294002.

CHAPTER 4

DISCUSSION

The role that the PI3-kinase pathway plays in oncogenesis has been well documented as many oncogenic downstream targets have been identified. One of these targets, Akt, has also been implicated in cancer, however the part it plays is not entirely clear. Many studies have been conducted in leukaemic cells to determine the effect that inhibiting the PI3-kinase/Akt pathway has on cytotoxic drug induced apoptosis. One such study was performed by O'Gorman and co-workers (2000), who determined that HL-60 cells are more susceptible to drug-induced apoptosis if the PI3-kinase pathway is inhibited. The PI3-kinase/Akt had been previously shown to mediate heterodimer interactions of BAD, a proapoptotic regulator, with Bcl-2 and Bcl-X_L. On phosphorylation by Akt, BAD is sequestered in the cytoplasm by the 14-3-3 protein and its interactions with anti-apoptotic Bcl members is prevented, thus inhibiting apoptosis. O'Gorman and colleagues (2000) found that inhibition of PI3-kinase didn't lead to BAD heterodimer formation with Bcl–X or Bcl-2 or the presence of non-phosphorylated BAD, suggesting that an alternative pathway is involved in the survival factor-mediated drug resistance in HL-60 cells. Other studies, including one conducted by Delhause and co-workers (2000) revealed that an interaction between Akt and IKK exists in HL-60 cells. This suggested that the pro-survival pathway responsible for

decreasing cytotoxic drug induced apoptosis in HL-60 cells is the IKK, IκB and NF-κB pathway.

This study was designed to confirm the observations that inhibiting the PI3-kinase/Akt pathway led to increased cytotoxic drug induced apoptosis, made by O'Gorman and co-workers (2000), as well as to confirm that this pathway activates IKK and IκB as was elucidated by Delhause and colleagues (2000).

The cytotoxic drug etoposide was used in this study and had been previously shown to cause apoptosis in HL-60 cells by O'Gorman and co-workers (2000). Their findings were confirmed in the present study by the cytotoxicity assay which revealed that cell death occurred at a concentration as little as 10 μg/ml etoposide, and cells treated with 60 μg/ml etoposide had a 70% decrease in survival. In the current study, the inhibition of the PI3-kinase pathway by the addition of 25 μM LY294002 resulted in an approximately 10% increase in cell death, whereas O'Gorman and co-workers demonstrated an approximate 30% increase in cell death. This indicates that the PI3-kinase pathway plays a small anti-cell death role in HL-60 cells treated with cytotoxic drugs. The disadvantage of this method was that it did not demonstrate whether the decrease in cell number was due to apoptosis or necrosis, and further experimentation was required to determine the mechanism of cell death. Therefore four other techniques were used to confirm apoptosis, the

acridine orange-ethidium bromide assay, flow cytometry, DNA fragmentation and the LDH activity assay. The flow cytometry assay was the only quantitative assay performed, whereas the acridine orange-ethidium bromide assay showed the changes in cell morphology. The DNA fragmentation assay was used to demonstrate internucleosomal digestion of DNA indicative of apoptosis, and the LDH assay was used to confirm that necrosis had not occurred.

As was previously described, the morphology of cells undergoing apoptosis and necrosis is substantially different. The acridine orange-ethidium bromide assay was used to identify the morphological changes in the HL-60 cells treated with etoposide, cyclohexamide and LY294002. The assay was described in T47D and HEK293 cell lines by Gibson and colleagues (1999). They used the technique to determine the percentage of apoptotic cells after adding anti-Fas antibody for several time periods. Unlike these authors, it was decided that the technique in this case was only usable as a qualitative and not a quantitative assay for two reasons. Firstly, large numbers of cells (2×10^6) need to be present in each field for the results to have any statistical relevance. Secondly, the classification of the cells into the different categories (H, EA, LA and N) is at the discretion of the individual doing the analysis.

The flow cytometry assay was used to quantitatively confirm the results obtained in the acridine orange-ethidium bromide assay. This is a very

sensitive technique as viable cells are not stained by either dye, apoptotic cells bind YO-PRO-1 and propidium iodide enters necrotic cells staining the DNA. Studies by Dylacht and co-workers in 1999 and 2000 described the use of propidium iodide and FITC to determine the percentage apoptosis of HL-60 cells treated with radiation, hyperthermia and etoposide. This technique used by Dylacht and co-workers (1999 & 2000) is highly sensitive, as they incubated the cells with a monoclonal antibody against human lamin B, an apoptosis marker. This was then incubated with a secondary antibody that was conjugated with FITC, and the cells were stained with propidium iodide (Dylacht *et al*, 1999; Dylacht *et al*, 2000). They obtained the same characteristic 'scorpion tail' in apoptotic samples as was found in this study, however they had a very high percentage of apoptotic cells (79%) when treated with 12 μg/ml etoposide for 6 hours.

In the present study both the confocal microscopy and flow cytometry assays confirmed that etoposide treated HL-60 cells have a decrease in cell survival due to apoptosis, however the flow cytometry allowed the cell death to be quantitatively differentiated into apoptosis and necrosis. Normal cell populations were shown to contain a large percentage of normal cells, with a few cells undergoing apoptosis and necrosis. Approximately 45% of the cells treated with 60 μg/ml etoposide for 48 hours were undergoing apoptosis and this is increased to 53% when they were pre-treated with 25 μM LY294002, confirming the findings of

O'Gorman and co-workers (2000) (70% and 100% respectively), but in this study there were lower levels of apoptosis. O'Gorman and colleagues (2000) also used flow cytometry to obtain these results, however they detected apoptosis by measuring the amount of light scatter and necrosis by the amount of propidium iodide included into the cell. Propidium iodide can only enter the cell once the membrane has been compromised as is the case with necrosis (Vermes *et al*, 1997). Therefore the technique used by O'Gorman and co-workers (2000) is less sensitive than the technique used in this study, as both light scatter and the uptake of two dyes were analysed.

The LDH activity of the medium surrounding the treated cells proved to be negligible, and the numbers of necrotic cells were low implying that little or no necrosis was occurring. Cyclohexamide was described as an apoptotic positive control (3 μg/ml) in HL-60 cells by Sigma, and was shown to cause apoptosis (20 μg/ml) in Human Jurkat and CEM C7 cell lines by Tang and co-workers (1999). Therefore 3 μg/ml cyclohexamide was used as a positive control in this study. The results were opposite to what was expected, as the majority of the cells in the field appeared healthy. This was also the case when 25 μM LY294002 was added prior to the addition of the cyclohexamide. These findings were confirmed with flow cytometry as the addition of cyclohexamide resulted in 1.97% apoptosis, which was increased to 6.91% when LY294002 was added. The cyclohexamide

used had passed its expiry date, and it is suspected that it was no longer active.

As previously mentioned DNA fragmentation is indicative of apoptosis and was attempted to confirm the results obtained with the experiments described above in the present study. This technique has been formerly used to demonstrate apoptosis in HL-60 cells that were serum starved for 4 hours then treated with GH (growth hormone)-blocking antibodies for 6 days (Costoya, *et al*, 1999). Dylacht and co-workers (2000) also demonstrated that low molecular weight DNA fragmentation occurs in HL-60 cells treated with 12 μg/ml etoposide for 3 hours. As stated previously, several different techniques were used for DNA fragmentation. It was decided to use Protocol 3, as all of the supernatants that could contain the DNA fragments were studied. According to the source of the technique (www.imoax1.unimo.it.HTM), the fraction most likely to contain the lower molecular weight DNA fragments was the 'T' fraction as the small DNA fragments would remain in solution. However, no fragmentation was present in any fraction, even though the alternative experiments prove that apoptosis is occurring. The experiments were repeated many times and the time frames of the incubation and the concentrations of the drugs were varied; however the same results were obtained. The reasons behind this lack of DNA fragmentation are unclear. It is possible that the concentration of DNA fragments is too low for detection by ethidium bromide, as a low percentage of cells had undergone apoptosis. Both

Dylacht and co-workers (2000) and Vermes and colleagues (1997) had the same difficulty with detecting DNA fragmentation, as they found that the apoptotic processes often occurred asynchronously. Vermes and colleagues (1997) state that the DNA fragmentation technique is essentially qualitative and is not sensitive enough to detect spontaneous apoptosis, or apoptosis in small populations of cells (Vermes *et al*, 1997). Other studies have shown that there is a preliminary step in DNA laddering, where the DNA is digested into multiples of 300 and 50 kilo bases which represent higher order chromatin structure. In some cases no further DNA fragmentation occurs, indicating that the endonucleases responsible for the continuation of the DNA cleavage are not uniform and that the production of DNA fragments is not a necessary step for apoptosis (Story & Kodym, 1998). It is possible that this was the case in the current study, as the morphological studies (confocal microscopy and flow cytometry) did show that apoptosis was occurring.

To elucidate the pathway by which the PI3-kinase pathway protects HL-60 cells from cytotoxic drug induced apoptosis, the activation of the downstream targets was assessed. The first step taken was to determine whether stimulation of the PI3-kinase pathway with PDGF resulted in cell proliferation and whether the addition of LY294002 caused a decrease in this growth. The proliferation assay revealed that optimum cell growth appeared to be at 10 ng/ml PDGF however a decrease in cell growth did occur at concentrations higher than 30 ng/ml PDGF. The reason for this

is unknown, but it is thought that a high concentration of PDGF may have a toxic effect on HL-60 cells. However, the preliminary Trypan Blue exclusion studies showed a marked increase in HL-60 cell proliferation when treated with 50 ng/ml PDGF. Another more probable explanation is that the cells grow at a higher rate and reach confluence after a short time frame. The over-confluence results in a decrease in proliferation and increase in cell death. Increased cell growth induced by PDGF was therefore not clearly demonstrated by the growth assay however, inhibition of the PI3-kinase pathway with 25 μM LY294002 decreased the mean percentage growth of the HL-60 cell population. Thus the PI3-kinase pathway may play a role in PDGF mediated growth as shown when Akt phosphorylation was studied as described below.

The PI3-kinase pathway has been reported to protect cells from apoptosis inducing drugs in many cell lines, as well as in HL-60 cells (O'Gorman *et al*, 2000; Brazil & Hemmings, 2001; Vivanco & Sawyers, 2002). It has also been reported that stimulation of PI3-kinase results in the phosphorylation of Akt, and that the treatment of HL-60 cells with LY294002 decreased the amount of Akt phosphorylation (O'Gorman *et al*, 2000). These findings were confirmed by this study as HL-60 cells treated with PDGF for 15 and 30 min had a higher proportion of phosphorylated Akt to those treated with LY294002 prior to the addition of PDGF. Unexpectedly, phosphorylated Akt levels in LY294002 and PDGF treated cells were higher than that of the cells grown under normal conditions.

This leads us to believe that Akt is also phosphorylated via another pathway, or that LY294002 does not inhibit the PI3-kinase pathway entirely. At the initiation of this study LY294002 was the most specific PI3-kinase pathway inhibitor available, but as mention previously (Chapter 2.3) other more specific inhibitors are currently being tested and becoming commercially available. Contradictory to the results obtained in this study, O'Gorman and colleagues reported that a small proportion of Total Akt is phosphorylated in HL-60 cells grown under normal conditions, a finding confirmed by several groups in other cell lines. The majority of the studies conducted in the literature insert a vector containing Akt into the cell lines (Franke *et al*, 1995; Chen *et al*, 1999; Ramaswamy *et al*, 1999; Ma *et al*, 2001). The advantage of performing this transfection is that there is higher expression of the protein and the phosphorylation is easier to detect, a problem experienced in the present study. The disadvantage is that the protein constitutively expressed with little or no control, and the results obtained are therefore not completely indicative of the processes occurring *in vivo*. It was decided not to perform the transfection in this study for that reason.

As previously stated in this report the PI3-kinase/Akt pathway has many downstream targets that are potentially responsible for protecting carcinogenic cells from cytotoxic drugs. A recent study has shown that the PI3-kinase pathway plays a role in the activation of NF-κB DNA-binding activity in AML (Birkenkamp *et al*, 2004). Delhause and co-

workers (2000) reported that this activation of NF-κB is due to the interaction of Akt with the IKK/IκB pathway. This however was not shown in this study as treatment of the HL-60 cells with LY294002 did not decrease the levels of phosphorylation of IKK or IκB. The exact opposite occurred as the phosphorylation of both IKK and IκB increased slightly when the HL-60 cells were incubated with LY294002. This confirms the observations of Birkenkamp and colleagues (2004), who found that the classical NIK/IKK/IκB pathway can be activated by external factors and other pathways (e.g. Ras), besides the PI3-kinase/Akt pathway. Romashkova and Makarov (1999) reported that under certain circumstances PI3-kinase can activate NF-κB in an IκB independent manner. It has also been shown that Akt can activate NF-κB transcriptional activity via an alternative IκB-independent pathway by modulating the transcriptional potential of RelA (Romashkova & Makarov, 1999). Due to time constraints on this study, the direct interaction between Akt and NF-κB could not be analysed.

Okano and co-workers (2000) performed a study on the expression of the three isoforms of Akt in different cell lines. They revealed that of the three isoforms, only Akt3 is differentially expressed. In this study the semi-quantitative method of multiplex RT-PCR was used to observe the expression of Akt1 mRNA in HL-60 cells treated with PDGF, LY294002, etoposide and cyclohexamide. Treatment of the HL-60 cells with 50 ng/ml PDGF did not show a significant difference in Akt1 mRNA expression to

the untreated cells. However, a decrease in expression was evident when the cells were treated with 25 μM LY294002, indicating that inhibition of the PI3-kinase pathway decreases transcription of Akt1 mRNA. RNA extracted from HL-60 cells treated with 60 μg/ml etoposide was of poor quality, and the resultant RT-PCR bands were also not of good quality. The study did reveal that when the cells were treated with etoposide that little transcription of Akt1 mRNA occurred. Once again, a decrease in expression of Akt1 mRNA was evident in the cells treated with 60 μg/ml etoposide and 25 μM LY294002. Thus the PI3-kinase pathway itself may play a role in regulating the transcription of pro-survival genes, including Akt.

CHAPTER 5

CONCLUSION

Further study on this project is continuing, as Akt phosphorylation and mRNA expression is being monitored in the blood samples of leukaemic patients. Due to time constraints on the study, the relationship between Akt and NF-κB was not determined. These along with the interactions of other protein cascades such as MAPK with Akt are planned for the future. The diversity of Akt downstream targets outlined by Steelman and co-workers (2004) also leaves many possibilities for future study.

In conclusion, we confirmed that PI3-kinase stimulates phosphorylation of Akt, but that a minor relationship exists between Akt, IκB and IKK. The expression of Akt mRNA was also shown to be affected by inhibition of the PI3-kinase pathway and etoposide. This study also confirmed that etoposide causes apoptosis in HL-60 cells, and that there is an increase in apoptosis when the PI3-kinase pathway is inhibited. This allows us to conclude that inhibition of the PI3-kinase pathway may sensitise leukaemic cells to cytotoxic-drug induced apoptosis, a finding that may be of therapeutic importance in the future.

APPENDIX 1

REAGENT AND EQUIPMENT SUPPLIERS

A1.1 HL-60 CELL CULTURE

Incubator	Heraeus, USA
Ethanol	ACE, RSA
Copper Sulphate ($CuSO_4$)	SAARCHEM, Muldersdrift, RSA
HL-60 Cell Line	ATCC, Maryland, USA
Sterile Culture Flasks	Nunc, Roskilde, Denmark
RPMI-1640	Highveld Biological, Lyndhurst,RSA
$NaHCO_3$	Analyzed Analytical Reagent, Vorna Valley, RSA
Penicillin	Sigma-Aldrich, St Louis, MO, USA
Streptomycin	Sigma-Aldrich, St Louis, MO, USA
Fungizone	Sigma-Aldrich, St Louis, MO, USA
Foetal Calf Serum	Delta, Kempton Park, RSA
Glutamine	Fluka, Sigma-Aldrich, USA
Light Microscope	Zeiss, West Germany
Trypan Blue	Merck, Darmstadt, Germany
Desk Top Centrifuge	Beckmann
Glycerol	AAR, Vorna Valley, RSA

Sterile cryotubes	Nunc, Roskilde, Denmark
Sterile 50 ml Nunc tubes	Nunc, Roskilde, Denmark
Sterile Petri Dishes	Nunc, Roskilde, Denmark
NaCl	SAARCHEM, Muldersdrift, RSA
KCl	SAARCHEM, Muldersdrift, RSA
Na_2HPO_4	SAARCHEM, Muldersdrift, RSA
KH_2PO_4	BDH Lab Reagents, England
Filtration Unit	Millipore Corporation, USA
22 μm filter	Whatmann, RSA
Thick paper prefilter	Whatmann, RSA
Pump	Millipore Corporation, USA

A1.2 STIMULATION OF CELLS

PDGF	Sigma-Aldrich, St Louis, MO, USA
HCl	SAARCHEM, Muldersdrift, RSA
Bovine Serum Albumin	Highveld Biological, Lyndhurst, RSA
Cyclohexamide	Sigma-Aldrich, St Louis, MO, USA
Etoposide	Sigma-Aldrich, St Louis, MO, USA
DMSO	SAARCHEM, Muldersdrift, RSA
LY294002	Sigma-Aldrich, St Louis, MO, USA

A1.3 GROWTH/CYTOTOXICTY ASSAY

Growth/cytotoxicity assay kit	Promega, Madison, WI, USA
96 well sterile plates	Nunc, Roskilde, Denmark
Multichannel pipette	Socarex, England
96 well plate reader	Thermo Star, ADP, RSA

A1.4 PROTEIN EXTRACTION

Tris Base	Roche Laboratories, JHB, RSA
Sucrose	SAARCHEM, Muldersdrift, RSA
Triton X-100	Lab Reagents, RSA
PMSF	Sigma-Aldrich, ST Louis, MO, USA
Sodium dodecyl sulphate (SDS)	ICN Biomedicals Inc, Ohio, USA
β-Mercaptoethanol	Merck, Darmstadt, Germany
NaCl	SAARCHEM, Muldersdrift, RSA
Na_3VO_3	Sigma-Aldrich, ST Louis, MO, USA
NaF	Sigma-Aldrich, ST Louis, MO, USA
Sodium pyrophosphate	Sigma-Aldrich, ST Louis, MO, USA
EDTA	BDH Lab Reagents, England
Microcentrifuge tube	Eppendorff, USA
Bench top microcentrifuge	Eppendorff, USA
Bromophenol Blue	Merck, Darmstadt, Germany

A1.5 TOTAL PROTEIN DETERMINATION

Sodium Potassium Tartrate	SAARCHEM, Muldersdrift, RSA
$CuSO_4$	SAARCHEM, Muldersdrift, RSA
NaOH	SAARCHEM, Muldersdrift, RSA
Sodium Carbonate	SAARCHEM, Muldersdrift, RSA
Folinciocalteau	Merck, Darmstadt, Germany
Spectrophotometer	DU-65 Spectrophotometer
	Soft Pac Module Quant II linear

A1.6 ELECTROPHORESIS

Mini Gel system	Hoefer, USA
Acrylamide	BDH, Lab Suppliers, England
Bisacrylamide	Merck, Darmstadt, Germany
Ammonium Persulphate (APS)	BDH, Lab Suppliers, England
TEMED	Merck, Darmstadt, Germany
Isopropanol	AAR, JHB, RSA
Molecular Weight Markers	Amersham Pharmacia Biotech, RSA
Electrophoresis apparatus	Hoefer Scientific Instruments
Cooling system	Hoefer Scientific Instruments

Power Pack	Hoefer Scientific Instruments
Coomassie Brilliant Blue R-250	Merck, Darmstadt, Germany
Acetic acid	AAR, JHB, RSA
Methanol	AAR, JHB, RSA

A1.7 WESTERN BLOTTING

Nitrocellulose Paper	Osmonics, JHB
Glycine	Merck, Darmstadt, Germany
Western blotting aparatus	Transfer Electrophoresis Unit TE Series
Amido Black	Merck, Darmstadt, Germany

A1.8 IMMUNOBLOTTING

Total Akt Antibody	Cell Signalling, Biolabs, USA
Phospho-Akt Antibody	Cell Signalling, Biolabs, USA
Phospho-IκB Antibody	Cell Signalling, Biolabs, USA
IKK Antibody	Cell Signalling, Biolabs, USA
Tween-20	Merck, Darmstadt, Germany
Donkey-anti-rabbit 2° Antibody	Amersham Life Science, UK
Sheep-anti-mouse 2° Antibody	Amersham Life Science, UK
Non-fat-dry milk powder	Elite, JHB, RSA

Advanced ECL™ kit	Amersham Life Science, UK
Cling Film	Glad, RSA
X-ray Film	Fuji, UK

A1.9 CONFOCAL MICROSCOPY

Acridine Orange	Merck, Darmstadt, Germany
Confocal Microscope	Zeiss, West Germany

A1.10 FLOW CYTOMETRY

Flow cytometry tubes	Beckmann-Coultier, Germany
YO-PRO-1	Molecular Probes Inc, Netherlands
Propridium Iodide	Fluka, Sigma-Aldrich, USA
Flow Cytometer	Beckmann-Coultier, Germany

A1.11 DNA EXTRACTION

RNase-A	Boehringer Mannheim, West Germany
NP-40	Boehringer Mannheim, West Germany

Proteinase K	Roche Laboratories, JHB, RSA
Sodium Acetate	Merck, Darmstadt, Germany
Vortex apparatus	Chilt Scientific, USA
Agarose	Tech Com Ltd, Hong Kong
Ethidium Bromide	Sigma-Aldrich, ST Louis, MO, USA
Gel Chamber	Hoefer, USA
DNA viewing apparatus	Syngene gel viewing system, USA

A1.12 LDH ASSAY

Triethanolamine	SAARCHEM, Muldersdrift, RSA
Monosodium Pyruvate	SAARCHEM, Muldersdrift, RSA
NADH	Sigma-Aldrich, ST Louis, MO, USA
Spectrophotometer	Perkin-Elmer spectrophotometer with a chart recorder

A1.13 RNA EXTRACTION

Diethyl Pyrocarbonate	SAARCHEM, Muldersdrift, RSA
Tri-Reagent™	Sigma-Aldrich, St Louis, MO, USA
Chloroform	AAR, Vorna Valley, RSA

A1.13.1 VISUALISATION OF RNA

MOPS	Merck, Darmstadt, Germany
Formamide	SAARCHEM, Muldersdrift, RSA
RNase Free water	Sabax, RSA

A1.14 REVERSE TRANSCRIPTION-POLYMERASE CHAIN REACTION ANALYSIS OF AKT1 MRNA

cDNA synthesis kit	Promega, Madison, WI, USA
PCR Machine	Hybaid Touchdown Thermocycler
AKT1 primers	Whitehead Scientific, Cape Town, RSA
GAP-DH primers	Whitehead Scientific, Cape Town, RSA
PCR kit	Roche Laboratories, JHB, RSA

A1.15 ENDONUCLEASE RESTRICTION OF AKT1 PCR PRODUCT

XhoI	Promega, Madison, WI, USA
AvaI	Promega, Madison, WI, USA

HaeIII	Promega, Madison, WI, USA
Buffer M	Promega, Madison, WI, USA
Buffer H	Promega, Madison, WI, USA
Buffer B	Promega, Madison, WI, USA

APPENDIX 2

SOLUTIONS AND TECHNIQUES

A2.1 CELL CULTURE

A2.1.1 FUMIGATION OF CULTURE ROOM

A2.1.1.1 Fumigation solution

2 g Potassium Permanganate

20 ml Formaldehyde

A2.1.1.2 Methodology

- Clean Incubator and remove $CuSO_4$ solution from the tray
- Prepare fumigation solution
- Place one beaker with solution in the switched off open incubator
- Place second beaker with solution in the switched on Laminar Flow hood
- Leave the room immediately, close door and leave for two days
- Potassium permanganate will release formalin and fumigate the area
- Remove beakers, dispose of solutions into a formalin waste container

- Put freshly prepared $CuSO_4$ solution into the tray in the incubator
- Switch on incubator

A2.1.2 STERILIZATION SOLUTIONS

A2.1.2.1 70% Ethanol

700 ml Ethanol

300 ml Distilled water

A2.1.2.2 Adcodyne

4 ml Adcodyne

996 ml Distilled Water

A2.1.1.3 10% $CuSO_4$

10 g $CuSO_4$

100 ml Distilled water

A2.1.3 THE RPMI-1640 MEDIUM

Prior to preparing medium, all objects to be used must be autoclaved using the water cycle. This includes the medium bottles and filtering unit.

Table A2.1 Recipe for RPMI-1640

Materials	1 Litre	5 Litres
RPMI-1640	10.41g	52.05g
NaHCOμ	2.00g	10.00g
Penicillin	0.26g	1.30g
Streptomycin	0.43g	2.15g

The above is made up in 800ml or 4.5l Baxter water and gently stirred using a magnetic stirrer. Make up to the final volume in a volumetric flask, then transfer back into a conical flask for easier filtration.

A2.1.4 FILTRATION

- On the tripod part of the filtering unit place:
  I. Round metal grid with the bars down
  II. Metal filter with rough side up
  III. 22μm filter – hold the edge with forceps, allowing the opposite edge to touch the metal filter and let it fall gently

IV. Thick paper prefilter with rough side up – wet with distilled water
V. Position top of unit so that the screw holes line up, put screws in loosely

- Wrap foil around the top of the glass bell and upper two nozzles – the central one with the lever up (open)
- Autoclave using the liquid cycle, with the schott bottles
- Remove the cotton filter from a sterile 10ml disposable pipette and attach to pump inlet tube. Place in Baxter water. Attach the shorter tube to the filtering unit. Swab glass bell and waste bottle with alcohol, flame and pump water through into the waste bottle
- Tighten nuts on the filtering unit using the key
- Pump water by switching from the central position on the pump to the right, speed < 1.0 (±0.8)
- Switch on the pump, when the water reaches the filter unit move the upright lever to the horizontal position
- Transfer pipette into unfiltered medium, allow some medium to pass through the filter into the waste bottle before filling the schott bottles to 900ml
- Store medium at 4°C until required

A2.1.5 ADDITIONS TO THE MEDIUM

A2.1.5.1 Foetal Calf Serum (FCS)

Heat inactivate the FCS at 56°C for 20 minutes

Add 100 ml inactive FCS to 900 ml RPMI-1640 = 10% FCS

A2.1.5.2 Fungizone

Add 200 µl fungizone to 1 L of 10% FCS in RMPI-1640

A2.1.5.3 Glutamine

3g tissue culture grade glutamine

100ml Baxter water

Makes up a 100X concentration, store in 10ml vials at -20°C

Glutamine has a 3-week half-life, if the medium has been stored for longer than 3 weeks then add 10ml to 1 L of medium

A2.1.6 CELL COUNTING

A2.1.6.1 2% Trypan Blue Stain

Solution 1: 0.2% w/v trypan blue

0.2g Trypan blue in 100 ml sterile water

Solution 2: 52 Saline

1.06g NaCl in 25 ml sterile water

Mix 4 parts solution 1 to 1 part solution 2

Store at RT

A2.1.7 PHOSPHATE BUFFERED SALINE (PBS)

0.9% NaCl	9 g
2.8 mM KCl	0.2 g

8.5 mM Na_2HPO_4	1.20 g
1.5 mM KH_2PO_4	0.2 g

A2.2 STIMULATION OF CELLS

A2.2.1 PLATELET DERVIVED GROWTH FACTOR

10 µg of PDGF was resuspended in 1 ml 4 mM HCl containing 0.1% BSA, aliquoted out and stored at -20°C until required. This gave a stock solution of 10 ng/µl. For experimental conditions cells were treated with 50 ng/ml PDGF that is equivalent to 5 µl in 1 ml of medium.

A2.2.1.1 4 mM HCl + 0.1% BSA

3.82 µl HCl
9.996 ml Sterile water
1 g BSA

A2.2.2 ETOPOSIDE

25 mg of etoposide was resuspended in 833 µl DMSO to give a stock solution of 30 mg/ml. The recommended concentration for experimental

conditions was 60 μg/ml that was equivalent to 2 μl of etoposide stock in 1 ml of medium.

A2.2.3 CYCLOHEXAMIDE

A stock solution of cyclohexamide (3 mg/ml) was prepared by dissolving 3 mg of cyclohexamide in 1 ml DMSO. Cyclohexamide was used as an apoptotic positive control at a concentration of 3 μg/ml (1 μl in 1 ml).

A2.2.4 LY294002

A stock solution (25 mM LY294002) was prepared by resuspending the obtained 5 mg LY294002 in 650 μl DMSO. This was aliquoted out and stored at -20°C. The PI3-kinase pathway was inhibited by incubating cells with 25 μM LY294002 (1 μl in 1 ml) for 1 hour prior to incubation with other stimulants.

A2.3 GROWTH/CYTOTOXICITY ASSAY

A2.3.1 PREPARATION OF PLATES

A2.3.1.1 PDGF

To give the correct final concentrations of PDGF the different concentrations were prepared as a 4X solution. 25µl of the corresponding concentration was added to the respective well. A 1 in 10 dilution of stock PDGF (10 ng/µl) was prepared to give a master solution with a concentration of 1 ng/µl

Table A2.2 Preparation of the five different concentrations of PDGF

Final PDGF Concentration	4X Concentration	µl of 1 ng/µl PDGF Added	µl Medium Added
10 ng/ml	40	1	24
30 ng/ml	120	3	22
50 ng/ml	200	5	20
70 ng/ml	280	7	18
90 ng/ml	360	9	16

A2.3.1.2 LY294002

To give the correct final concentration of LY294002, the stock solution was prepared as a 4X solution. The samples to be treated with LY294002 had 25µl of the stock solution added to its well.

Final concentration of LY294002 = 25 µM

4X concentration = 100 µM

µl LY294002 added = 4 µl

µl Medium added = 996 µl

A2.3.1.3 Etoposide

A 4X stock solution of the different concentrations of etoposide were prepared in order to obtain the correct final concentrations. 25µl of the corresponding concentration was added to the respective well. A 1 in 10 dilution of stock etoposide (30 mg/ml) was prepared to give a master solution with a concentration of 3 mg/ml

Table A2.3 Preparation of the five different concentrations of Etoposide

Final etoposide Concentration	4X Concentration	µl (3 mg/ml) etoposide Added	µl Medium Added
20 µg/ml	80	0.6	24.4
40 µg/ml	160	1.3	23.7
60 µg/ml	240	2	23
80 µg/ml	320	2.7	22.3
100 µg/ml	400	3.3	21.7

A2.4 PROTEIN EXTRACTION

A2.4.1 LYSING BUFFER A

20 mM Tris-HCl (pH 7.5)	0.24 g
Sucrose	8.55 g
1% Triton-X 100	1 ml

Dissolve in 80 ml distilled water

Adjust pH with HCl

Make up to 100 ml

Store in a dark bottle

A2.4.2 LYSING BUFFER B

20 mM Tris-HCl (pH 7.5)	0.24 g
Sucrose	8.55 g
1% Triton-X 100	1 ml

Dissolve in 80 ml distilled water

Adjust pH with HCl

Make up to 99 ml

Store in a dark bottle

Prior to lysing cells, add 1 µl 100 mM PMSF per 99 µl lysis buffer

A2.4.3 LYSING BUFFER C (SDS-LYSIS BUFFER)

62 mM Tris-HCl (pH6.8)	0.75 g
2% SDS	2 g
10% glycerol	10 g
0.5% β-mercaptoethanol	0.5 ml

Dissolve in 80 ml distilled water

Adjust pH with HCl

Make up to 100 ml

Store in a dark bottle

A2.4.4 LYSING BUFFER D

20 mM Tris-HCl (pH 7.5)	0.24 g
100 mM NaCl	0.58 g
1% Triton-X 100	1 ml
0.1% SDS	0.1 g

Dissolve in 80 ml distilled water

Adjust pH with HCl

Make up to 93 ml

Store in a dark bottle

Prior to lysis add the following to 93 µl lysis buffer:

1 µl 100mM Na_3VO_3

1 µl 100 mM PMSF

5 µl 100 mM NaF

A2.4.5 LYSING BUFFER E (AKT LYSING BUFFER)

20 mM Tris-HCl (pH 7.2)	0.24 g
150 mM NaCl	0.876 g
10% glycerol	10 ml
1% Triton-X	1 ml
30 mM Sodium Pyrophosphate	0.797 g
1 mM EDTA	0.037 g

Aliquot into 10 ml tubes and store at -20°C until required

Prior to lysing cells, add the following to 97 µl lysis buffer:

1 µl 100mM Na_3VO_3

1 µl 100 mM PMSF

1 µl 1 M NaF

A2.4.6 ADDITIONS TO LYSING BUFFERS

A2.4.6.1 PMSF (100 mM Stock)

0.17 g PMSF

Dissolve in 10 ml isopropanol to reduce degradation in aqueous water

Aliquot in to eppendorff tubes and store at -20°C until required

A2.4.6.2 Sodium Vanadate (100 mM Stock)

2.5 g Sodium Vanadate

Dissolve in 8 ml distilled water

Adjust pH to 10

Boil until translucent

Readjust pH to 10

Store in aliquots frozen at -20°C

A2.4.6.3 NaF (1 M Stock)

0.42 g NaF

Dissolve in 10 ml distilled water

Store at -20°C in aliquots

A2.5 TOTAL PROTEIN DETERMINATION

A2.5.1 STOCK SOLUTIONS

A2.5.1.1 0.1% BSA

0.1g BSA

100ml distilled water

Aliquoted and stored at -10°C

A2.5.1.2 0.1M Sodium Hydroxide

4g NaOH

1 litre distilled water

Store at RT

A2.5.1.3 2% Sodium Carbonate in 0.1M NaOH

10g Sodium carbonate

500ml 0.1M NaOH

Store at RT

A2.5.1.4 2% w/v Sodium Potassium Tartrate

1g sodium potassium tartrate

50ml sterile water

Store at RT

A2.5.1.5 1% w/v Copper Sulphate

0.5g $CuSO_4$

50ml sterile water

Store at RT

A2.5.2 WORKING REAGENT A

Prepare freshly by adding the following components in strict order with constant stirring:

1ml 2% w/v sodium potassium tartrate

1ml 1% w/v copper sulphate

100ml 2% sodium carbonate in 0.1M NaOH

A2.5.3 THE PROTEIN STANDARD CURVE

Table A2.4 The protein standard curve that was prepared in duplicate

Sample Number	Protein Concentration	1% BSA (µl)	Water (µl)
1	0	0	1000
2	25	25	975
3	50	50	950
4	75	75	925
5	100	100	900
6	150	150	850
Sample	X	10 µl of sample	990

A2.6 SDS-PAGE ELECTROPHORESIS

A2.6.1 RUNNING GEL SOLUTIONS

A2.6.1.1 Stock Acrylamide (RGA) (30%)

30% Acrylamide	15 g
0.8% Bisacrylamide	0.4 g

Make up to 50 ml with distilled water

Store in a dark bottle in the fridge

A2.6.1.2 Running Gel buffer (RGB) (pH 8.8)

1.5 M Tris HCl	9.085 g
0.4% SDS	0.2 g

Make up to 50 ml with distilled water

Correct pH with HCl and store in the fridge

A2.6.2 STACKING GEL SOLUTIONS

A2.6.2.1 Stacking Gel Acrylamide (SGA) (16%)

16% Acrylamide	8 g
0.512% Bisacrylamide	0.256 g

Make up to 50 ml with distilled water

Store in a dark bottle

A2.6.2.2 Stacking Gel Buffer (SGB) (pH 6.8)

0.5 M Tris	3.0285 g
0.4% SDS	0.2 g

Make up to 50 ml with distilled water

Correct pH with HCl (*pH drops rapidly after a certain point)*

Store in the fridge

A2.6.3 PREPARATION OF SDS-PAGE

- Wash the casting chamber well, rinse with distilled water
- Wipe plates down with alcohol and allow to dry
- Assemble casting chamber

Table A2.5 Three different concentrations of Running Gels

Reagent	10%	12.5%	15%
Distilled Water	5 ml	4 ml	3 ml
RGB	3 ml	3 ml	3 ml
RGA (30%)	4 ml	5ml	6 ml

- A 12.5% gel was generally prepared
- Mix the solutions well and degas for 10 minutes
- Make up fresh 0.1 g/ml ammonium persulphate in distilled water
- Add 0.25 μg/ml TEMED (3 μl per gel)
- Add 0.5 μg/ml APS (60 μl per gel)
- Gently swirl to mix
- Pour into casting chamber, allow to set for 15-20 minutes
- Overlay with isopropanol to ensure a flat surface and to exclude air
- Once the gels have set pour off the isopropanol and rinse with a 1 in 4 dilution of SGB

Table A2.6 The Stacking Gel

Reagent	4 %
Distilled Water	2.5 ml
SGB	1.25 ml
SGA (16%)	1.25 ml

- Mix solutions well and degas for 10 minutes
- Add 0.25 μg/ml TEMED (1.5 μl per gel)
- Add 0.5 μg/ml APS (25 μl per gel)
- Pour off 1 in 4 dilution of SGB
- Pour over running gel
- Insert combs and allow to set overnight

A2.6.4 ELECTROPHORESIS

A2.6.4.1 Running Buffer (pH 8.3)

0.025 M Tris	3.0285 g
0.192 M glycine	14.4 g
0.1% SDS	1 g

Make up to 1 L with milli-Q water

Check pH, if not correct, throw solution away and remake.

DON'T correct pH with HCl

Store in the fridge

A2.6.4.2 Loading Buffer (pH 6.8)

62 mM Tris-HCl (pH6.8)	0.75 g
2% SDS	2 g
10% glycerol	10 g
0.5% β-mercaptoethanol	0.5 ml

Dissolve in 80 ml distilled water

Adjust pH with HCl

Make up to 100 ml

Store in a dark bottle

A2.6.5 STAINING GELS

A2.6.5.1 Coomassie Blue Stain (0.1%)

H_2O	:	Acetic Acid	:	Methanol
17	:	1.5	:	20
34ml	:	3 ml	:	40 ml

Add a few grains of Coomassie blue

Gels are removed from the plates, washed with tap water and then placed in stain overnight.

A2.6.5.2 Coomassie Blue Destain

H_2O	:	Acetic Acid	:	Methanol
17	:	1.5	:	20
34ml	:	3 ml	:	40 ml

Can be recycled by filtering through active charcoal

The stain is poured off the gels, and the destain added. This is left to destain until the blue protein bands are visible on a clear background.

A2.7 WESTERN BLOTTING

A2.7.1 TRANSFER BUFFER (PH 8.5)

25 mM Tris	6.055 g
0.2 M Glycine	30.028 g
20% Methanol	400 ml
Make up to 2 L	

A2.7.2 STAINING A WESTERN BLOT

A2.7.2.1 Amido Black Stain

0.1% Amido Black Stain	0.1 g
10% Methanol	10 ml
2% Acetic Acid	10 ml
88 ml Water	

The blots were removed from the cassettes, washed with tap water and then placed in stain overnight.

A2.7.2.2 Amido Black Destain

50% Methanol	50 ml
7% Acetic Acid	7 ml
43 ml Water	

Can be recycled by filtering through active charcoal

The stain is poured off the blots, and the destain added. This is left to destain until the blue protein bands are visible on a white background.

A2.8 IMMUNOBLOTTING

A2.8.1 SOLUTIONS

A2.8.1.1 10X Tris buffered saline (TBS) (pH 7.6)

24.2g Tris

80g NaCl

Adjust pH with HCl and make up to 1 L with distilled water

Make a 1 in 10 dilution for 1X TBS

A2.8.1.2 Wash Buffer (TBS-T)

999 ml 1X TBS	
0.1% Tween-20	1 ml

A2.8.1.3 BSA Blocking Buffer & 1° Antibody dilution buffer

1X TBS-T	3 ml
5% Bovine serum albumin (BSA)	0.15 g

A2.8.1.4 Milk powder Blocking Buffer & 2° Antibody dilution buffer

1X TBS-T	25 ml
5% w/v non-fat dry milk	1 g

A2.8.2 STRIPPING AND REPROBING MEMBRANES

A2.8.2.1 Stripping Buffer (100ml)

2% SDS	2 g
62.5 mM Tris-HCl (pH 6.7)	0.757g

Prior to use add 100 mM β-mercaptoethanol (140 µl in 20 ml stripping buffer)

A2.8.2.2 Methodology

- Submerge membrane in stripping buffer and incubate at 50°C for 30 min with occasional agitation
- Wash membrane in 1X TBS twice for 10min each
- Block and immunoblot as usual

A2.8.3 DEVELOPMENT OF THE X-RAY FILM

A2.8.3.1 Developer

200 ml Solution 1

2.2 ml Solution 2

Make a 1 in 5 dilution with distilled water

Store in a dark bottle and replace every month

A2.8.3.2 Fixer

Make a 1 in 5 dilution with distilled water

A2.8.3.3 Method

- Place exposed X-ray in developer until bands start to appear
- Wash X-ray in water bath
- Place X-ray in fixer until the background appears clear
- Wash X-ray in water bath
- Allow X-ray to dry

A2.9 CONFOCAL MICROSCOPY

A2.9.1 ACRIDINE ORANGE-ETHIDIUM BROMIDE STAIN

100 mg Acridine Orange

100 mg Ethidium Bromide

1 ml PBS

Mix well and store at 4°C

A2.10 FLOW CYTOMETRY

A2.10.1 PROPIDIUM IODIDE

1 mg Propidium Iodide

100 µl DMSO

Mix well and store at -20°C

A2.11 DNA EXTRACTION

A2.11.1 RNASE A

Dissolve 10 mg RNase A in 1 ml TE buffer

Heat for 10 min at 70°C

Cool slowly

Aliquot and store at -20°C

A2.11.2 PROTEINASE K (10 MG/ML)

10 mg Proteinase K

4 µl 0.5 M EDTA

100 µl 10% SDS

Make up to 1 ml with distilled water

A2.11.3 TE BUFFER PH 7.6

12.1 g Tris

2 ml 0.5 M EDTA

Dissolve in 90 ml distilled water

Adjust pH with HCl

Make up to 100 ml

A2.11.4 10% SDS

0.1 g SDS

Dissolve in 10 ml distilled water

A2.11.5 0.5 M EDTA (PH 7.5)

18.61 g NaEDTA

Dissolve in 80 ml distilled water

Adjust pH with HCl

Make up to 100 ml

A2.11.6 1 M EDTA (PH 7.5)

37.2 g EDTA

Dissolve in 80 ml distilled water

Adjust pH with HCl

Make up to 100 ml

A2.11.7 1 M TRIS HCL (PH 7.4)

12.1 g Tris

Dissolve in 80 ml distilled water

Adjust pH with HCl

Make up to 100 ml

A2.11.8 GEL LOADING BUFFER

40mM Tris

20mM sodium acetate.$3H_2O$

1mM EDTA-Na_2.$2H_2O$

50% glycerol

pH to 7.2 with acetic acid

A2.11.9 3 M SODIUM ACETATE

3.657 g Sodium Acetate

Dissolve in 100 ml distilled water

A2.11.10 70 % ETHANOL

700 ml ethanol

300 ml distilled water

A2.11.11 5 M NaCl

222 g NaCl

100 ml distilled water

A2.11.12 LYSIS BUFFER 1

0.5 ml 1M Tris-HCl (pH 7.4)

0.5ml 1M EDTA

10 µl RNase-A

2.5 µl NP-40

A2.11.13 LYSIS BUFFER 2

0.5 ml 1M Tris-HCl (pH 7.4)

0.5ml 1M EDTA

10 µl RNase-A

2.5 µl NP-40

A2.11.14 TTE BUFFER

100 ml TE buffer (pH 7.4)

200 µl Triton-X

Store at 4°C

A2.11.15 BROMOPHENOL BLUE LOADING BUFFER

50 g Sucrose

50 mM EDTA

0.1 g Bromophenol Blue

10 g Ficoll

Make up to 100 ml with distilled water

A2.11.16 50X TAE BUFFER (STOCK SOLUTION)

242 g Tris

100 ml 0.5M EDTA (pH 8.0)

57.1 ml glacial acetic acid

Make up to 1 L with distilled water

Dilute to a 1X buffer when running gels

A2.11.17 1X TAE BUFFER

20 ml 50X TAE buffer

980 ml distilled water

A2.11.18 ETHIDIUM BROMIDE (STOCK SOLUTION)

100mg Ethidium Bromide

Dissolve in 10ml distilled water

Store in a glass bottle wrapped in foil at 4°C

A2.11.19 1% AGAROSE GEL

1 g Agarose

100 ml 1X TAE Buffer

Boil to dissolve agarose

Allow to cool to approximately 60°C

Add 5 µl Ethidium Bromide

Pour into gel chamber

A2.12 LDH ASSAY

A2.12.1 LDH BUFFER (PH 7.4)

50 mM Triethanolamine	665 µl
5 mM EDTA	0.186 g
100 ml distilled water	

A2.12.2 85 mM POTASSIUM PYRUVATE

0.019 g Potassium Pyruvate

2 ml LDH buffer

A2.12.3 4.5 mM NADH

0.016 g NADH

5 ml LDH buffer

A2.12.4 REACTION MIXTURE

100 µl 4.5 mM NADH

2.6 ml LDH buffer

200 µl Sample

100 µl 87 mM Pyruvate (Added to start the reaction)

A2.13 RNA EXTRACTION, QUANTIFICATION AND ANALYSIS

A2.13.1 DEPC WATER

200 µl DEPC

1 L Baxter water

Shake to release gasses

Allow solution to stand overnight

Autoclave on wet cycle to destroy DEPC

Tighten lid and store at RT

Note: DEPC is toxic and should be worked with in a fume cupboard

A2.13.2 VISUALISATION OF ISOLATED RNA INTEGRITY

A2.13.2.1 10X MOPS (pH 5.5-7.0)

Add the following reagents into a sterile schott bottle:

20.93 g MOPS

2.05 g Anhydrous Sodium Acetate

1.86 g EDTA

Make up to 500 ml with sterile water

Measure pH

Add 100 µl DEPC (in the fume cupboard)

Autoclave on the wet cycle

Store at RT in a dark bottle

Extreme care must be taken in order not to introduce RNases into the solution

A2.13.2.2 1% Denaturing Agarose Gel

0.5 g Agarose (RNA grade)

42.3 ml DEPC water

5 ml 10X MOPS

Dissolve by boiling for 5 min

Allow to cool to approximately 60°C

Add 2.7 µl Formaldehyde

Add 2.5 µl Ethidium Bromide

A2.13.2.3 RNA Sample Buffer

360 µl Formamide

80 µl 10X MOPS

130 µl Formaldehyde

135 µl DEPC

80 µl Glycerol

5 µl Saturated Bromophenol Blue

A2.13.2.4 Denaturing Gel Running Buffer

40 ml 10X MOPS

360 ml DEPC water

20 µl Ethidium Bromide

A2.14 REVERSE TRANSCRIPTION-POLYMERASE CHAIN REACTION ANALYSIS OF AKT1 MRNA

Table A2.7 The RT-PCR Master Mix

Reagent	Final Concentration	Volume per Sample
10 X Reaction Buffer	12	2 µl
25 mM $MgCl_2$	5 mM	4 µl
10 mM dNTP Mix	1 mM	2 µl
Oligo-p$(dT)_{15}$ Primer	0.025 µg/µl	1 µl
RNase Inhibitor	20 Units	0.5 µl
Reverse Transcriptase	15 Units	0.63 µl
Sterile Water	-	Variable
RNA Sample	2 µg	Variable
Final Volume		20 µl

Following cDNA synthesis, the product was made up to 100 µl with nuclease free water

A2.14.1 AKT PRIMERS

The Akt forward and reverse primers were diluted to a stock concentration of 100 pmole/µl by adding 1 µl primer to 99 µl Sterile water. The stock solution was stored at -70°C. A working dilution of 10 pmole/µl (10 µM) was prepared by diluting the stock solution 1:10 with sterile water. Small quantities of working dilution were prepared and stored at -20°C.

A2.14.1 GAP-DH PRIMERS

The GAP-DH primers were diluted to a stock concentration of 250 pmole/µl. This stock solution was stored at -70°C. A working dilution of 10 pmole/µl (10 µM) was prepared by diluting the primers 1:50 with nuclease free water. The working dilution was prepared in small volumes and stored at -20°C.

A2.14.3 THE MULTIPLEX PCR MASTER MIX

The dNTP mix that was added to the PCR master mix was the difference between the Reverse Transcription and PCR reactions. This was to ensure that the dNTP concentration remained at 0.2 mM throughout the RT-PCR reaction.

Table A2.8 The Multiplex PCR Master Mix

Reagent	Final Concentration	Volume (µl) per Sample
10X Reaction Buffer	12	5 µl
$MgCl_2$	1.5 mM	3 µl
10 mM dNTP Mix	0.2 mM	0.5 µl
Akt Forward Primer	0.4 µM	2 µl
Akt Reverse Primer	0.4 µM	2 µl
GAP-DH Forward Primer	0.05 µM	0.5 µl
GAP-DH Reverse Primer	0.05 µM	0.5 µl
Taq Polymerase	2.5 Units	0.5 µl
Sterile Water	-	Variable
cDNA	-	10 µl
Final Volume		50 µl

A2.14.4 VISUALISATION OF THE PCR PRODUCT

A2.14.4.1 2% Agarose Gel

1 g Agarose

50 ml 12 TAE Buffer

Boil to dissolve agarose

Allow to cool to approximately 60°C

Add 2.5 µl Ethidium Bromide

Pour into gel chamber

A2.14.4.2 DNA molecular weight marker

4 µl DNA molecular weight marker

3 µl Bromophenol blue loading buffer

3 µl Distilled water

A2.15 ENDONUCLEASE RESTRICTION OF AKT1 PCR PRODUCT

Table A2.9 The Restriction Enzyme Master Mix for the three Restriction enzymes used

Reagent	Buffer	Volume
PCR Product		6 µl
Sterile Water		12µl
Xho I	M	2 µl
Ava I	H	2 µl
Hae III	B	2µl
Final Volume		20 µl

REFERENCES

Alberts, B., Bray, D., Lewis, J., Raff, M., Roberts, K. & Watson, J.D. (1994) *Molecular Biology of the Cell*, Garland Publishing Inc., New York.

Adrain, C. & Marti, S.J. (2001) The mitochondrial apoptosome: a killer unleashed by the cytochrome seas. *TiBS.*, 26(6), pp. 390-397.

Alessi, D.R., Caudwell, B., Andjelkovic, M., Hemmings, B.A. & Cohen, P. (1996) Molecular basis for the substrate specificity of protein kinase B; comparison with MAPKAP kinase-1 and p70 S6 kinase. *FEBS Letters*, 399, pp. 333-338.

Andjelkovic, M., Jakubowicz, T., Cron, P., Ming, X., Han, J. & Hemmings, B.A. (1996) Activation and phosphorylation of a pleckstrin homology domain containing protein kinase (RAC-PK/PKB) promoted by serum and protein phosphatase inhibitors. *PNAS*, 93, pp. 5699-5704.

Andjelkovic, M., Suidan, H.S., Meier, R., Frech, M., Alessi, D.R. & Hemmings, B.A. (1998) Nerve growth factor promotes activation of the α, $\beta$and λ isoforms of protein kinase B in PC12 pheochromocytoma cells. *Eur J. Biochem,* pp. 195-200.

Astoul, E., Edmunds, C., Cantrell, D.A. & Ward, S.G. (2001) PI 3-K and T-cell activation: limitations of T-leukaemic cell lines as signalling models. *Trends Immunol,* 22(9) pp. 490-496.

Bellacosa, A., Testa, J.R., Staal, S.P. & Tsichlis, P.N. (1991) A retroviral oncogene, *akt,* encoding a serine-threonine kinase containing an SH2-like region. *Science*, 254, pp. 274-277.

Beraud, C., Henzel, W.J. & Baeuerle, P.A. (1999) Involvement of regulatory and catalytic subunits of phosphoinositide 3-kinase in NF-κB activation. *PNAS*, 96, pp. 429-434.

Birkenkamp, K.U., Geugien, M., Schepers, H., Westra, J., Lemmick, H.H. & Vellenga, E. (2004) Constitutive NF-κB DNA-binding activity in AML is frequently mediated by a Ras/PI3-K/PKB-dependent pathway. *Leukemia*, 18, pp. 103-112.

Borgatti, P., Martelli, A.M., Bellacosa, A., Casto, R., Massari, L., Capitani, S. & Neri, L.M. (2000) Translocation of Akt/PKB to the nucleus of osteoblast-like MC3T3-E1 cells exposed to proliferative growth factors. *FEBS Letters*, 477, pp. 27-32.

Brazil, D.P. & Hemmings, B.A. (2001) Ten years of protein kinase B signalling: a hard Akt to follow. *TiBS*, 26(11), pp. 657-664.

Brazil, D.P., Yang, Z. & Hemmings, B.A. (2004) Advances in protein kinase B signalling: *AKT*ion on multiple fronts. *TiBS*, 29(5), pp. 233-242.

Brunet, A., Bonni, A., Zigmond, M.J., Lin, M.Z., Juo, P., Hu, L.S., Anderson, M.J., Arden, K.C., Blenis, J. & Greenberg, M.E. (1999) Akt promotes cell survival by phosphorylating and inhibiting a Forkhead transcription factor. *Cell*, 96, pp. 857-868.

Burgering, B.M.T. & Kops, G.J.P.L. (2002) Cell cycle and death control: Long live Forkheads. *TiBS*, 27(7), pp. 352-360.

Burow, M.E., Weldon, C.B., Melnik, L.I., Duong, B.N., Collins-Burow, B.M., Beckman, B.S. & McLachlan, J.A. (2000) PI3-K/Akt regulation of NF-κB signalling events in suppression of TNF-induced apoptosis. *BBRC*, 271, pp. 342-345.

Chen, R., Chang, M., Su, Y., Tsai, Y. & Kuo, M. (1999) Interleukin-6 inhibits transforming growth factor-β-induced apoptosis through the phosphatidylinositol 3-kinase/Akt and signal transducers and activators of transcription 3 pathways. *J. Biol. Chem*, 274(33), pp. 23013-23019.

Collins, S.J. (1987) The HL-60 promyelocytic leukaemia cell line: proliferation, differentiation and cellular oncogene expression. *Blood*, 70(5), pp. 1233-1244.

Corfe, B. (2002) Suicide: A way of life. *The Biochemist*, June, pp. 9-11.

Costoya, J.A., Finidori, J., Moutoussamy, S., Senaris, R., Devesa, J. & Arce, V.M. (1999) Activation of growth hormone receptor delivers an antiapoptotic signal: evidence for a role of Akt in this pathway. *Endocrinology*, 140(12), pp. 5937-5943.

Delhaus, M., Li, N. & Karin, M. (2000) Kinase regulation in inflammatory response. *Nature*, 406, pp. 367-368.

Domin, J. & Waterfield, M.D. (1997) Using structure to define the function of phosphoinositide 3-kinase family members. *FEBS Letters,* 410, pp. 91-95.

Dynlacht, D.R., Earles, M., Henthorn, J., Roberts, Z.V., Howard, E.W, Seno, J.D., Sparling, D. & Story, M.D. (1999) Degradation of the nuclear matrix is a common element during radiation-induced apoptosis and necrosis. *Radiat. Res.,* 52, pp. 590-603.

Dynlacht, J.R., Roberts, Z.V., Earles, M., Henthorn, J. & Seno, J.D. (2000) Different patterns of DNA fragmentation and degradation of nuclear matrix proteins during apoptosis induced by radiation, hyperthermia or etoposide. *Radiat. Res.,* 154, pp. 515-530.

Franke, T.F., Yang, S., Chan, T.O., Datta, K., Kaziauskas, A., Morrison, D.K., Kaplan, D.R. & Tsichlis, P.N. (1995) The protein kinase encoded by the *Akt* proto-oncogene is a target of the PDGF-activated phosphatidylinositol 3-kinase. *Cell*, 81, pp. 727-736.

Franke, T.F., Kaplan, D.R. & Cantley, L.C. (1997a) PI3K: Downstream AKTion blocks apoptosis. *Cell*, 88, pp. 435-437.

Franke, T.F., Kaplan, D.R., Cantley, L.C. & Toker, A. (1997b) Direct regulation of the *Akt* proto-oncogene product by phosphatidylinositol-3,4-bisphosphate. *Science*, 275, pp. 665-667.

Frech, M., Andjelkovic, M., Ingley, E., Reddy, K.K., Falck, J.R & Hemmings, B.A. (1997) High affinity binding of inositol phosphates and phosphoinositides to the pleckstrin homology of RAC/Protein kinase B and their influence on kinase activity. *J. Biol. Chem.,* 272(13), pp. 8474-8481.

Gibson, S., Tu, S., Oyer, R., Anderson, S.M. & Johnson, G.L. (1999) Epidermal growth factor protects epithelial cells against Fas-induced apoptosis. *J. Biol. Chem.,* 274(25), pp. 17612-17618.

Glencross, D. (1994) Flow Cytometry: Basic Priciples and Applications. *The Leech*, 63(1), pp. 18-21.

Golstein, P., Aubry, L. & Levraud, J. (2003) Cell-death alternative model organisms: why and which? *Nature Reviews: Mol. Cell Biology,* 4, pp. 1-10.

Green, D.R. & Reed, J.C. (1998) Mitochondria and apoptosis. *Science*, 281, pp. 1309-1312.

Hsu, S.M., Chen, Y.C. & Jiang, M.C. (2000) 17 β-Estradiol inhibits Tumor necrosis factor-α-induced Nuclear factor-κB activation by increasing Nuclear factor-κB p105 level in MCF-7 breast cancer cells. *BBRC*, 279, pp. 47-52.

Janssen-Heininger, Y.M.W., Poynter, M.E. & Baeuerle, P.A. (2000) Recent advances towards understanding redox mechanisms in the activation of Nuclear factor κB. *Free Radical Biology & Medicine,* 28(9), pp. 1317-1327.

Jones, R.G., Parsons, M., Bonnard, M., Chan, V.S.F., Yeh, W., Woodgett, J.R. & Ohashi, P.S. (2000) Protein kinase B regulates T lymphocyte survival, Nuclear Factor κB activation and Bcl-X_L levels in vivo. *J. Exp. Med.,* 191(10), pp. 1721-1733.

Kane, L.P., Shapiro, V.S., Stokoe, D. & Weiss, A. (1999) Induction of NF-κB by the Akt/PKB kinase. *Curr. Biol.,* 9, pp. 601-604.

Li, H. & Yuan, J. (1999) Deciphering the pathways of life and death. *Curr. Opinion in Cell Biology,* 11, pp. 261-266.

Ma, N., Jin, J., Lu, F., Woodgett, J. & Liu, F. (2001) The role of protein kinase B (PKB) in modulating heat sensitivity in a human breast cancer cell line. *Int. J. Radiation Oncology Biol. Phys.*, 50(4), pp. 1041-1050.

Madge, L.A. & Pober, J.S. (2000) A phosphatidylinositol 3-kinase pathway, activated by tumour necrosis factor or interleukin-1 inhibits apoptosis but does not activate NF-κB in human endothelial cells. *J. Biol. Chem.*, 275(20), pp. 15458-15465.

Madrid, L.V., Mayo, M.W., Reuther, J.Y. & Baldwin, A.S. (2001) Akt stimulates he transactivation potential of the RelA/p65 subunit of NF-κB through the utilization of the IκB Kinase and activation of the Mitogen-activated Protein Kinase p38. *J. Biol. Chem.,* 276(22), pp. 18934-18940.

Masure, S., Haefner, B., Wesselink, J., Hoefnagel, E., Mortier, E., Verhasselt, P., Tuytelaars, A., Gordon, R. & Richardson, A. (1999) Molecular cloning, expression and characterization of the human serine/threonine kinase Akt-3. *Eur. J. Biochem.,* 265, pp. 353-360.

McKenna, W.G. (2001) Apoptosis, Radiosensitivity and the Cell Cycle. www.oncolink.org

O'Gorman, D.M., McKenna, S., McGahon, A.J., Knox, K.A. & Cotter, T.G. (2000) Sensitization of HL-60 human leukaemic cells to cytotoxic drug-

induced apoptosis by inhibition of PI3-kinase survival signals. *Leukaemia*, 14, pp. 602-611.

Okano, J., Gaslightwala, I., Birnbaum, M.J., Rustgi, A.K. & Nakagawa, H. (2000) Akt/protein kinase B isoforms are differently regulated by epidermal growth factor stimulation. *J. Biol. Chem.*, 275(40), pp. 30934-30942.

Ozes, O.N., Mayo, L.D., Gustin, J.A., Pfeffer, S.R., Pfeffer, L.M. & Donner, D.B. (1999) NF-κB activation by tumour necrosis factor requires the Akt serine-threonine kinase. *Nature*, 401, pp. 82-85.

Perkins, N.D. (2000) The Rel/NF-κB family: friend and foe. *TIBS*, 25, pp. 434-440.

Pomerantz, J.L. & Baltimore, D. (2000) A cellular rescue team. *Nature*, 406, pp. 26-29.

Pommier, Y., Sordet, O., Antony, S., Hayward, R.L. & Kohn, K.W. (2004) Apoptosis defects and chemotherapy resistance: molecular interaction maps and networks. *Oncogene*, 23, pp. 2934-2949.

Ramaswamy, S., Nakamura, N., Vazquez, F., Batt, D.B., Perera, S., Roberts, T.M. & Sellers, W.R. (1999) Regulation of G_1 progression by the *PTEN* tumour suppressor protein is linked to inhibition of the phosphatidylinositol 3-kinase/Akt pathway. *PNAS*, 96, pp. 2110-2115.

Raven, P.H. & Johnson, G.B. (1996), *Biology*, 4th ed., Wm. C. Brown Publishers, Dubuque.

Romashkova, J.A. & Makarov, S.S. (1999) NF-κB is target of AKT in anti-apoptotic PDGF signalling. *Nature,* 401, pp. 86-89.

Schmitz, M.L., Bacher, S. & Kracht, M. (2001) IκB-independent control of NF-κB activity by modulatory phosphorylations. *TIBS*, 26(3), pp. 186-190.

Shah, N., Thomas, T., Shirahata, A., Sigal, L.H. & Thomas, T.J. (1999) Activation of nuclear factor κB by polyamines in breast cancer cells. *Biochemistry*, 38, pp. 14763-14774.

Shin, I., Yakes, M., Rojo, F., Shin, N., Bakin, A.V., Basselga, G. & Artega, C.L. (2002) PKB/Akt mediates cell-cycle progression by phosphorylation of $p27^{Kip1}$ at threonine 157 and modulation of its cellular localization. *Nature Medicine*, 8(10), pp. 1145-1152.

Sizemore, N., Lerner, N., Dombrowski, N., Sakurai, H. & Stark, G.R. (2002) Distinct roles of Ikappa B kinase alpha and beta subunits in liberating nuclear factor kappa b (NF-kappa B) from IKappa B and in phosphorylating the p65 subunit of NF-kappa B. *J. Biol. Chem.*, 277(6), pp. 3863-3869.

Staal, S. (1987) Molecular cloning of the *akt* oncogene and its human homologues *AKT1 and AKT2*: Amplification of *AKT1* in primary human gastric adenocarcinoma. *PNAS*, 84, pp. 5034-5037.

Steelman, L.S., Pohnert, S.C., Shelton, J.G., Franklin, R.A., Bertrand, F.E. & McCubrey, J.A. (2004) JAK/STAT, Raf/MEK/ERK, PI3-k/Akt and BCR-ABL in cell cycle progression and leukemogenesis. *Leukemia*, 18, pp. 189-218.

Stephens, L., Anderson, K., Stokoe, D., Erdjument-Bromage, H., Painter, G.F., Holmes, A.B., Gaffney, P.R.J., Reese, C.B., McCormick, F., Tempst, P., Coadwell, J. & Hawkins, P.T. (1998) Protein kinase B kinases that mediate phosphatidylinositol 3,4,5-triphosphate-dependent activation of protein kinase B. *Science*, 279, pp. 710-714.

Stokoe, D., Stephens, L.R., Copeland, T., Gaffney, P.R.J., Reese, C.B., Painter, G.F., Holmes, A.B., McCormick, F. & Hawkins, P.T. (1997) Dual role of phosphatidylinositol-3,4,5-triphosphate in the activation of protein kinase B. *Science*, 277, pp. 567-570.

Story, M. & Kodym, R. (1998) Signal transduction during apoptosis; implications for cancer therapy. *Frontiers in Bioscience*, 3, pp. 365-375.

Tang, D., Lahti. J.M., Grenet, J. & Kidd, V.J. (1999) Cycloheximide-induced T-cell death is mediated by a Fas-associated death domain dependent mechanism. *J. Biol. Chem.*, 274(11), pp. 7245-7252.

Tang, X., Downes, C.P., Whetton, A.D. & Owen-Lynch, P.J. (2000) Role of phosphatidylinositol 3-kinase and specific protein kinase B isoforms in the suppression of apoptosis mediated by the Abelson protein-tyrosine kinase. *J. Biol. Chem.*, 275(17), pp. 13142-13148.

Tang, D., Okado, H., Ruland, J., Liu, L., Stambolic, V., Mak, T.W. & Ingram, A.J. (2001) Akt is activated in response to an apoptotic signal. *J. Biol. Chem.,* 276(10). pp. 30461-30466.

Thornberry, N.A. & Lazebnik, Y. (1998) Caspases: Enemy within. *Science*, 281, pp. 1312-1316.

Toker, A. & Newton, A.C. (2000) Cellular signalling: Pivoting around PDK-1. *Cell*, 103, pp. 185-188.

Tu, Y., Gardner, A. & Lichtenstein, A. (2000) The phoshatidylinositol 3-kinase/AKT kinase pathway in multiple myeloma plasma cells: Roles in cytokine-dependent survival and proliferative responses. *Cancer Research*, 60, pp., 6763-6770.

Ui, M., Okada, T., Hazeki, K. & Hazeki, O. (1995) Wortmannin as a unique probe for an intracellular signalling protein, phosphoinositide 3-kinase. *TIBS*, 20, pp. 303-307.

Vermes, I., Haanen, C. & Reutelingsperger, C.P.M. (1997) Apoptosis – the genetically controlled physiological cell death: biochemistry and measurement. *Ned. Tijdschr Klin. Chem.,* 22, pp. 43-50.

Vivanco, I. & Sawyers, C.L. (2002) The phosphatidylinositol 3-kinase-Akt pathway in human cancer. *Nature Reviews: Cancer*, 2, pp. 489-501.

Vlahos, C.J., Matter, W.F., Hui, K.Y. & Brown, R.F. (1994) A specific inhibitor of phosphatidylinositol 3-kinase, 2-(4-morpholinyl)-8-phenyl-4H-1-benzopyran-4-one (LY294002). *J. Biol. Chem.,* 269(7), pp. 5241-5248.

Yang, X.H., Sladek,T.L., Liu, X., Butler, B.R., Froelich, C.J. & Thor, A.D. (2001) Reconstitution of caspase-3 sensitizes MCF-7 breast cancer cells to doxorubicin- and etoposide-induced apoptosis. *Cancer Research*, 61, pp. 348-354.

Zhao, S., Konopleva, M., Cabreira-Hansen, M., Xie, Z., Hu, W., Milella, M., Estrov, Z., Mills, G.B. & Andreeff, M. (2004) Inhibition of

phosphatidylinositol 3-kinase dephosphorylates BAD and promotes apoptosis in myeloid leukaemias. *Leukemia*, 18, pp. 267-275.

Zhou, B.P., Hu, M.C.-T., Miller, S.A., Yu, Z., Xia, W., Lin, S.-Y. Hung, M.-C. (2000) *Her-2/neu* blocks tumour necrosis factor-induced apoptosis via the Akt/NF-κB pathway. *J. Biol. Chem.,* 275(11), pp. 8027-8031.